Addis Ababa University

Addis Ababa Institute of Technology

School of Electrical and Computer Engineering

Design and Simulation of Traction Power Supply System: Case study of Modjo~Hawassa line

A Thesis Submitted to Addis Ababa University

Addis Ababa Institute of technology

In Partial Fulfillment of the Requirement for the Degree of Master of Science in Electrical Engineering for railway systems

By**: Asegid Belay**

Advisor

Dr.Ing Getachew Biru

June, 2016

Addis Ababa, Ethiopia

Addis Ababa University

Addis Ababa Institute of Technology (AAIT) School of

Electrical and Computer Engineering

Design and Simulation of Traction Power Supply System: Case Study of Hawassa~Modjo Line

By: Asegid Belay

Approved by board of Examiners

Dr. Birhanu Beshah		
Chairman, Department Graduate Committee	Signature	Date
Dr-Ing Getachew Biru		
Advisor	Signature	Date
Ato Abebe Teklu		
Internal examiner	Signature	Date
Dr. Mengesha Mamo		
External Examiner	Signature	Date

Declaration

I, Asegid Belay, declare that this thesis is my original work, has not been presented for a degree in this or other universities. All sources of materials used for this thesis work have been fully acknowledged.

Name: Asegid Belay Signature: _____

Place: Addis Ababa Institute of Technology, Addis Ababa University, Addis Ababa

Date of Submission: _____

This thesis has been submitted for examination with my approval as a university advisor.

Dr.Ing Getachew Biru Signature: _____

Advisor's Name

Abstract

For more than a decade, the railway has experienced a renaissance in many countries after several years of decay. The main reasons for the renewed interest in the railway are environmental, economical, and safety related. This has quite naturally, in turn, increased the interest in railway associated research. Both passenger and freight transports on railway are increasing. In order to cope with this increase, large railway infrastructure investments are expected. An important part of this infrastructure is the railway power supply system – without it, only the weaker and less energy efficient steam and diesel locomotives could be used.

This thesis work presents the design and simulation of traction power supply system for the case of Modjo~Hawassa railway line. For this purpose, all the necessary electrical parameters data are collected through literature survey and the traction power supply system major components such as traction substation transformer, autotransformer, the catenary system and the loads are designed.

In connection with this, a model that represents the designed components of the power supply system using an existing blocks in the MATLAB/Simulink library were built and integrated into a system called a traction power supply system, which has a total length of 64 kilometer including 60 kilometer single track and 4 kilometer double track railway line and simulated using MATLAB/Simulink environment.

Accordingly, the simulation result of the traction power supply system for the three cascaded train which is found at a distance of 64 kilometers from the traction substation reveals that a train voltage of 19.81 kV and current of 414.63 A, a rail voltage of 87.12 V and autotransformer voltage of 19.82 kV in worst case scenario. In addition, the maximum percentage voltage regulation is found to be 26.45 %. As the result, it was found that the voltages and the currents waveform are according to BS EN 50163:2004, EN 50388:2012 and BS EN 50122-1 (IEC 62128-1) standard limits. This shows the performance of designed traction power supply system is within the industry standard.

Keywords: Traction power supply system, Design, Model, MATLAB/Simulink, Simulation, Currents, Voltages, Standards.

Acknowledgment

I would like to express my deepest thanks to Dr.-Ing Getachew Biru, My research advisor, for his guidance, support, motivation and encouragement to work on this research. His readiness for consultation at all times, his educative comments, his concern and assistance have been invaluable.

Moreover, I am really thankful to all of my family and my wife Yenealem Eyassu who were always there for me.

Special thanks to Ethiopian Railway Corporation (ERC), for sponsoring me this MSc program in Electrical Railway Engineering.

Finally, I would like to thank my fellow Msc students and other colleagues at Ethiopian Railway Corporation for making the coffee and lunch breaks pleasant.

At last but above all I would like to thank my father (God) who gave me his only son to save me from eternal death and revealed me heavenly wisdom.

Table of Contents

List of Figures

List of Table

List of Symbols and Abbreviations

AT	Autotransformers
A + Bv	Rolling resistance
AREMA	American railway enginering and maintenance of way asociation
a	Transformer transformation ratio
AC	Alternate Current
A_f	Projected cross sectional area
BT	Booster transformer
Cv^2	Aerodynamic resistance
C	Catenary
C1	Contact wire for track 1
CWR	Continuously welded rail
DC	Direct current
D_{ad}	Equivalent conductor at depth
D_{sa}	Distance between conductors
E_1, E_2	Electromotive forces of AT's primary and Secondary windings
E	Earth
F_{max}	Maximum tractive effort
f	Frequency
F1	Negative feeder wire for track 1
Fi	Forces acting on the train
F_{ex}	Forces against the train
F_c	Curve resistance

F_{gr}	Gradient resistance
F_r	Resistance force
F_D	Aerodynamic Drag
F	Feeder
G	Traction weight
GMR	Geometrical mean distance
GMD	Geometrical mean radius
Hz	Hertz
HVDC	High voltage direct current
HVAC	High voltage alternate current
HV	High-voltage
IEEE	Institute of Electrical and Electronics Engineers
IEC	International Electro technical Commission
i	Gradient
I_{ave}	Average Current
I_{effmax}	Effective Feeder Current
I_C	Catenary current
I_R	Rail current
I_{TR}	Negative feeder current
I_m	Train current
I_1 , I_2	Substation current-injected model
I_F	AT's primary and secondary current
JSS	AT's magnetizing current

K_1	Fluctuation coefficient
K_2	Over design coefficient
Ke (m)	Coefficient depending on the track gauge
km/h	Kilometer per hour
KV	Kilovolt
LRT	Light railway transit
L_{kk}	Self-inductance
L_{kj}	Mutual inductance
L	Inductance per phase
L_T	Total length of the train
m	Mass of a train
m^*	Dynamic mass of a train
M1	Messenger wire for track 1
MVA	Mega volt ampere
N	Number of train
N1, N2	Turns of the two windings
N_{axle}	Number of trailing axle
N.O	Normally open
ONAN	Oil Natural Air Natural
OCS	Overhead catenary system
P_D	Power demand
P_{aux}	Auxiliary power consumption
PSB	Power System Block set
PS	Paralleling stations
P	Traction probability

$P(v)$	Power as a function of velocity
pu	Per unit value
ρ	Autotransformer admittance matrix
PsYmat	Air density
R	Rails
$\mathbf{r_F}$	Freight train net weight coefficient
r	Radius of curve
rms	Route mean square
R11	Rail line for track 1
S1	Static wire for track 1
SS	Traction power substation
SWS	Switching stations
S	Transformer capacity
S_{TR}	Train Power
TPF	Traction power facilities
t	Tone
TSI	Technical Specifications for Interoperability
U_n	Nominal voltage
U_{max1}	Highest permanent voltage
U_{min1}	Lowest permanent voltage
U_{min2}	Lowest non-permanent voltage
U_{max2}	Highest non-permanent voltage
V_C	Catenary voltage

V_R	Rail voltage
V_F	Negative feeder voltage
V_O	Substation transformer Input side voltage
$\mathbf{V}SS$	Substation voltage
$\mathbf{V}$	Velocity
V_1	Substation transformer primary side voltage
V_2	Substation transformer Output voltage
W	Dead weight
W_a	Adhesive weight
ω	Angular velocity
X	Inductance
$\boldsymbol{Y}SS$	Substation admittance
Y_{AT}	Auto transformer admittance
Z_{AT}	Autotransformer impedance
Z_{TPSS}	Impedance of traction power substation
Z_{aa}	Self-impedance
Z'_1	Primary side impedance referred to secondary
Z_{eq}	Equivalent impedance
Z_1, Z_2	AT's primary and secondary leakage impedances
Z_m	AT's magnetizing impedance
Z_{cc}	Contact line self-impedance
Z_{ad^1}	Mutual impedance
Z_{base}	Base impedance
Z_e	Earth resistance

Z_{mm}	Messenger wire self-impedance
Z_{RR}	Rail line self-impedance
Z_{SS}	Static wire self-impedance
Z_{FF}	Negative feeder self-impedance
α	Gradient angle
μ_a	Adhesion Coefficient
ξ	Slippage ratio
η_{loco}	Locomotive efficiency
%Z	Percentage impedance
Ω/km	Kilometer per ohm
δ	Skin depth
X/R	Inductance resistance ratio
λ_k	Flux linkage for the Kth conductor
Ω	Ohm
Γ	Annual transportation

1 INTRODUCTION

This chapter provides an introduction to railway power supply systems in general, and also defines the aim and the objectives of the thesis work.

1.1 Background

For more than a decade, the railway has experienced a renaissance in many countries after several years of decay. The main reasons for the renewed interest in the railway are environmental, economical, and safety related.

This has quite naturally, in turn, increased the interest in railway associated research. Both passenger and freight transports on railway are increasing. This is not an increase only in the number of departures, but also heavier trains for goods, and faster trains for personal transports. In order to cope with this increase, large railway infrastructure investments are expected. An important part of this infrastructure is the railway power supply system – without it, only the weaker and less energy efficient [1] steam and diesel locomotives could be used.

Due to massive advantages of electric power supply compare to diesel fuel, there has been a gigantic acceleration in railway traction development in Ethiopia and other parts of the world.

The main advantage of electric traction is a higher power-to-weight ratio than types such as diesel or steam that carry power generators on board. This was particularly the case when compared to steam engines and diesels of the mid-twentieth century. This results in a higher rate of acceleration and higher tractive effort on steep grades. Electrification is also a more efficient way of transmitting power, especially on the busiest and most heavily trafficked routes where any additional capacity (either through longer trains or more frequent services) will require proportionally less additional energy when it comes from a common source rather than on each train. Electric locomotives can deliver as much as 2½ times the tractive power output of an equivalent diesel [1][2].

With electric traction it is also possible to further increase efficiency through regenerative braking, which means that a slowing-down train can use its electric motors as generators

and recycle energy back into the system for other electric trains to use. Electric traction offers significantly improved performance when ascending gradients, plus the possibility of using regenerative braking to cost efficiently maintain safety whilst descending [5].

Other advantages include the lack of exhaust fumes at point of use, less noise and lower maintenance requirements of the traction units. In countries where electricity comes primarily from non-fossil sources, such as Ethiopia ,Austria and France, electric trains also produce fewer carbon emissions than diesel trains. Electric railways have the potential to be the least environmentally damaging form of traction. Although this depends on how the power is sourced.

With the trend of increasing energy prices and the environmental impact of wasting energy in mind, power consumption, is also an important parameter to study in traction power supply system. The studies of power consumption will also be helpful when placing the traction power substation. The determination of traction Substation capacities is important, because it is desirable to transport power over as short distances as possible on the overhead contact wire, called the catenary. The possible choice between power transmissions in 50 Hz high voltage lines, through transformers depends much on the local prerequisites. A slightly under-dimensioned power supply system might lead to higher energy consumption because of increased losses, whereas a severely under-dimensioned system would hardly allow the trains to consume any power at all.

An under-dimensioned power system, i.e. an electric power system which is too weak, is in general characterized by substantial voltage drops when stressed. Accurate power supply system analysis provides the necessary information for design, planning and operation. Simulation is commonly adopted as the most cost-effective tool for traction power supply system studies. There are two major considerations in traction power supply simulation [2], namely accurate modeling of power networks and loads and efficient system or algorithms for solution. A number of traction power simulators have been developed [2-4] and they cover a wide range of applications and systems [5-7].

In this study, an alternative approach, using MATLAB software, is developed to simulate the traction power supply systems for the case of Modjo~Hawassa rail line. It has to be stressed that

the traditional traction power simulators are very expensive and owned by giant companies in the industry. Due to this, as mentioned above, an alternative approach using MATLAB software is developed.

1.2 Overview of a Traction Power Supply System Under Study

Selection of an appropriate traction power supply system is always very dependent on the railway system objectives. The system considered under study for Modjo~Hawassa railway line is bi-phase or autotransformer fed traction power supply system. In this system, the traction transformers are supplied from state grid, normally at 132 kV voltage levels. This voltage is further step down to 55 kV nominal voltage at traction substation of using 132/55 kV (no load voltage) transformers. Each traction substation has two 132kV independent power lines. Branch connection is used at 132 kV side and single bus bar section is applied at 27.5 kV bus bar. Permanent spare system is used. Figure 1.1 shows the autotransformer feeding system configuration under study [34].

In this research, the proposed line is 202 kilometer long, but for simulation purpose only 64 kilometer is considered (the first 60 km represents a single track line and the second 4 km represents double track line) which is ranging from Modjo to Arsi Negealea; this is because in design of railway traction power supply systems unless there exist special case, the equipment rating used for one feeding section could be a complete duplicate of the other. Due to this, simulation result obtained for Modjo to Arsi Negealea can represent the whole 202 kilometer railway line.

In the proposed feeding system, the catenary-rail voltage is delivered by the feeder-catenary distribution system via autotransformers. Autotransformers are installed at each paralleling station and at each switching station. The autotransformer winding ratio must correspond to the distribution voltage (feeder-to-catenary) and the traction voltage (catenary-to-rail) ratio.

The autotransformer-fed system enables power to be distributed along the system at higher than the train utilization voltage. For example, in the 2x27.5 kV autotransformer system, power is distributed at 55 kV (line-to-line) while the trains operate at 27.5 kV (line-to-ground). This arrangement results in a system with lower voltage drop along the alignment than is possible

with 25 kV direct-fed systems or booster fed system, resulting in an improved train voltage profile along the line. Depending on the train position along the system, the current in the feeder may flow in the opposite direction than the current in the catenary. In this event, certain electromagnetic field cancelation occurs. This field cancelation mitigates, to some degree, the effects of electromagnetic interference on other wayside equipment as well as communications and signaling circuits [9] [11].

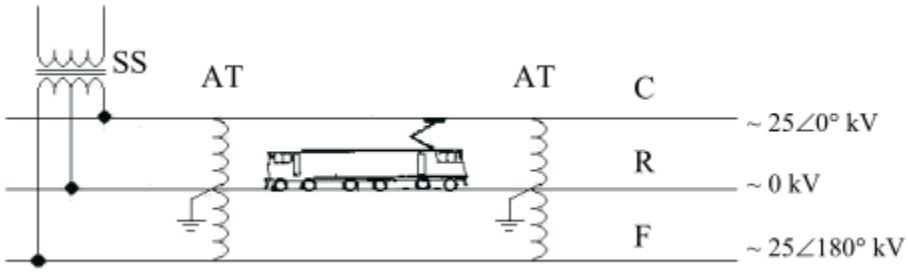

Figure 0.1: Autotransformer feeding system

The type of locomotives chosen in this thesis is MTAB (MalmTrafik i Kiruna AB) locomotive which is a common Swedish freight train. Its maximum speed is 100 km/h and designed for freight transport and can consume up to 15 MW [25]. The locomotive has six axle loads each weighing 25 ton whereas each trailing car has two axle load and the length of the locomotive and the trailing train is 15.5 m and 14.27 m respectively.

In actual train operation the voltage variation at the vehicle current pickup devices affects the train performance. When the voltage decreases, lower power is available to the train, and as a result the acceleration may be reduced and sometimes the top speed the train can attain may be also reduced. Conversely, when the system presents high voltage to the vehicle, the rolling stock can accelerate at full rate and reach the maximum operating speed in short time. Therefore load flow analysis for the evaluation of the performance of the traction power supply system is mandatory. Hence, in this research, the effort is focused on designing a traction power supply system, studying the impact of distance and number of train on the system and evaluating the performance of the designed system in terms of voltages, currents and voltage regulation.

1.3 Statement of the problem

The transportation demand in Ethiopia is increasing as a product of economic development and population growth. To cop up with this demand, the Ethiopian government is implementing a rail transport system in two phases. In the first phase the country is constructing light rail transit (LRT) in the capital city, Addis Ababa and freight and passenger train transport from Addis Ababa to Djibouti. In the second phase construction of a rail transport system that joins the main cities of the country including rail line connection with neighboring Kenya will take place.

The Modjo~Hawassa railway line will be one of the largest projects that starts very soon and its importance is twofold.

First, it connects Hawassa, the capital of Southern Nations Nationalities and Peoples of Ethiopia, to Addis Ababa-Djibouti rail line, which facilitates socioeconomic development of the country.

Second, this rail line will be extended up to Ethio-Kenya border, which enables us to use Kenya's Mombasa or Lamu Port, which reduces dependency on Djibouti port and also significantly decreases the cost and the amount of time that is needed to transport goods from south to all the way north and vise versa.

Since the investment is very expensive and almost impossible for this poor country to achieve its future goal depending only on foreign contractors and professionals, we have to start developing our own project by our own experts.

Motivated by the above reasons, design and simulation of the traction power supply system for the case of Modjo~Hawassa rail way line performed, which enable our country to move one step forward for the construction of its own rail line.

1.4 Objective

The research work is aimed at the design and simulation of traction power supply system for the case of Modjo~Hawassa rail line with the following general and specific objective.

1.4.1 General Objectives

The general objective of this master thesis is to design and simulate AC traction power supply system using the power system toolbox of MATLAB/ Simulink and verify the obtained solution for practical implementation.

1.4.2 Specific Objectives

The design incorporated the following specific design and simulation objectives to achieve the main goal.

1. Collect primary data required for the design of the railway power supply system.
2. Determine power and energy requirement for the railway system.
3. Identify appropriate supply voltage type and levels.
4. Design power transformers for the traction substation, paralleling stations and switching stations for the required power supply system and calculate the transformer capacity and other major elements.
5. Model and simulate the overall system using MATLAB/Simulink to make power flow analysis and evaluate the performance of the power supply system in terms voltages, currents and voltage regulation.
6. Draw conclusions and recommendations which are helpful for improvement of the construction of the railway system.

1.5 Methodology

In order to achieve the main aim of the study there are various procedural tasks followed by the author. The first method towards processing the work is started with reviewing different literatures where all the theoretical information regarding the design and simulation of traction power supply system is gathered and a comparison of previous similar research is studied. Alongside with reviewing current specification and standards, the collection and verification of data for the design is performed. This is followed by studying and designing the major components of the traction power supply system. Once the design is completed, a model is developed using MATLAB/Simulink environment and simulation is performed. Finally, based

on the simulation results, the performance of the designed traction power supply system is evaluated. The general block diagram of the methodology is given below.

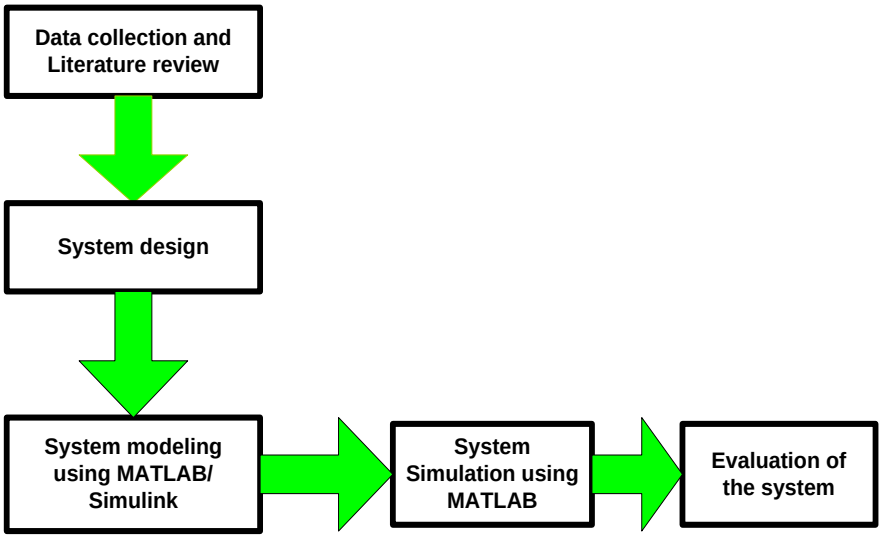

Figure 1.2 Summary of methodology

1.6 Aim of Research and Structure of Thesis

The aim of the research was to carry out design and modeling of traction power supply system and verify the results based on MATLAB software simulation.

1.6.1 Outline of the Manuscript

This thesis paper is organized into six chapters. These are:

Chapter 1

This chapter provides an introduction to the topic of traction power supply systems by describing the background, defining the research problems, and presenting the objectives of the thesis.

Chapter 2

This chapter generally covers about theoretical background and literature survey of a traction power supply system. Presents detail explanation about major components of traction power supply system such as substation traction power transformer, catenary system, the moving load

and the railway load flow and also reviews various related research works. This chapter also aimed to present system configuration of the autotransformer feeding system for the proposed line. Finally explains steps that should be followed in designing traction power supply system.

Chapter 3

This chapter starts with estimation of power consumption of the locomotive followed by calculations of traction power transformer capacity and continued with the design of traction power transformer and autotransformer. It also focuses on calculation of the transmission line impedance using Carson line model.

Chapter 4

Models of the different system components are presented using MATLAB/Simulink. These components are the substation transformer model, the catenary system model, autotransformer model and the train model.

Chapter 5

This chapter provides simulation results and discussions for different scenarios. In addition, graphic results were presented.

Chapter 6

Ends the thesis with conclusions from the work done for the completion of the master study and also gives recommendations and suggestions towards future work.

2 THEORETICAL BACKGROUND AND LITERATURE SURVEY

This chapter primarily presents theoretical background to the subject of traction power supply system and discusses previous research related to this thesis.

2.1 Introduction

The knowledge of railway and steam engines has been around since the sixteenth century. Wagon roads for coalmines using heavy planks were first designed and built in 1633 [1]. Mathew Murray of Leeds in England invented a steam locomotive that could run on timber rails in 1804 and this was probably the first railway engine [12]. Although railway and locomotive technologies were continually developed, the first electrified railway was introduced in the 1880s [12-14]. As a result of this revolution, motors and the traction power supply system have become important parts of modern electrified railways.

Apart from traction motors, traction power supply systems are physically huge electrical circuits which generally consists of traction substation, the catenary system, time-varying and moving loads and other electrical system[13].

2.2 Traction substation

In general substations serve as sources of energy supply for the local areas of distribution in which they are located. Their main functions are to receive energy transmitted at high voltage from the generating stations, reduce the voltage to a value appropriate for local use, and provide facilities for switching. Substations have some additional functions. They provide points where safety devices may be installed to disconnect circuits or equipment in the event of trouble. Voltage on the outgoing distribution feeders can be regulated at a substation. A substation is a convenient place to make measurements to check the operation of various parts of the system. Street lighting equipment as well as on-and-off controls for street lights can be installed in a substation though this is a diminishing function. Some substations are simply switching stations where different connections can be made

between various transmission lines. Whereas some are used only for specific purposes such as powering locomotives which is called traction power substation.

A traction power substation is an electrical substation that converts electric power from the form provided by the electrical power industry for public utility service to an appropriate voltage, current type and frequency to supply railways, trams (streetcars) or trolleybuses with traction current. In a substation many electrical components work together to carry out its functions, these include Lightning arresters, Switches, Distribution Bus, Circuit Breakers, Current Transformers, Isolators, Conductor systems, Insulation, Overhead line terminations, Bushings and Power transformers.

2.2.1 Traction power Transformers

The high voltage utility power is transformed to the distribution voltage by the traction power transformers. Normally, each substation is equipped with two equally-sized transformers, each transformer should be rated to be capable of handling the entire substation load and to allow for continuous system feeding in the event of outage of one of the utility feeders, transformer, or other item of high voltage equipment [14].

The single-phase traction power transformer primary windings are connected to two of the three phases of the utility power system. Because power is being drawn from only two phases of a three-phase system, a certain amount of current and voltage unbalance will occur. In order to mitigate the effects of the unbalanced currents and voltages, the single-phase connections should be alternated at successive transformers. Therefore, in an interconnected power utility network, the unbalanced currents and voltages will tend to balance out by the time they reach the utility generators or consumer motors [16].

2.3 Catenary

Electrical power will be supplied to the trains from wayside traction power substations through the catenary, which distributes the power to the train pantographs. The pantographs, mounted on the roof of the rolling stock, collect the electrical power from the catenary through mechanical contact by running or sliding under the contact wire.

There are three main types of technologies used for catenaries where return currents are supposed to flow in overhead power lines instead of in the rail or through the ground. These are direct feeding with return conductor (DR), Auto Transformer (AT) and Booster Transformer (BT). In [51], a detailed description of DR, AT and BT catenary systems can be found.

The introduction of Booster Transformers (BT) in some countries catenary systems was necessary as a result of the high ground resistances. A high ground resistance complicates the return conduction through rail and ground [25]. The complications are primarily disturbances on phone and signal systems, caused by ground currents and magnetic fields [8]. The normal distance between BT transformers is around 5 km, and between these, there is a connection between the return conductor and the rail, see figure 2.1. The purpose of the BTs is to draw the current from the return rail to an overhead return conductor. In Sweden one rail is conducting, and is called "S-rail", whereas the other rail is used for signaling and is called "I-rail" [25].

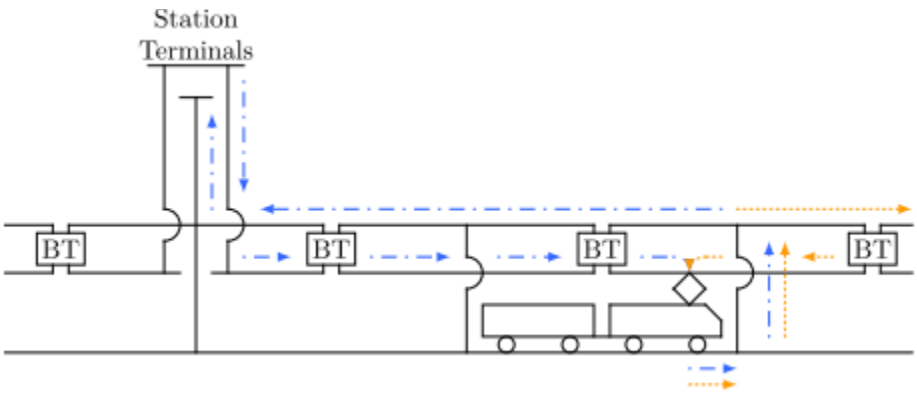

Figure 2.1: An illustration of a typical BT catenary system [25]

Through a BT the sum of currents needs to be zero, therefore it will draw the return current from the rail through the return line all the way to the return current bus. The purpose of using the BTs is mainly to reduce the stray currents in the rail [52]. Since the train is moving, the impedances between the locomotives and the nodes of power inflows vary in time. The impedances between the nodes are dependent not only on the physical distances between them, but also on the locomotive's distance to the BTs and return line connectors. Thus, one can say that the impedances vary in a complicated way.

Where a BT balances currents, an AT balances voltage. AT catenaries doubles the voltage between catenary and the feeder line, but still maintains the same rail-to-catenary voltage as in the BT system. The doubling of voltage is created by a 180 degrees voltage phase shift between the contact wire and the feeder line. This is a way of reducing impedances in a cost-efficient way. The higher voltage leads to smaller currents, and thereby also reduced power losses and reduced telephone interferences [41]. AT transformers are normally distributed with 10 km in between. Having allowed power to be transmitted at the voltage twice as high as the operating voltage, AT feeding improves system efficiency. Interference suppression is another advantage of AT feeding. In addition, AT feeding provides better voltage regulation and allows longer interval between transformers [19], which is essential for service reliability of long-distance rail lines.

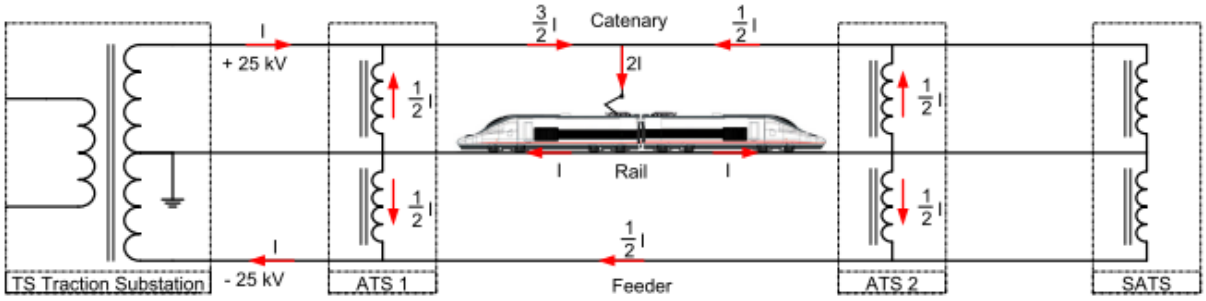

Figure 2.2: Autotransformer feeding system

In AT+BT system, the AT transformers can be sparser distributed than in a pure AT system. This is possibly a cheaper choice when upgrading old BT systems that have become too weak due to increased traffic. A smaller discussion of AT+BT can be found in [41].

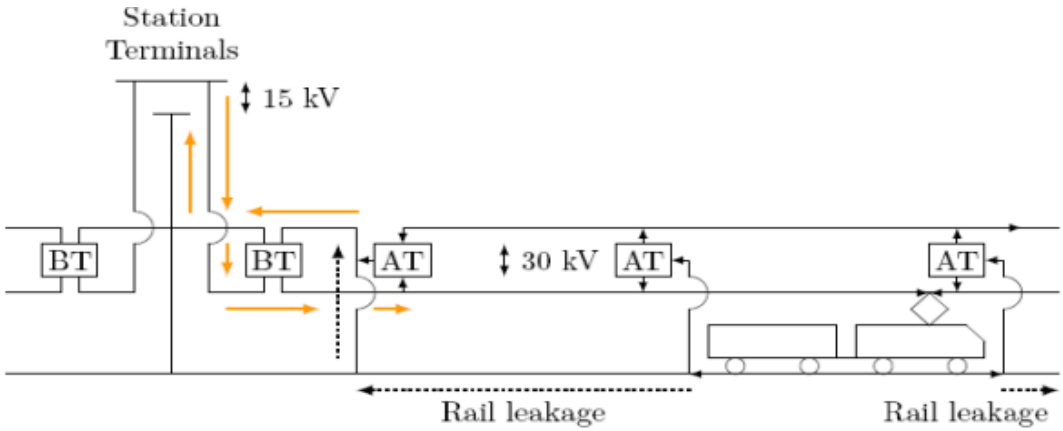

Figure 2.3: AT+BT configuration [25]

2.4 Loads

Train speed and operation mode are the decisive factors of the immediate amount of power required by the train as a load. They are however determined by the traction equipment characteristics, train weight, aerodynamics, track geometry and drive control.

For an inter-station run, a train goes through different speeds and operation modes and the power demand may thus vary significantly within a short period of time. A simple and quick reference linking train speed and operation mode to the power required is essential to load flow calculation. The fact that the trains are moving and carrying variable loads does not impose any difficulty on traction power system simulation [20] in which the details of power flow and energy consumption at every instant are available.

In order to provide a general and simple picture of loading conditions in the system over a long span of time, load flow study is a simple and viable tool for any power system [21]. Given that the loads are moving with time-varying demands. The number of trains in a feeding section is also vital to the calculation as they may be running at different speeds, drawing (or feeding) different amount of power from (or into) the feeding network and thus attributing different effects to the supply system. Nominal separation among trains is yet another important consideration and it should follow the timetables or headway of the train services.

2.5 Power Requirements of the Load

Energy resources are quite scarce in many countries. One of the most important energy resources is electricity. In the last few years, Ethiopia has suffered from electricity shortage problem. For this reason, the government has encouraged all public and private sectors to reduce power losses.

In order to avoid wastage of electricity in railway, selection of power supply system and an accurate energy estimation model is necessary. As early as in 1985, Majumdar proposes four main stages of train movement including (1) acceleration, (2) balancing, (3) coasting, and (4) deceleration.

During the first state (I), the vehicle moves with constant positive acceleration, so the speed increases. When the vehicle reaches a determined speed lower than the constant speed, the second operation state starts. In this state, the acceleration decreases, but the speed keeps increasing. In the third state (III), the cruise speed is reached and the acceleration is zero. In the final stage (IV), the braking operation starts with negative acceleration until the moment it decelerates with a constant rate and finally it stops at the destination station [40].

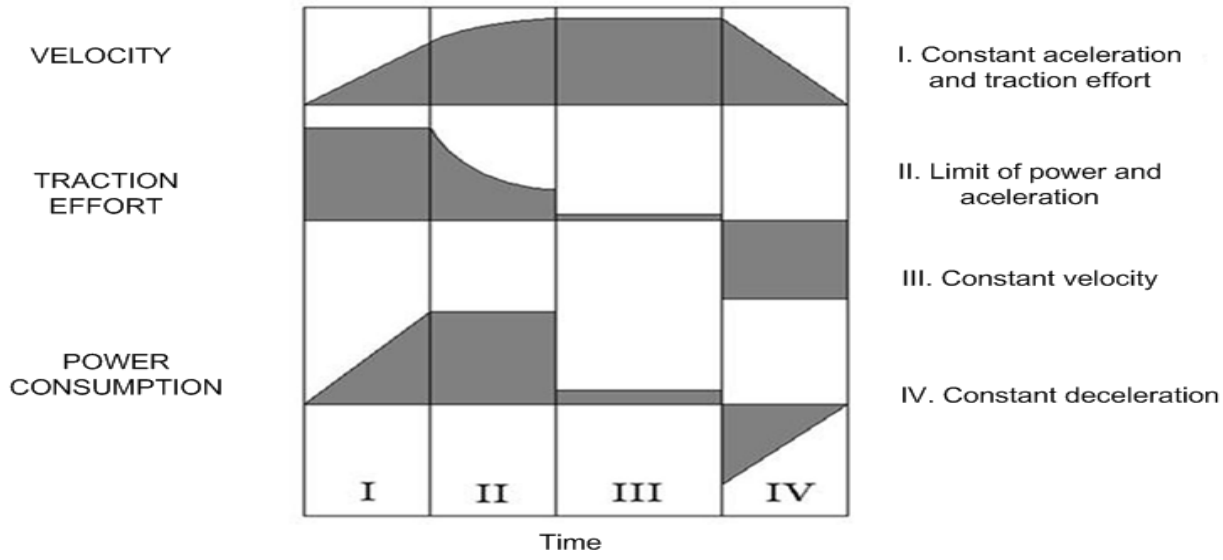

Figure 2.4: Velocity, Traction Effort, and Power Consumption of a train [40].

For determining the power requirements it is important to know the forces acting against their direction of travel and the available adhesion for traction and breaking. The total resistance, called running resistance, consists mainly of mechanical rolling resistance, air drag and resistance due to curves and grades. Adhesion is a term for the grip between a wheel and the rail, or in this context the part of the wheel-rail-friction in the longitudinal direction that can be used for actual propulsion or deceleration. Both the running resistance and the adhesion are affecting the performance of a train; acceleration, driving times and also energy consumption and they both vary in time and space [40].

The motion of the train can be described by the one-dimensional Newton's equation. Indeed the Train can be modeled as a point following the track.

$$\overrightarrow{\sum_{i=1}^{n} Fi} = m^{*}a \qquad 2.1$$

Where Fi are the different forces acting on the train, m* is the mass of the train, corrected to take into account the inertia of the rotating mass ($m^{*}= \xi m$) and a is the acceleration of the train along the track.

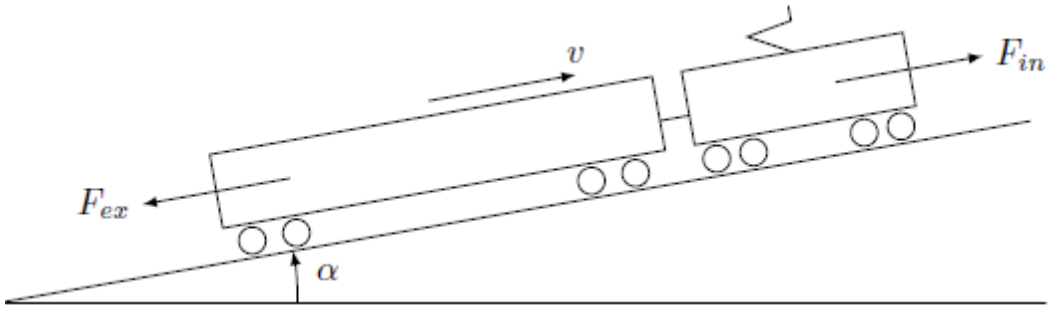

Figure 2.5: Train running on a track [12]

The different forces acting on the train can be split in two categories:

- F_{in}: forces produced by the train, positive in traction, negative in braking
- F_{ex}: Forces mainly against train motion

The equation 2.1 can therefore be written

$$F_{in} - F_{ex} = m^{*}a \qquad 2.2$$

The force opposing train movement can be written:

$$F_{ex} = F_r + F_{gr} + F_c \quad 2.3$$

Where F_r is the train resistance (resistance to forward motion), F_{gr} is the force due to gradients, and F_c is the resistance due to the curves.

Then F_r is always modeled as follows

$$F_r = A + Bv + cv^2 \quad 2.4$$

The term A increases linearly with the number of axle and can be divided into two parts. One part is constant for a given type of running gear, while the other part increases approximately linearly with axle load.

Term BV can be divided into two parts and increases approximately with number of axle or train length but does not show any systematic variation with axle load. This implies that term BV is probably affected by parts of aerodynamic drag not covered by the quadratic term.

Term cv^2 can be divided into two parts. The first part is constant and depends mainly upon the front and rear of the train. The second term increases approximately linearly with train length. Several formulas exist to derive A, B and C, many of them can be found in [37].

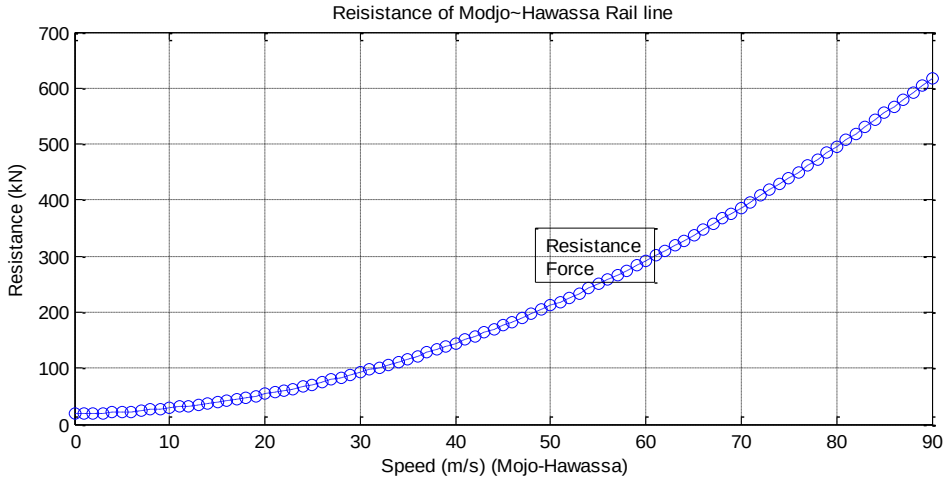

Figure 2.6: Train resistance force Vs speed

As shown in the figure 2.6 above the resistance force increases with the speed. The calculated results and the matlab code of figure 2.6 can be found in chapter three and in appendix A respectively.

Trains are heavy and require substantial effort to push them up slopes. If a train of mass M is on a slope making an angle α to the horizontal the vertical force Mg (g is the acceleration due to gravity, 9.81 m/s 2) can be resolved into horizontal force along the track and vertical force perpendicular to the track, as shown in figure 2.5.

Gradients on railways are small and usually expressed in the form 1 in X, where X is the horizontal distance moved to rise 1 unit.

Then the gradient force is simply:

$$F_{gr} = Mg\sin(\alpha) \qquad 2.5$$

Where α is the gradient angle (figure 2.5), the gradient is usually defined by the tangent of this angle in mm/m or ‰. For gradients below 120 mm/m , that is to say in almost every cases in railways, it is common to assume that the $\sin(\alpha)$ and the tangent are similar. The gradient resistance is therefore given by:

$$F_{gr} = i\ 10^{-3}mg \qquad 2.6$$

Where i is the gradient in mm/m or ‰. By convention, i is positive if the train is going up, and Negative if the train is going down.

A train running in a curve is subjected to an additional rolling resistance, due to the friction between the wheels and the rail. This friction phenomenon is quite complicated and depends very much on the type of the bogies, and the shape of the rails. For travel time calculation purposes there is no need to derive complicated models. The resisting force produced by the curve is modeled by the following equation [37]:

$$F_c = \frac{k_e}{r} 10^{-3}\ m\ g \qquad 2.7$$

Where ke (m) is a coefficient depending on the track gauge (Table 2.1) and r is the radius of the curve. The tighter the curve is, the higher is the resisting force. This equation is empirically derived and is widely adopted when performing running time and power consumption calculations.

Table 2.1: Track gauge coefficient for curve resistance [35]

ke (m)	Track gauge (mm)
750	1435
530	1000
400	750
325	600

The available frictional force between the steel wheels of the train and the steel of the rails is a fundamental physical property limiting the performance of the trains in a very significant way. The coefficient of friction μ_a, sometimes simply called the adhesion, is the fraction of the perpendicular force on the rails which can be exerted along the rails before slipping occurs. It has a value between 5% and 50% depending on conditions, although the range 10% to 30% is more normally assumed for performance calculations [35].

In 1943 Curtius and Kniffler derived an adhesion curve for a dry rail as a function of the vehicle speed (Figure 2.7).

The adhesion coefficient follows the equation:

$$\mu_a = 0.161 + \frac{7.5}{3.6v+44} \qquad 2.8$$

With v the speed in km/h.

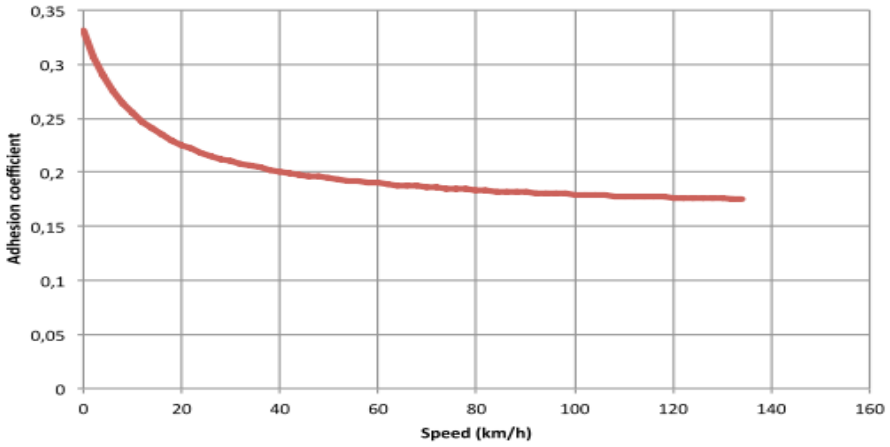

Figure 2.7: Adhesion curve of Curtius and Kniffler

It has been found that tractive effort can be increased by increasing the motor torque but only up to a certain point. Beyond this point any increase in the motor does not increase the tractive effort but merely cause the driving wheels to slip. Which mean the force developed by the traction motor is transmitted by the wheel-rail contact. The transmitted force is limited by adhesion and the maximum force that can be transmitted can be written as

$$F_{max} = 1000.\mu_a.M.9.8 = 9800.\mu_a.M \qquad 2.9$$

Where M, μ_a, x are mass of the train, coefficient of adhesion and fraction varying from 0.6 to 0.8 due to adhesive weight of the train respectively.

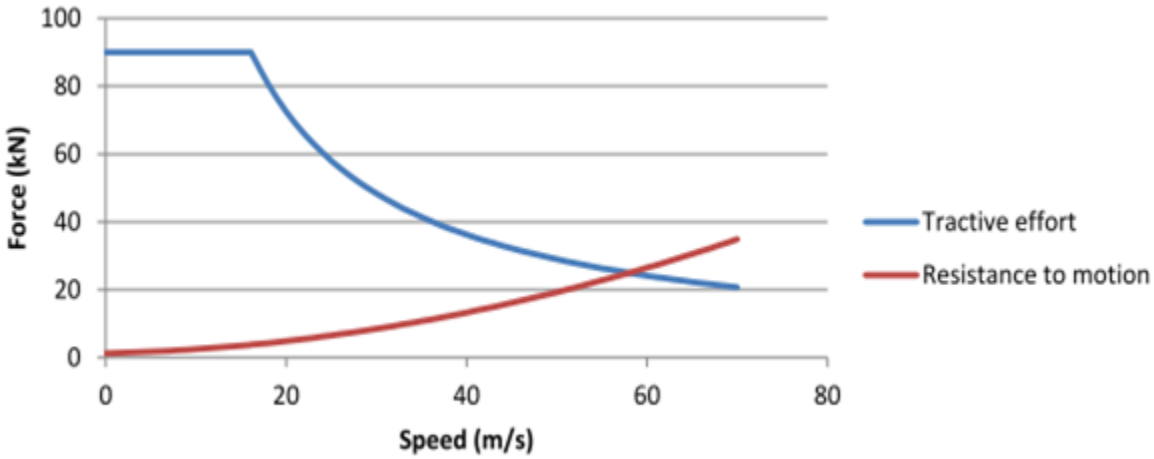

Figure 2.8: Tractive effort vs speed

The tractive effort- vs- speed diagram can also be limited by the adhesion and the comfort. The tractive effort-vs- speed diagram represents the performances of the traction motor(s), until the train reaches up to a certain speed the curve is horizontal (the graph doesn't show the horizontal line) which correspond to the range of speed in which the tractive effort is limited either by the maximum torque, the adhesion or the maximum acceleration allowed for comfort reasons. The next part of the curve corresponds to maximum power of the traction motor(s). The product $P(v) \times v$ remains constant (Power $= P(v) \times v$) and thus the curve has the shape of the function $x \rightarrow \frac{1}{x}$ [29].

The mechanical tractive power of the motors is then computed.

$$P_{motor} = F_{max}.v.(1 + \xi) \quad 2.10$$

Where v is the speed of the train and ξ is the slippage ratio which is equal to 0 for dry rail and 1 for wet rail.

In order to obtain more realistic results some losses and auxiliary power consumptions can be taken into account. Indeed, there are mechanical and electrical losses inside the locomotive between the wheel and the pantograph. These losses can be modeled with the parameter η_{loco} which is the locomotive's efficiency [25].

$$P_D = \frac{P_{motor}}{\eta_{loco}} \quad 2.11$$

Aiming a more realistic model, the auxiliary power consumption, P_{aux}, can be considered as well.

$$P_D = \frac{P_{motor}}{\eta_{loco}} + P_{aux} \quad 2.12$$

Auxiliary equipment's include lighting, air conditioning, etc. In general, their energy consumption rate is considered as a constant [25].

2.6 Load Flow in Railway

Load flow studies are the determination of the voltage, current, power, power factor and reactive power at various points in an AC electrical power system under existing or contemplated Conditions of normal or extreme operation [12]. They provide vital knowledge of system

dynamics of the existing set-up for system operation and maintenance, as well as the effects of interconnection with other power systems, and of new loads, generation stations and transmission line for future planning.

The scale of an electrified railway line is large enough to warrant substantial performance studies [13]. However, there are distinct operational differences between power system and railway traction power system. Because of the multiple sources (i.e. Generators) in power system, the bus-bars are classified as slack, PV and PQ to ease convergence in the conventional load flow methods, such as Newton Raphson and Fast Decoupled and complicated algorithms are required to form the Jacobian matrix. In an AC traction system, there is only a single source in each feeding section (although there are always a number of feeding sections along a railway line). Whilst the loads in power systems are usually assumed to be of constant (or at least not fast-changing) MVA, the traction load is dynamic (dependent on train operation mode) and moving. The conventional methods are thus not as effective for load flow analysis in AC railways [14].

Power supplies for AC traction are obtained from the utility supply system, at transmission or sub-transmission voltage levels, through traction feeder substations. Different feeding systems are available, including direct supply with or without return conductors, booster transformer (BT) and autotransformer (AT) systems. A number of considerations, such as power transmission efficiency and interference suppression, have to be taken on the adoption of appropriate feeding system. The trains are the loads of the circuit and they are obviously not standing still.

The power demand depends upon the train speed that in turn is related to a number of factors categorized by system specifications and operation conditions. The former includes traction equipment characteristics, track layout, signaling and speed restrictions whilst the latter covers the positions of trains, headway, traffic pattern and drivers‟ behavior. As if it were not complicated enough, a train might become a generator should regenerative braking be possible. As a result, the study of traction power supply system becomes the major focus for many researchers recently.

2.7 System Configuration of Modjo ~Hawassa Rail line

2.7.1 General

The proposed TPSS configuration utilizes traction power substations (SS) with main transformers, and switching stations (SWS) and paralleling stations (PS), both with autotransformers, which provide 25kV (nominal) voltage to the catenary with respect to remote ground and also 25kV to along-track negative feeders (NF) with respect to remote ground. Both of these voltages are 180 out-of-phases with each other, and hence, the catenary is at 50kV with respect to the NF.

Autotransformers will be provided periodically along the line, interconnecting catenary, NF and rails. The autotransformer turns ratio will be 2:1 of primary (catenary-to-NF) to secondary (catenary-to-Rails) windings, in order to step down the 50kV distribution voltage between catenary and NF, to 25kV nominal between catenary and rails, suitable for the trains[27-30].

2.7.2 Traction Power Substations

At each traction power substation two separate 3-phase HV circuits will be drawn from the power utility network. These circuits should be originating from different utility substations, at least from different bus systems. These may however, be carried on the same transmission towers. Each SS will have two equally sized HV traction power transformers, each transformer supplied from a separate incoming circuit. Both transformers will be energized under normal TPSS configuration, with one of them supplying power to the feed section north of the SS, the other to the section to the south, with the two feed sections separated by a phase-break (neutral section) at the SS. Both the HV power transformers will be individually capable of supplying the full normal load of the SS [19].

The HV transformers will be single-phase, with their primary windings connected to two phases of the utility HV 3-phase system. The secondary winding of the HV transformer will be either a single winding with a grounded midpoint connected also to the running rails, or comprise two separate counter-phase secondary windings connected in series, with the common point grounded and connected to the running rails. The HV transformers will be outdoor type, mineral

oil insulated, self-cooled, with appropriate rating. Each HV transformer will have a no-load tap changer on the primary side and on-load tap changer on the secondary side [19].

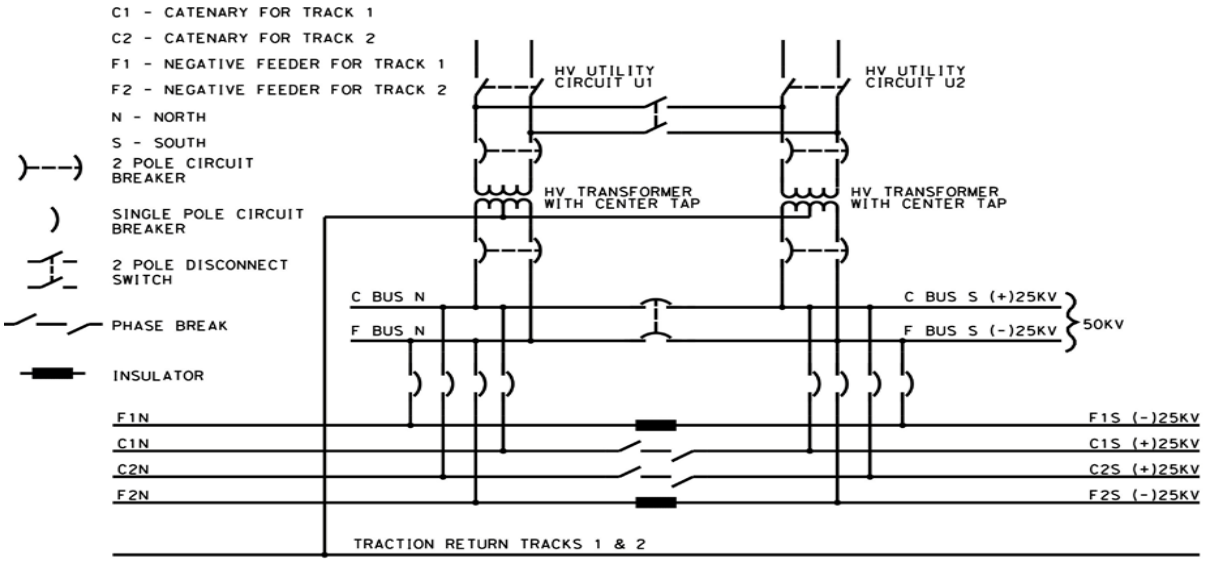

Figure 2.9: 2x25KV substation transformer configurations [19]

The 'positive' bus of the SS (the bus supplying power to the catenary) will be split into two sections interconnected via normally open (N.O.) motorized tie circuit breaker, with each bus section supplied by a different transformer under normal conditions. Each section of the positive bus will feed two different catenary electrical sections in normal TPSS configuration for two main line tracks. The 'negative' bus of the SS (the bus supplying power to the along-track NF) will be sectionalized likewise. Tie-breakers of both the catenary and the NF buses will be interlocked with each other so that they open and close together.

The outer terminals of the secondary winding of each HV transformer will be connected to the positive and negative buses (the bus sections corresponding to the particular transformer) through a two-pole circuit breaker. The positive and negative buses in turn will be connected to the catenary and NF, respectively, through single-pole circuit breakers and in-series connected no-load motorized disconnect switches.

2.7.3 Switching Stations

The switching stations are a facility interfacing the feeding sections of adjacent SS. This is an installation at which electrical energy can be supplied to an adjacent, but normally separated electrical section during contingency power supply conditions (An electrical section may be defined as the entire section of the OCS which, during normal system operation, is powered from a circuit breaker of the traction substation).

Because the ac voltages on either side of any SWS will be of different phases (or even if of the same phase sequence, the angular displacement may be different) the SWS will include a phase break. In normal operations the phase break will be open, isolating the two feed sections. Autotransformers (AT) will be connected on either side of the phase break, one AT per side, serving as the last AT of the respective feed section [34].

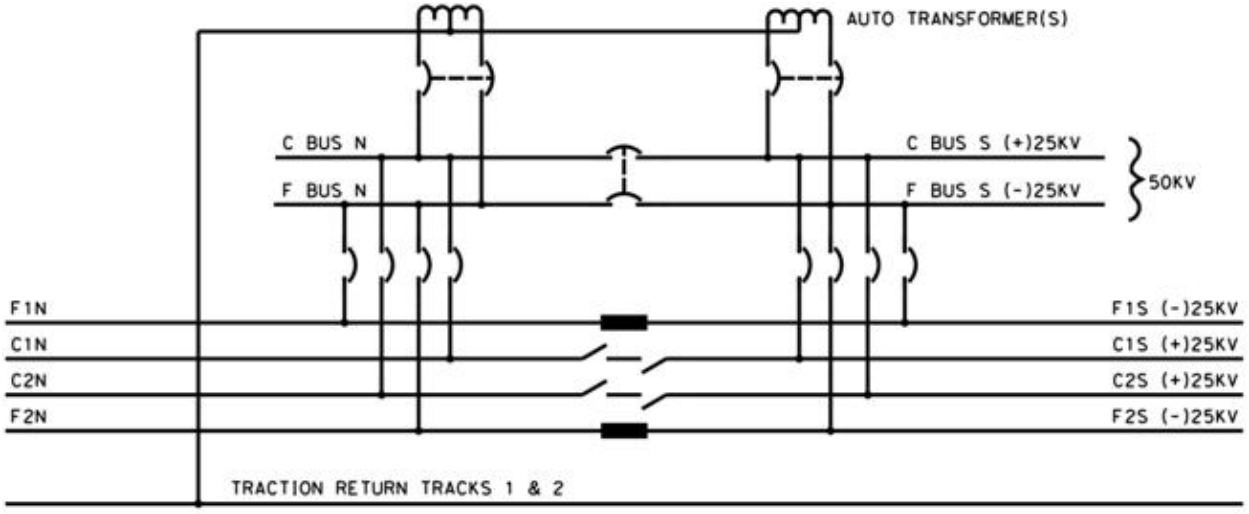

Figure 2.10: 2x25KV autotransformer switching station [19]

The catenary and NF buses will be connected in turn to the primary winding terminals of the AT via a two-pole circuit breaker. The AT winding center tap will be connected to a neutral bus, which will be locally grounded and connected also to the running rails of both tracks and to the static wires.

The SWS equipment will include switchgear (25kV circuit breakers) and motorized disconnect and bypass switches in a configuration that allows isolation of an AT in case of problems, and as

required for maintenance. The SWS design will provide for electrical continuity across the phase break in contingency operations, in the event the SS on one side is out-of-service. In such eventuality, the SS on the other side of the SWS will be used to provide power to the sections normally served by the out-of-service SS. This will be achieved by interconnecting the catenary and NF on both sides of the SWS, by closing N.O. circuit breakers. Furthermore, N.O. trackside, motorized, load-break disconnect switches will be installed at the SWS phase break, to provide for electrical continuity in emergency conditions between the OCS and NF, respectively, on either side of the phase break [36].

2.7.4 Paralleling Stations

The paralleling stations are a facility featuring an AT and associated switchgear and disconnect switches. The PS helps boost the OCS voltage and reduce the running rail return current by means of the autotransformer feed configuration. The AT installed along the line in the PS steps down the 50kV nominal voltage between catenary and NF to the 25kV level between catenary and running rails. Similar to the SS, the number and locations of the PS have been determined based on the results of a traction power study, and by taking into account mainly environmental considerations.

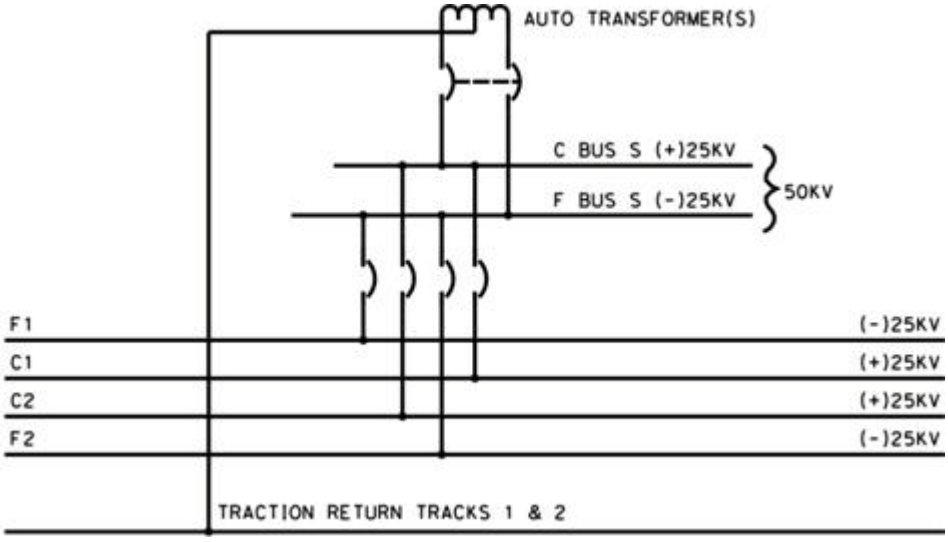

Figure 2.11: 2x25KV autotransformer paralleling station [19]

One AT of 10 MVA rating serving all tracks will be installed at each PS, along with a line-up of medium voltage switchgear containing separate buses for connections to the catenary and NF circuits. The switchgear will include single-pole 25kV catenary circuit breakers and NF circuit

breakers, and double-pole 50kV AT circuit breaker. The catenary and NF conductors will be connected to the switchgear buses via no-load type motorized disconnect switches and the switchgear. The catenary and NF buses will be connected in turn to the primary winding terminals of the AT via a two-pole circuit breaker. The AT winding center tap will be connected to a neutral bus, which will be locally grounded and connected also to the running rails of both tracks and to the static wires [19].

2.7.5 System Voltage

The system voltages for the proposed line conformed to *European standards EN 50163: 2004, "Railway Applications – Supply Voltage of Traction Systems" and EN 50388: 2005, "Railway Applications – Power Supply and Rolling Stock – Technical Criteria for the Coordination between Power Supply (Substation) and the Rolling Stock to Achieve Interoperability".*

The system voltage (U) will be the potential at the train's current collector or elsewhere on the catenary, measured between the catenary and the rail return circuit. It will be the rms value of the fundamental ac voltage and its values will be as following.

1. The nominal voltage (U_n), that is, the designated value for the system voltage, will be 25kV.
2. The highest permanent voltage (U_{max1}), that is, the maximum value of the voltage likely to be present indefinitely, will be 27.5kV.
3. The highest non-permanent voltage (U_{max2}) that is, the maximum value voltage likely to be present for a limited period of time (as defined below), will be 29.0kV.
4. The lowest permanent voltage (U_{min1}), that is, the minimum value of voltage likely to be present for a long period, will be 19.0kV.
5. The lowest non-permanent voltage (U_{min2}) that is, the minimum value of voltage likely to be present for a limited period of time (as defined below), will be 17.5kV.

2.7.6 Voltage Related Requirements

1. The duration of voltages between U_{min1} and U_{min2} will not exceed 2 minutes.
2. The duration of voltages between U_{max1} and U_{max2} will not exceed 5 minutes. (If voltage between U_{max1} and U_{max2} is reached, it will be followed by a level below or equal to U_{max1} for an unspecified period). Voltages between U_{max1} and U_{max2} will only be reached for non-permanent conditions such as regenerative braking.
3. The voltage at the busbar of the substation at no-load conditions will be less than or equal to U_{max1}V
4. Under normal operating conditions (including single contingency situation), voltages will lie within the range $U_{min1} \leq U \leq U_{max2}$.
5. Under double contingency conditions, the voltage in the range $U_{min1} \leq U \leq U_{min2}$ will not cause any damage or failure, and will permit continuing vehicle operation with some degradation. Rated vehicle power and performance will not be available but reduced operation will be possible assuming on-board logic will automatically degrade the performance of the traction system (rolling stock) and auxiliaries [33].

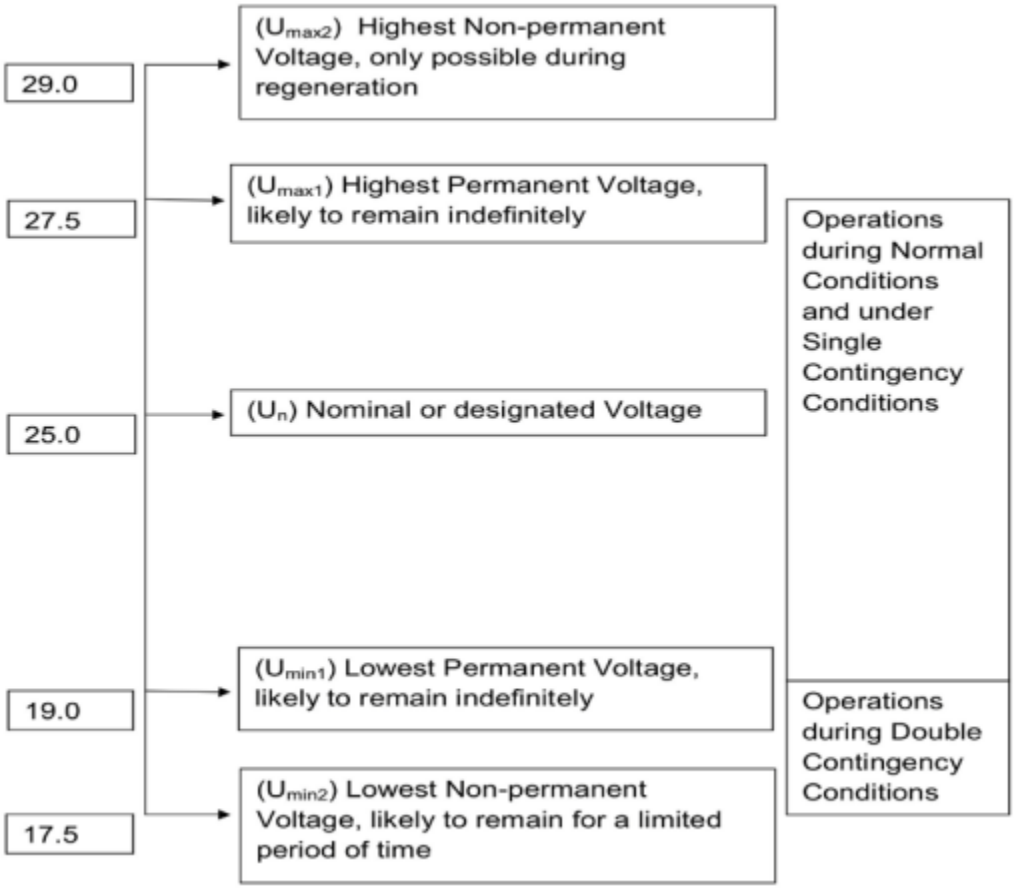

Figure 2.12: System voltage in kilovolt [33]

2.7.7 Model of the Locomotives and Trains

Before modeling the power system structure of the railway, the train model needs to be introduced. The type of locomotives chosen in this thesis is MTAB (MalmTrafik i Kiruna AB) locomotive which is a common Swedish freight train. Its maximum speed is 100 km/h and designed for freight transport and can consume up to 15 MW [25]. This train has chosen not because of it has a special properties but the availability of train data which are validated through full scale test. For the design purpose 60 trailing trains which has two axle loads at each car is considered. The locomotive has six axle loads each weighing 25 ton. The length of a single locomotive and trailing train is 15.5 m and 14.27 m respectively and the total train weight is 5000T.

2.8 Designing Techniques of Traction Power Supply System (TPSS)

The **TPSS** is a subsystem of the overall railway system and cannot be designed in vacuum. Therefore, to specify the requirements of the TPSS, the starting point is the physical layout of the route, the location of the passenger stations, the topography of the track route including the curves to be encountered and their physical characteristics. This information together with the required acceleration and speed of the train as a function of position along the track can be used, (using Newtonian mechanic), to determine the tractive effort requirement of the train as a function of position.

Depending on the type of motor used, the motor drive, and efficiency, the electric power demand by the train as a function of position can be calculated using the tractive effort and speed (power = tractive effort x speed). Next, different operation scenarios are assumed starting with the number of trains per hour to run**,** in what station a train should stop, what are the speed limits at various lengths of the route, the required acceleration and deceleration, etc. All this is to determine where the trains are on the tracks at any instant of time.

Having those snapshots, the engineer determines the power requirements at the different points on the tracks (where the trains are). This information provides the interface between the overall system and the TPSS (the power system providing electric energy to the trains).The specifications of the power supply system constitute a subset of the overall specifications, for example, voltage specifications are specified by international standards such as BS EN 50163 and IEC 60850. These take into account the number of trains drawing current and their distance from the substation [37] [52].

Designing TPSS is done in several stages. In the first stage the following information is generated:

I. **Locations and speeds of trains**: This is based on design specification (speed, headway...), topography, and type of trains.
II. **Power requirements**: The power requirement of each train on each track and the location of each train are calculated using the speed and the traction effort. This

calculation is usually done using software that takes the slope of the track, the acceleration of the train, etc., into consideration when using Newton's laws of motion but due to lack of resources the author performed the calculation by hand.

III. **Certain power system configuration and wire sizes are selected**. The wires are: The messenger, the catenary, the static, and the feeder wires; one for each track. In some literature, the messenger wire and the catenary wire are called the catenary system or the Overhead Catenary System (OCS). The rails are used as return conductors also. The configuration of the system specifies the coordinates of each conductor (horizontal and vertical distances, usually from the center of the track) and also what type of conductors are to be used.

The second stage receives the train locations, the power requirements of each train and the system data. The output of this stage is the catenary voltage at the location of every train, the currents in the different conductors, and the rail voltage. This last item is important for public safety consideration and usually the acceptable limits are specified by regulation.

Having the output of the second stage, the designer verifies that no line is overloaded, the rail voltage is within specifications, and the train's powers requirements are met. If any of these requirements is found to be violated, the design is modified and the calculations in the second stage repeated. Almost both stages are the subject of this thesis.

2.9 Literature survey

In this part, we would like to analyze some of the interesting works done in area of traction power modeling and simulation. Though papers on traction power system models are available, they lack detailed presentation and discussion. It is not only scarceness of publications that makes the search challenging, but the terminologies used in the field is not uniform. Terms like electrified railways, mass transit, ground transport, traction systems, trolley systems, railway power supply, railroad electrification, train power supply, traction power supply and many others exist in parallel.

In America [19], the first Phase of California High-Speed Train Project implemented between San Francisco and Anaheim is a 520 route-miles long state-of-the-art rail system providing

intercity travel with modern high-speed trains running at speeds up to 220 miles per hour. The traction power supply system (TPSS) for this project is a 2x25kV ac autotransformer feed system, and is designed to provide traction power for safe, efficient, and reliable operation of trains per the operations plan. The TPSS design is based on the European Union's Technical Specifications for Interoperability (TSI) relating to the 'Energy' and other related subsystems, and conforms to North American standards (AREMA, IEEE) and relevant International and European standards (EN, IEC).

The TPSS has in general, traction power substations (SS) spaced approximately 30 miles apart, located close to HV utility transmission network/grid substations, switching stations (SWS) located midway between adjacent SS, and paralleling stations (PS) located at approximately 5-mile spacing between SS and SWS. The capacity of the main transformers and autotransformers has been arrived at based on the train operations plans, rolling stock parameters, track alignment, and spacing of these facilities. The TPS configuration has been verified by running traction power supply load flow analyses over representative sections of the project.

The paper describes the main features of the traction power system design for California High-Speed Train Project including system configuration, reliability, system protection, interface options with HV power supply utility networks, and other related aspects.

In [20], modeling and simulation of AC traction power supply system using MATLAB/Simulink software package for the case of Sebeta~Adama~Mieso railway line in Ethiopia were treated. In this study three models of traction power supply system are used to illustrate modeling, however direct power with return wire mode is selected. Modeling of traction substation for different transformer is implemented based on direct power with return wire mode (TR). The Author conducts simulation of traction network impedance, traction network voltage loss, maximum traction network voltage loss and it is observed that in single track traction network voltage loss is greater than double track traction network voltage loss. In addition Matlab calculation is carried out to determine catenary-rail voltage and rail potential. In this work, however, no attention is paid to the tractive force of locomotives and the power consumption of the train. It didn't show how the traction substation capacity is determined.

In [51], with its probabilistic load flow approach. Instead of making tedious simulations, one proper simulation is done – once and for all. In that particular simulation model, it is assumed that the tractive force curves of the trains are independent of catenary voltage. The train positions are used as primary parameter in the probabilistic load flows, a position is assumed to determine the consumed, or possibly regenerated, electric power. A probability density function (PDF) for the location of trains on a railway section is derived out of the simulation results.

The probability of each train location is modeled as inversely proportional to the train speed in that particular location. This leads roughly to a bathtub curve since the trains drive slower when accelerating and braking. Once the PDF is known, train positions and power flows can be realized. Trains that normally depart with a certain periodicity can be placed out after and in front of the randomly placed train at a fixed or, if so desired, a randomly disturbed distance. For lots of cases studied, PDFs describing the voltages and power flows at the feeding points can be calculated. The probabilistic load flow models are verified with simulations. This type of study does, however interesting, not seem to be suitable for studies of the voltage dependency of the running times.

In [24] Load flow of power distribution system of Tabriz (Iran) urban railway is analyzed. Dynamic load flow behavior of a bi-phase (AT power supply system) electrified train sets and fault analysis is considered in selecting the appropriate ratings of the electrical equipment in the railway electrification system through the study. The simulation and analysis of the power distribution system is done with Power World simulator software.

In [21], one can find a detailed study for the design of AT catenary systems on the basis of cost effectiveness. The tradeoff is between how dense the AT transformers should be distributed along the catenary and the impedance of the actual conducting wire.

In [22] U. J. Shenoy, Senior Member of IEEE presents the modeling and simulation of a 25 kV 50 Hz AC traction system using Power System Block set (PSB) / SIMULINK software package. The three-phase system with substations with rectifier-fed DC locomotives and traction load are included in the model. The model has been used to study the effect of loading and fault conditions in 25 kV AC traction.

Authors called L. Abrahamsson, T. Kjellqvist, and S.Ostlund [23] present high voltage direct current (HVDC) Feeder Solution for Electric Railways, and the authors argue railway power supply systems in many sparsely populated countries are relatively weak. Weak railway power supply system cause problems with power quality, voltage drops, and high transmission losses. For AC railway power supply systems with a different frequency than the public grid, high-voltage AC (HVAC) transmission lines are common, connected to the catenary by transformers. In this paper an alternative design based on an HVDC feeder is suggested. The HVDC feeder is connected to the catenary by converters. Such an HVDC line would also be appropriate for DC-fed railways and AC-fed railways working at public frequency. The converter stations between the public grid and the HVDC feeder can be sparsely distributed, in the range of 100 km or more, whereas the converters connecting the HVDC feeder to the catenary are distributed with a much closer spacing. Their ratings can be lower than substation transformers or electro-mechanical converters, since the power flow can be fully controlled. Despite a relatively low power rating, the proposed converters can be highly efficient due to the use of medium frequency technology. The HVDC-based feeding system results in lower material usage, lower losses and higher controllability compared to present solutions. But Simulations of the proposed solution does not show clear advantage regarding transmission losses and voltages compared to conventional systems, especially for cases with long distances between feeding points to the catenary, and when there are small amounts of regeneration (energy) from the trains.

In [25], the Madrid-servile line which is commenced operation in 1992 is 470 km long described;-450 km between the two system separating sections were electrified with single phase AC 25 KV 50 Hz and can be travelled at 300km/h. The traction power supply of the line provided by twelve AC 25 KV 50 Hz substations which are fed by AC 220 KV and 132 KV three phase installations from the Spanish public grids. The primary connection of the AC 25 KV 50 Hz substations to the three phase network was made to take advantage of the highest possible symmetry of the load on the AC circuits. As shown in figure 2.13 for substations with cyclic connection, three voltages result at secondary side of the substations SS1, SS2 and SS3 which are electrically offset by 120 degree respectively. If the pointer bases are earthed instead of the pointers peaks results for SS1', SS2' and SS3'. If SS1 and SS2 were adjacent substations a voltage difference of $\Delta U_{2-1} = 25 \times \sqrt{3}$ KV≈43.3KV would be applied to the phase separation

section. Because this voltage can reach the substation through damaged switches or on an unintentional phase short circuit, the medium voltage installations in other 25 kV 50 Hz lines had to be rated for increased insulation value. Due to limited procurement facilities for switching equipment, they were usually designed as open air switching equipment for 72.5 KV.

For the Madrid-Seville line, the two 120 degree switching variants were combined. This resulted in 60 degree switching and the connection of the substation as shown below. This allows design of the 25 KV part of the substation in accordance with a 36 KV voltage level. In contrast, 120 degree connections would require to the 52 KV voltage level because the voltage existing at the phase separation sections during a phase short-circuit of around 43.3KV would be applied in the substations. All substations of the Madrid-Seville line have uniform design. The main transformers have a nominal power rating of 20 MVA each and are designed for a load of 150 % for 15 minutes and 200 % for six minutes following operation at nominal power.

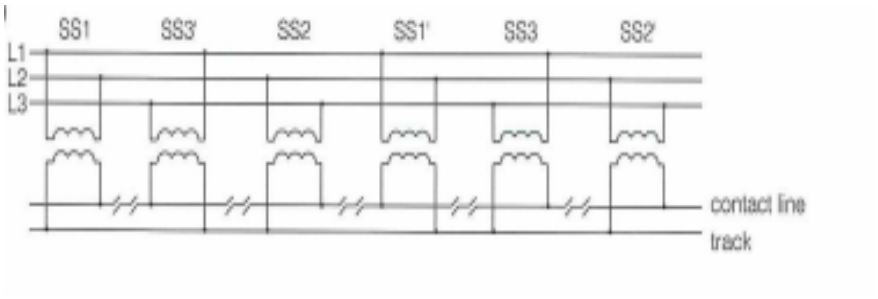

Figure 2.13: Connection Substation by 60 degree offset [25]

In [26], the paper describes an integrated calculation methodology which, by simulating railway traffic, allows analysis of the performance of 2x25KV 50Hz electric traction systems. This methodology performs a multi-conductor electrical analysis of the traction circuit utilizing ATP-EMTP software (alternative transient program-electromagnetic transient program) and therefore additionally allows calculation of electromagnetic transients and all possible failure regimes. The analyses presented refer to the application of the methodology in question to the study of a high speed railway line section in steady state operation with particular emphasis on electrical and energetic effects of train regenerative braking. Comparison of simulation results under various normal and extreme operational conditions are given to verify the methodology.

In [55], parts of the mechanical modeling of the SimERT (Simulation of energy and running time of trains) PhD thesis are used whereas the electrical modeling is considered to be too imprecise. For example, voltage is assumed to decrease linearly with power usage. In reality, the line voltage depends on the distance between the train and the traction substation or possible transformer stations connecting the catenary line electrically to the high voltage transmission line.

In [32] a partly new simple methodology for determining running resistance called by energy coasting method is developed and demonstrated. An error analysis for this method is performed. Running resistance of high speed train SJ X2000, conventional loco hauled passenger trains and MTAB freight train is systematically parameterized. Influence of speed, number of axles, axle load, track type, train length and train configuration is studied. A model taking into account the ground boundary layer for determining the influence of measured head and tail wind is developed.

Different factors and parameters of a train that are vital for the accuracy is computed, energy consumption and running time is identified, analyzed and finally synthesized into a train model. Empirical models of braking and the traction system, including the energy efficiency, are developed for the electrical locomotive type SJRC4 without energy regeneration.

In [50] the issue of transformer station breakdowns has been discussed. According to the paper most common outage is down-torn catenaries, this is however not a problem that can be invested away. Tearing down of catenaries can occur when trains drive too fast and when the pantographs are somehow damaged. Thus, the reliability issue is of smaller interest regarding traction power supply system. In this thesis, the reliability of feeding stations is not considered.

In [7], issues like running resistance of trains, the modeling of traction loads, and descriptions of traction drives using DC machines can be found.

In [56], aspects of single-phase AC traction power transmission systems, including the main differences between AT and BT catenary systems treated.
In [8], electromagnetic compatibility and interference are treated.

3 DESIGN OF TRACTION POWER SUPPLY SYSTEM

In this chapter design of the most common traction power supply elements performed. These models will be used in the next chapter during modeling of different components in MATLAB/Simulink.

3.1 Introduction

All designs in the engineering sciences starts with the formulation of appropriate models. A model, in power system analysis almost invariably mean a mathematical model, and is a set of equations or relations, which appropriately describes the interactions between different quantities and with the desired accuracy of a physical or engineered component or system. Hence, depending on the purpose of the analysis different models of the same physical system or components might be valid. In this section the traction power supply system components will be independently designed.

3.2 Power Consumption of the Load

Again designs in enginering science starts with the load, in the previous chapter we have seen the type of the locomotive or load which is used in this study, in this section based on the available data of the locomotive the power consumption of the load will be computed.

Train, as a load, is on the move and railway traction is considered to be one of the main problems of longitudinal rail dynamics. It is seen as a one-dimensional problem located in the longitudinal direction of the track, governed by the Fundamental Law of Dynamics or Newton's Second Law, applied in the longitudinal direction of the train's forward motion:

$$\overrightarrow{\sum_{\iota=1}^{n} F\iota} = \mathrm{M}^{*}\mathrm{a} \qquad 3.1$$

Where the term to the left of the equal sign is the sum of all the forces acting in the longitudinal direction of the train, "M^{*}" is the total mass and "a" is the longitudinal acceleration experienced by the train.

The sum of forces consists of the tractive or braking effort " F_t" and the passive resistances opposing the forward motion of the train, "F_{ex}". The tractive or braking effort " F_t", in a final instance, is the resultant of the longitudinal adhesion forces that appear in the wheel-rail contact zones, either when the train's motors make the wheels rotate in the direction of forward motion, or when the braking forces act to stop the wheels rotating (in this case, these forces will obviously be negative or counter to the direction of the train's forward motion).

$$F_t - F_{ex} = M^* a \qquad 3.2$$

The maximum design weight of the trains including its load (freight) is **5000T** and when a train accelerates along a track the total mass (tare mass + passenger or freight mass) is accelerated linearly but the rotating parts are also accelerated in a rotational sense. It is usual to express this rotational inertia effect as an increase in the effective linear mass of the train called the 'rotary allowance' and expressed as a fraction of the tare weight of the train.

The value of the rotary allowance varies from 5% to 15% depending on the number of motored axles, the gear ratio and the type of car construction. For this case 10% is taken.

Therefore the total mass of the train increases by 10 percent. In other word the total mass of the train increases by 500T.

Then the dynamic mass M^* becomes:

$$M^* = 5{,}500T$$

Various literature [32][19][25] shows different countries use different starting acceleration that ranges from $0.08\ m/s^2$ to $0.25\ m/s^2$ for freight trains and for passenger train the maximal acceleration is not determined with respect to adhesion but to comfort. Nowadays traction control system can achieve accelerations higher than $1.5\ m/s^2$ but for comfort purposes the acceleration is usually limited to approximately $1.1 m/s^2$.

The train must be able to accelerate after it has been brought into motion. The desired amount of acceleration, however, is dependent on the performance requirements of the train and on the desired capacity of the line; a slow acceleration of the freight train may block the line for a long

time, thus reducing the line capacity. Considering the above case **0.15 $\mathbf{m/s^2}$** acceleration is taken which is very sufficient to solve problems related with the line capacity of the track.

Then the sum of the tractive and the resistive force becomes:

$$F_t - F_{ex} = 5{,}500{,}000 \text{ Kg x } 0.15 \text{ m/s}^2$$

$$F_t - F_{ex} = 825000 \text{ N}$$

$$F_t - F_{ex} = 825 \text{ KN}$$

Where N is newton and K is kilo

The total forces acting on a train against its direction of travel F_{ex} are can be divided in to three main categories:

- Mechanical and aerodynamics resistance, F_r.
- Gradient resistance, F_{gr}.
- Curves resistance, F_c .

Then these forces can be expressed mathematically as:

$$F_{ex} = F_r + F_{gr} + F_c \qquad 3.3$$

The force created due to mechanical and aerodynamic resistance, F_r is given by:

$$F_r = A + Bv + cv^2 \qquad 3.4$$

Where A related to axle load, Bv depends on quality of the track and stability of the trains. Generally $A + Bv$ is rolling resistance and cv^2 is aerodynamic resistance.

The value of A can be approximately computed as:

$$A \approx 2450 + 175N_{axle}(\text{N}) \qquad 3.5$$

N_{axle} is number of trailing car axle and there are 60 wagons which have two axle load at each wagon.

Then

$$A \approx 2450 + 175 \times 120\ (\text{N}) = 23450 \text{ N}$$

$$A = 23.450 \text{ KN}$$

Although there are statistical uncertainties in the determined B-coefficients, in [32] indicated that the main parts of this coefficient is not due to mechanical resistance but rather originates from portion of air drag not covered by cv^2,therefore coefficient B may be expressed as a function of total train length rather than train mass.

Then the design equation for the value of B is [32]:

$$B \approx -22 + 0.58L_T(N\,s/m) \qquad 3.6$$

Where L_T is the total length of the train.

The length of locomotive and the trailing car is 15.5 m and 14.27 m respectively and the total length of the train can be found as [32]:

$$L_T = 14.27m \times 60 + 3.(15.5) = 902.7m$$

Then the value of B becomes:

$$B \approx -22 + 0.58 \times 902.7m\ (N\,s/m) = 510.556\ (N\,s/m)$$

$$B = 510.556\ (N\,s/m)$$

Aerodynamics drag, the part which dependent upon the speed squared is usually written for no wind condition as [32]:

$$F_D = \frac{1}{2}\rho A_f C_D v^2 = Cv^2 \qquad 3.7$$

Where A_f is the projected cross sectional area and it is convenient to express C as air drag area A_fC_D.

$$A_fC_D = 2\frac{C}{\rho}$$

For the proposed freight train A_fC_D can be expressed approximately as:

$$A_fC_D \approx 8.3 + 0.149L_T\ (m^2)$$

$$A_fC_D \approx 8.3 + 136.8(m^2)$$

$$A_fC_D = 145.1(m^2)$$

$$C = \frac{1}{2}\rho A_fC_D$$

Where ρ is the air density which equal to 1.3 kg/m^3

Then

$$C = \frac{1}{2} \times 1.3 \times 145.1\ \mathrm{N\,s^2/m^2} = 94.25\ \mathrm{N\,s^2/m^2}$$

According to European standards the maximum speed for freight train ranges from 80 km/hr to 120 km/hr [32]. For this thesis a maximum speed of 90 km per hour is taken.

$$A = 23.450\ \mathrm{KN}$$

$$Bv = 510.556 \times 25\ \ \mathrm{N} = 12.763\ \mathrm{KN}\ \text{ and}$$

$$Cv^2 = 94.25 \times 25^2\ \mathrm{N} = 58.906\ \mathrm{KN}$$

Then mechanical and aerodynamic resistance of the proposed train becomes:

$$F_r = 23.450\ \mathrm{KN} + 12.763\ \mathrm{KN}\ \ + 58.906\ \mathrm{KN} = 95.119\ \mathrm{KN}$$

Gradient resistance is also the component of the train load against the direction of travel. It is positive for uphill gradients and negative for downhill gradients (i.e. pushes the train forward). Thus the gradient resistance is determined by:

$$F_{gr} = i10^{-3}mg \qquad 3.8$$

For freight and passenger lines, the location where the maximum gradient needs to be used in design. Therefore, for the profile design of railway, we need to lower the maximum gradient to ensure the freight train passes through this section at no less than calculated or stipulated speed. In this thesis because of lack of resources and equipment's which used to measure the gradient profile of the line under study, the ruling gradient of the locomotive **6‰** is taken.

$$F_{gr} = 6 \times 10^{-3} \times 5000{,}000\mathrm{kg} \times 9.8\ \mathrm{m/s^2}$$

The gradient resistance of Modjo~Hawassa rail line corridor becomes:

$$F_{gr} = 294\ \mathrm{KN}$$

Additional curving resistance F_c mainly corresponds to the increased energy dissipation that occurs in the wheel rail interface, due to sliding motions (creep) and friction phenomena, at curve negotiation. It is dependent on wheel rail friction and the stiffness and character of the

wheel set guidance. The resistive force produced by the curve is modeled by the following equation [32]:

$$F_c = \frac{k_e}{r} 10^{-3} mg \quad 3.9$$

Where ke (m) is the track gauge coefficient, which is equal to **750** for standard track as shown in table 2.1 and r is the radius of the curve, which is 1600 m.

Then the value of the curve resistance F_c becomes as follows:

$$F_c = \frac{750}{1600} \times 10^{-3} \times 5000{,}000\ \text{Kg} \times 9.8\ \text{m/s}^2 = 22.96\ \text{KN}$$

The total resistive force of the train F_{ex} becomes:

$$F_{ex} = 95.119\ \text{KN} + 294\ \text{KN} + 22.96\ \text{KN} = 412.079\ \text{KN}$$

The locomotive of the freight train must be able to produce a sufficient tractive force in order to bring the train into motion and to maintain a certain speed or acceleration. The tractive force has firstly to balance the total running resistance, including gradient resistance, secondly to accelerate the train. The tractive force F_t to overcome the resistance at the starting moment and thus bring the train into motion becomes:

$$F_t = 825\ \text{KN} + F_{ex}$$
$$F_t = 825\ \text{KN} + 412.079\ \text{KN} = 1237.079\ \text{KN}$$

This means we need a tractive force of 1237.079 KN to move 5000T full loaded train with an acceleration of 0.15 m/s^2 until it reaches a maximum speed of 90 km per hour, keeping in mind that when the train speed increases the tractive forces required to move the train forward decreases while the aerodynamic resistance of the train increases.

As explained in chapter two, the tractive effort can be increased by increasing the motor torque but only up to a certain point. Beyond this point any increase in the motor torque does not increase the tractive effort but merely cause the driving wheels to slip. Which mean the force

developed by the traction motor is transmitted by the wheel-rail contact. The transmitted force is limited by adhesion and the maximum force that can be transmitted can be written as:

$$F_{t-max} = \mu_a . Mg \quad 3.10$$

This can be re-written as:

$$F_{t-max} = 1000 \text{ x } \mu_a \text{x M x } 9.8 = 9800.\mu_a . M \quad 3.11$$

Where M, μ_a are mass of the train in ton and coefficient of adhesion respectively.

The adhesion coefficient μ_a can be found based on Curtius and Kniffler derived adhesion curve which is shown in figure 2.7 and the adhesion coefficient equation as shown below [34].

$$\mu_a = 0.161 + \frac{7.5}{3.6v+44} \quad 3.12$$

Then the adhesion coefficient at the design speed, 90 km per hour can be computed as:

$$\mu_a = 0.161 + \frac{7.5}{3.6(90)+44} = 0.161 + 0.0226 = 0.183$$

But at low speed the tractive effort is very high, see figure 2.8,corresponding to adhession utilisation of more than 0.3. therefore, during starting or at low speeds, the tractive force is frequently limmited by adhesion. Then we can assume an adhesion of 0.3 for the design purpose,which is a common level.

We know that the proposed train has six axle load each weighing 25 ton. Then the total mass of the locomotive will be 150 ton. Based on this values, the maximum tractive effort of the locomotive be:

$$F_{t-max} = 9800.\mu_a \text{ M} = 9800 \times 0.3 \times 150 \text{ N}$$

$$F_{t-max} = 441\text{KN}$$

This means we can get a maximum of 441 KN tractive force from a single locomotive, beyound this the driving wheel slips. Which means only some part of the freight is hauled. Inorder to find the number of locomotives required to hual the full load train, we use the following simple mathematical equation:

$$\text{Number of train} = \frac{\text{Tractive effort required to move full load}}{\text{Maximum tractive effort of locomotive}}$$

$$\text{Number of train} = \frac{1237.079\ \text{KN}}{441\text{KN}} = 2.805$$

Since fraction is meanigles, it means that 3 locomotives are needed for starting or braking a full loaded train.

The maximal tractive force of a MTAB locomotive is a function of the catenary voltage, U, the velocity of the train, v, and the current which flows through the motor, I_{TR}. This force multiplied by the train velocity gives the maximum power that a locomotive consumed. The mechanical tractive power of the motor is computed by [25]:

$$P_{motor} = F_{t-max}.v.(1+\xi) \qquad 3.13$$

Where v is the speed of the train, which is 90 km per hour or 25 m/s , F_{t-max} is the maximum tractive force of the locomotive (441KN) and ξ is slippage ratio, which is zero for dry rail. Then the power of the motor becomes:

$$P_{motor} = F_{t-max}.v. = 441\ \text{kN} \times 25\ \text{m/s}$$
$$P_{motor} = 10.9798\text{MW}$$

In order to obtain more realistic results some losses and auxiliary power consumptions must be taken into account. Indeed, there are mechanical and electrical losses inside the locomotive between the wheel and the pantograph. These losses will be modeled with the parameter η_{loco} which is the locomotive's efficiency. It is always less than one. In reality the efficiency depends of the train's velocity [32] [44]. Nevertheless an average value equal to 0.8 will be considered in this thesis work. This efficiency includes neither air condition nor auxiliary power consumption.

$$P_D = \frac{P_{motor}}{\eta_{loco}} \quad 3.14$$

Aiming a more realistic model, the auxiliary power consumption,P_{aux}, will be considered as well. Auxiliary power includes the cooling systems, train heating and the power available for travelers (for the case of passenger train). A power factor of this auxiliary power is also taken into account, PF_{aux}. Auxiliary equipment's include lighting, air conditioning, etc. In general, their energy consumption rate is considered as a constant. Which is assumed 42kW [45]. The electrical active power demand will be:

$$P_D = \frac{P_{motor}}{\eta_{loco}} + P_{aux} \quad 3.15$$

$$S_{TR} = \frac{P_{motor}}{\eta_{loco}} + P_{aux} = \frac{10.978MW}{0.8} + \frac{42KW}{0.8}$$

$$S_{TR} = 13.724\ MVA + 52\ KVA$$

$$S_{TR} = 13.772\ MVA$$

Based on the above result maximum power consumption of a single train is found to be $13.772\ MVA$, which means the electrical system of the line including the catenary system must be sufficient for the required power to be transmitted from the traction substation to the train without excessive voltage drop and energy losses.

3.3 Train or Locomotive Model

One of the major traction power supply system component is the electric train. It requires a simple model to reduce problem complexity. In this research **constant power model** is used because powers and power factor are the two quantities that can be measured by the on-board traction controller. This model is widely used in railway load flow. Figure 3.1 (a) shows the power model.

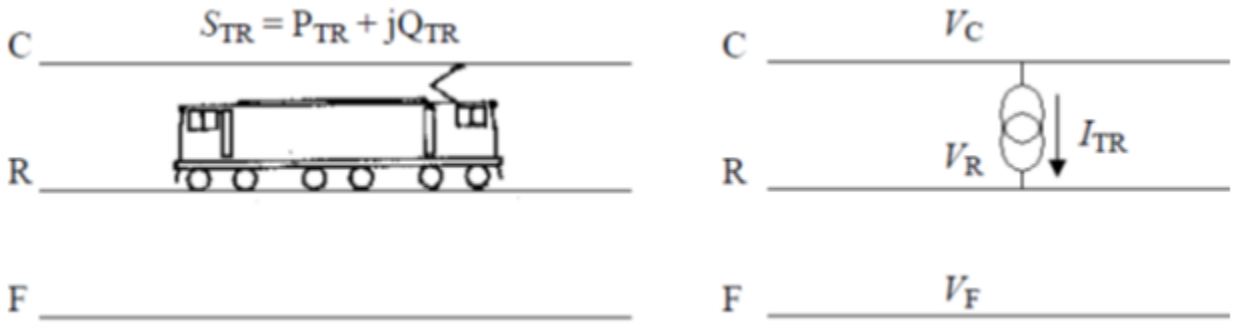

a) Train drawing power from the catenary b) current model

Figure 3.1: Train and its equivalent circuit [3]

$$\text{Train current} = I_{TR} = \left(\frac{S_{TR}}{V_C - V_R}\right)^* \quad 3.16$$

$$\text{Contact line current} = I_C = I_{TR} \quad 3.17$$

$$\text{Rail line current} = I_R = -I_{TR} \quad 3.18$$

$$\text{Negative feeder current } I_F = 0 \quad 3.19$$

$$\begin{bmatrix} I_C \\ I_R \\ I_F \end{bmatrix} = I_{TR} \begin{bmatrix} 1 \\ -1 \\ 0 \end{bmatrix} \quad 3.20$$

Where S_{TR} , V_R, V_C are power demand of the train, rail voltage and the contact line voltage respectively.

The nominal contact line to ground voltage is 25 kV and the rail voltage is zero, based on the above results the nominal train current can be calculated as:

$$I_{TR} = \left(\frac{S_{TR}}{V_C - V_R}\right)^* = \frac{13.772\ \text{MVA}}{25\ \text{kV}} = \mathbf{550.88\ A}$$

The designed system must provide a current of **550.88 A** at the pantograph for the efficient performance of the train, if the train current decreases from the calculated result, lower power will be available to the train and as a result the train acceleration may be reduced and sometimes the top speed of the train can be attain may be also reduced. In addition to this the change in vehicle propulsion current demand results in a corresponding change of the traction

power system loading. Due to this for the better performance of the train the catenary system and the capacity of the traction power substation transformer must be modeled, designed and represented accurately.

3.4 Substation Power Transformer Capacity

Traction power substations experience highly fluctuating loading due to the abrupt, impulse like changes in the power requirements of the trains as they accelerate, decelerate, or as they encounter or leave track grades. The magnitude and the frequency of the impulses increase during peak power demand time periods, since longer trains are likely to operate at shorter headways. The peak power demand time occurs twice a day, during morning peak period and evening period. For the traction power substation to supply this load cycles, the substation equipment must have sufficient continuous and overload power rating as recommended by the AREMA guidelines 22.

The capacity of traction transformer depends on the load current of feeding section or the maximum effective feeder current which is mainly determined by traction calculation results, traffic volume and line passing capacity conditions. The most critical factor is annual transportation. Train load density which is called line carrying capacity is calculated from annual transportation.

3.4.1 Number of Train

Train density is the line carrying capacity computed from traffic transportation requirement and maintains some overdesigned capacity. For the general consideration, overdesigned coefficient can be considered as 20% for singlet line and 15% for double line (track). Under short-term situation, according to investigated freight volume calculation and transportation fluctuation, fluctuation coefficient generally uses 20%. While under long term situation, according to the requirements of the national transmission capacity, overdesigned capacity is only considered.

Considering long term transportation

$$N = \frac{K_1.K_2.\Gamma \times 10^4}{365.G.r} \qquad 3.21$$

Where

$\mathbf{K_1}, \boldsymbol{K_2}, \boldsymbol{\Gamma}, \boldsymbol{G}, \mathbf{r}$ are fluctuation coefficient, over design coefficient, annual transportation (tone/year), traction weight(t) and freight trains net weight coefficient, weight ratio between net freight weight and gross weight respectively.

The design is performed based on the following consideration.

a. Long term annual transportation for the given line is 3500×10^4t
b. Traction weight of 5000T(G)
c. Ratio between freight net weight and gross weight is 0.7.

Based on the characteristics of this line and the freight transportation features along the line, the freight flow fluctuation coefficient is taken as 1.3 and over design coefficient of a single line is 1.2 and for a double track 1.15 [47].

With consideration of the distribution of cities and towns, number of population, socioeconomic development and also agricultural activities along the line, we can predict or assume the future or long term annual carrying capacity of the line from Modjo to Hawassa as $3500\times 10^4 t$. The section with largest freight volume is expected to be Hawassa to Shashemenea. With the above assumption, the number of freight train can be calculated as:

$$\mathrm{N} = \frac{1.2 \times 1.3 \times 3500 \times 10^4}{365 \times 5000 \times 0.7}$$

$$\mathrm{N} = 43 \ \text{trains/day}$$

The total number of train required per day considering long term transportation is 43 trains.

3.4.2 Maximum Effective Feeder Current

Maximum effective feeder current is the maximum current (probabilistic) that required from the feeding substation in the case of maximum number of train, which in this case are three trains.

Feeding section segment n represented as the largest number of train under traction operation. N is train density which is daily train operation number,tg is train traction running time when travelling through a feeding section and A train energy consumption when travelling through a feeding section.

$$\mathrm{Ig} = \frac{60\mathrm{A1(KVA)}}{\mathrm{tg.U(KV)}} + 7(\mathrm{A}) \qquad 3.22$$

Where 7(A) represents self-electricity of the locomotive and Ig represents traction average current in feeding section.

$$\mathrm{Ig} = \frac{60\times 13772(\mathrm{KVA})}{26\times 25(\mathrm{KV})} + 7(A)$$

$$\mathrm{Ig} = 1271.26 + 7 = 1278.26\ \mathrm{A}$$

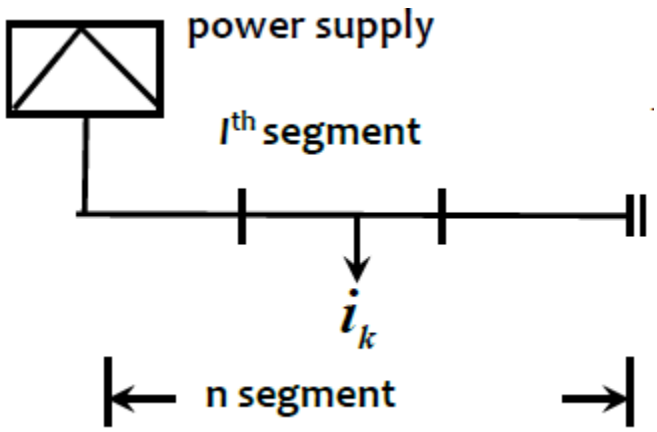

Figure 3.2: Unilateral power supply system

The design considers three segments for the given feeding section segment traction time

$\mathrm{tg1} = \mathrm{tg2} = \mathrm{tg3} = \frac{\mathrm{tg}}{\mathrm{n}} = \frac{76.8}{3} = 26$ minute Assuming operational speed of 50 km/hr

Traction probability $$\mathrm{P} = \frac{2\mathrm{Ntg}}{\mathrm{nT}} \qquad 3.23$$

$$\mathrm{P} = \frac{2\times 14\times 26}{3\times 1440} = 0.168$$

Average current $$\mathrm{I_{ave}} = \mathrm{nPIg} = \frac{2\mathrm{Ntg\ Ig}}{\mathrm{T}} \qquad 3.24$$

$$I_{ave} = 3 \times 0.168 \times 1278.26\ A = 646.23\ A$$

Effective feeder current $$I_{effmax} = I_{ave}\sqrt{1 + \frac{K_{eg}{}^2 - P}{nP}} \quad 3.25$$

$$I_{effmax} = 646.23\sqrt{1 + \frac{1.08 - 0.168}{3 \times 0.168}}$$

Where K_{eg} is train effective current coefficient which ranges from 1.03 to 1.05 and usually 1.04 taken for calculation

$$I_{effmax} = 646.23\ A \times 1.676 = 1083.187\ A.$$

A more detailed explanation with regards to probabilistic load flow in traction power supply system can be found in [51].

3.4.3 Transformer Capacity

Computing transformer capacity

$$S = U.I_{effmax} \quad 3.26$$

Where S, U, I_{effmax} are the transformer capacity in MVA, secondary winding output voltage of the transformer and maximum effective current of the transformer respectively.

The maximum secondary output voltage of the transformer is 55 kV and the maximum effective current of the transformer is 1083.187 A. Then

$$U = 55\ kV$$

$$I_{effmax} = 1083.187\ A$$

Traction transformer capacity= $S = 55\ kV \times 1083.187A = 59.575\ MVA$

The calculated capacity of the traction power transformer is 59.575 MVA but the nearest standard transformer rating available compared with the calculated results is 60 MVA. Then 60MVA is taken as the traction power transformer, which will be used in the next section for the design of the substation power transformer parameters. On the other hand, during intensive operation, the traction transformer may incidentally overload which last longer than the winding thermal time constant. This overload scenario enables the winding insulation temperature rise

rapidly, which in turn decreases the life of the transformer unless the overload capacity of the transformer calculated accurately. In this thesis the traction transformer overload capacity is taken as 50%. With this value we can achieve the requirement of the short-term or long-term intensive operation.

3.5 Design of Substation Power Transformer

The other important parts of a traction power supply system is the traction power transformers connecting the high-voltage transmission line to the catenary. The model of the transformer always influences the calculations of load flow and power losses in the system. Power transformers are commonly designed to give a very low magnetizing current [12], and therefore it is assumed that the influence of the magnetization reactance can be neglected, which gives an approximation of a transformer that can be seen in figure 3.1. This model still contains most of the electrical properties of a transformer, including losses, as needed to give a reasonable level of accuracy for the loss calculations. In this section traction substation power transformer is modeled.

3.5.1 Modeling of Substation Power Transformer

Today, there are many transformers which are used in railway power supply system such as open delta or Vv, Scott, YNd11, Wood-Bridge , single phase transformers, etc. These different transformers are used in various feeding configurations, for example, in direct feeding system, Vv transformers are the best choice where as in an autotransformer feeding arrangement, single-phase traction transformers with three windings are used to provide electricity supply to trains overhead catenary systems and are connected on the HV side to two phases of the transmission or distribution network. In these transformers, the secondary nominal voltage is 55 kV and their HV voltage may be 132, 275 or 400 kV. For the proposed line this single phase three winding transformer drives its supply from 132 kV and the voltage of the system arranged in such a way 132 kV/27.5 kV-0-27.5 kV. Figure 3.1 illustrate such connections.

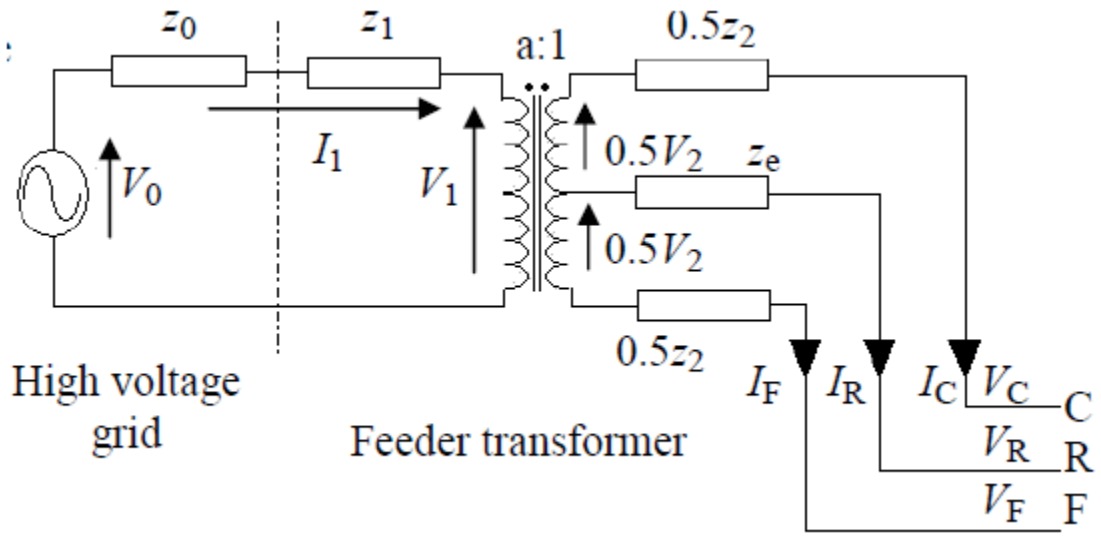

Figure 3.3: Equivalent circuit of a power substation [3]

I_1 is the primary current of the transformer caused by two secondary current, the contact line current I_C and the negative feeder current I_F as follows.

$$I_1 = \frac{1}{2a}(-I_C + I_F) \quad 3.27$$

Consider the primary-side circuit, using Kirchhoff's law, and replacing I_1 in equation 3.27, we will have,

$$V_1 = V_O - \frac{1}{2a}(Z_O + Z_1)(-I_C + I_F) \quad 3.28$$

Where a is the transformer transformation ratio which is equal to 2.4 , and considering the secondary-side contact to rail line (C-R) circuit,

$$V_C - V_R + \frac{1}{2}V_2 + \frac{1}{2}Z_2 I_C + Z_e(I_C + I_F) = 0 \quad 3.29$$

Substitute $V_2 = 0.41V_1$ where V_1 is as in equation 5.3 hence,

$$(Z'_1 + 12Z_2 + 24Z_e)I_C + (Z_e - Z'_1)I_F = -24V_C + 24V_R - 5V_O \quad 3.30$$

Similarly, the secondary-side negative feeder to rail line (F-R) circuit can be expressed as

$$(24Z_e - Z'_1)I_C + (Z'_1 + 12Z_2 + 24Z_e)I_F = 24V_R - 24V_F + 5V_O \quad 3.31$$

Where

$$Z'_1 = Z_O + Z_1 \quad 3.32$$

Based on the assumption that all currents are supplied by the substation and eventually returned to the substation, that is

$$I_C + I_R + I_F = 0 \tag{3.33}$$

By defining $Z_A = Z'_1 + 6Z_2$ and $Z_B = 6Z_2 + 24Z_e$ thus, 3.34

$$(Z_A + Z_B)I_C + (-Z_A + Z_B)I_F = -24V_C + 24V_R - 5V_O \tag{3.35}$$

$$(-Z_A + Z_B)I_C + (Z_A + Z_B)I_F = 24V_F - 24V_R + 5V_O \tag{3.36}$$

With equations 3.33-3.36, the equivalent voltage source in series with the impedance or the so called Thevenin equivalent circuit in the multi-conductor model is formed as shown in equation 3.37.

$$\begin{bmatrix} Z_A + Z_B & 0 & -Z_A + Z_B \\ 1 & 1 & 1 \\ -Z_A + Z_B & 0 & Z_A + Z_B \end{bmatrix} \begin{bmatrix} I_C \\ I_R \\ I_F \end{bmatrix} = 5V_O \begin{bmatrix} -1 \\ 0 \\ 1 \end{bmatrix} + 24 \begin{bmatrix} -1 & 1 & 0 \\ 0 & 0 & 0 \\ 0 & 1 & -1 \end{bmatrix} \begin{bmatrix} V_C \\ V_R \\ V_F \end{bmatrix} \tag{3.37}$$

Since

$$\begin{bmatrix} Z_A + Z_B & 0 & -Z_A + Z_B \\ 1 & 1 & 1 \\ -Z_A + Z_B & 0 & Z_A + Z_B \end{bmatrix}^{-1} = \begin{bmatrix} \frac{Z_A + Z_B}{4Z_A Z_B} & 0 & \frac{Z_A - Z_B}{4Z_A Z_B} \\ -\frac{1}{2Z_B} & 1 & -\frac{1}{2Z_B} \\ \frac{Z_A - Z_B}{4Z_A Z_B} & 0 & \frac{Z_A + Z_B}{4Z_A Z_B} \end{bmatrix} \tag{3.38}$$

Equation 3.37 can be written in the other form as the Norton equivalent circuit as shown in equation 3.39.

$$\begin{bmatrix} I_C \\ I_R \\ I_F \end{bmatrix} = 2.5\frac{V_O}{Z_A} \begin{bmatrix} 1 \\ 0 \\ -1 \end{bmatrix} + \begin{bmatrix} \frac{6}{Z_A} + \frac{6}{Z_B} & \frac{12}{Z_B} & \frac{6}{Z_A} - \frac{6}{Z_B} \\ \frac{12}{Z_B} & \frac{-24}{Z_B} & \frac{12}{Z_B} \\ \frac{6}{Z_A} - \frac{6}{Z_B} & \frac{12}{Z_B} & \frac{6}{Z_A} + \frac{6}{Z_B} \end{bmatrix} \begin{bmatrix} V_C \\ V_R \\ V_F \end{bmatrix} \tag{3.39}$$

$$I_{SS} = J_{SS} + Y_{SS}V_{SS}$$

Where

JSS is the substation current-injected model

VSS and **Y**SS are the substation voltage and the substation admittance, respectively.

3.5.2 Admittance Matrix of the Transformer

The short circuit impedance of the grid is assumed zero, this is equivalent to assuming the primary voltage of the substation transformer an infinite bus with a voltage of 132 kV. The no-load secondary voltage between the OCS and feeder is 55 kV with a grounded center tap. The nameplate data of the substation transformer are assumed to be: 132/55 kV, 60 MVA(traction transformer capacity found in section 3.4), X/R ratio equal to 10 based on ANSI/IEEE C37.010-1979 and the impedance of the traction transformer will be 10% based on IEC 60076 standards. The base impedance (Z_{base}) in the secondary side can be calculated as:

$$Z_{base2} = \frac{V_{rated}^2}{\text{Rated MVA}} \qquad 3.40$$

Then

$$Z_{base2} = \frac{55^2}{60} = 50.41\Omega$$

The percentage impedance $\%Z$ of a transformer is an important parameter in power-supply system design, which represents the percentage drop from normal rated primary voltage that would occur when full rated load current flows in the secondary; thus the percentage impedance can be used to determine the impedances (in ohms) of the primary and secondary. Typical value for such medium capacity power transformers ranges from 7 to 15 % according IEC 60076 and for this thesis 10 % is taken.

Therefore, in reference to the secondary, the traction power substation transformer impedance is:

$$Z_{TPSS} = Z_{base2} \times {}^{\%Z}/_{100} \qquad 3.41$$

$$Z_{TPSS} = 50.41\Omega \times 0.1 = 5.041\Omega$$

In power systems, the X/R ratios are higher for generating units and transformers and lower for the transmission lines. Typically the lower the voltage, the lower the X/R ratio. A transmission line X/R ratio may vary considerably, but it will always be less than the transformer X/R ratio because much of the short circuit contribution comes over transmission lines that have a lower X/R ratio than a transformer. Generally, in a generation station or a substation with many transformers the X/R ratio is fairly high.

The X/R ratio for power transformers can be between about 10 and 125, lower for smaller transformers and low voltage transformers and higher for larger transformers and high power transformers. ANSI/IEEE C37.010-1979, page 42, recommends the typically range of the X/R ratio for a power transformer. For this case:

$$\frac{X}{R} = 10 \qquad 3.42$$

Then

$$X = 10R$$

Using right angle rule

$$Z_{Tpss}{}^2 = (10R)^2 + R^2 = 101R^2$$

$$(5.041\Omega)^2 = 101R^2$$

$$25.4116\ \Omega^2 = 101R^2$$

$$\sqrt{\frac{25.4116}{101}} = R = 0.5016\Omega$$

Where

$$X = 10 \times 0.5016\Omega = 5.016\Omega$$

Then

The equivalent impedance of the transformer referring to the secondary side is:

$$Z_{eq} = 0.5016 + 5.016i \qquad 3.43$$

Then let's assume that half of Z_{eq} will be primary side impedance referring to secondary side and the other half will be secondary side impedance of the substation transformer.

Then

$Z_2 = 0.250799 + 2.50799i\ \Omega$ And $Z_1{}' = 0.250799 + 2.50799i$ (the primary impedance referred to secondary)

Then

$$Z_1 = Z_1{}' \times (\text{transformation ratio})^2 \qquad 3.44$$

$$\text{Transformation ratio} = \frac{N_2}{N_1} = \frac{V_1}{V_2} = \frac{132}{55} = 2.4 \qquad 3.45$$

$$Z_1 = (0.250799 + 2.50799i\ ) \times 2.4^2$$

$$Z_1 = 1.213 + 12.13i\ \Omega$$

Per unit value of the primary and secondary impedance can solved as follows. For the secondary side Z_2 has to be divided into two equal values, that is:

$$Z_{2P} = \frac{Z_2}{2} = \frac{0.250799+2.50799i}{2} = 0.1253 + 1.253i\ \Omega \text{ And}$$

$$Z_{2N} = \frac{Z_2}{2} = \frac{0.250799+2.50799i}{2} = 0.1253 + 1.253i\ \Omega$$

Then per unit value of secondary side will be:

$$Z_{2P}(p.u) = \frac{0.1253+1.253i\ \Omega}{Z_{base2}} = \frac{0.1253+1.253i\ \Omega}{50.41} = 0.002487 + 0.02487i$$

And

$$Z_{2N}(p.u) = \frac{0.1253+1.253i\ \Omega}{Z_{base2}} = \frac{0.1253+1.253i\ \Omega}{50.41} = 0.002487 + 0.02487i$$

For the primary side

$$Z_{base1} = \frac{V_{1rated}^2}{\text{Rated MVA}} \qquad 3.46$$

$$Z_{base1} = \frac{132^2}{60} = 290.4\Omega$$

Per unit value of the primary winding will be

$$Z_1(p.u) = \frac{Z_1}{Z_{base1}} = \frac{1.213+12.13i}{290.4} = 0.00417699 + 0.0417699i$$

Based on these data we can find the relationship between the three currents and the three voltages using MATLAB script.

$Z_1 = 1.213 + 12.13i\ \Omega$, $Z_2 = 0.250799 + 2.50799i\ \Omega$, a=2.4, $Z_e = 0.1$ and $V_o = 13200$

The following Y matrix representing the substation transformer is obtained:

```
i_source =

  1.0e+004 *
  -0.1202 + 1.2022i
  -0.0000
   0.1202 - 1.2022i

 Y_station =

  -0.1188 + 0.5922i    0.1939 - 0.7471i   -0.0751 + 0.1550i
   0.1939 - 0.7471i   -0.3878 + 1.4943i    0.1939 - 0.7471i
  -0.0751 + 0.1550i    0.1939 - 0.7471i   -0.1188 + 0.5922i
```

3.6 Design of Autotransformer

The autotransformer has a single winding connected between the catenary and the feeder wires. The rail system (rails and grounded wires) is connected to a center point on the winding. The usual voltage rating is 50 kV supply between the catenary and feeder with a transformation ratio of 2:1 to obtain a 25 kV catenary to rail and from rail to the return feeder. The station where the autotransformer is located is also called paralleling station because the two tracks (C wire and F wire) are connected in parallel as shown in figure 3.4.

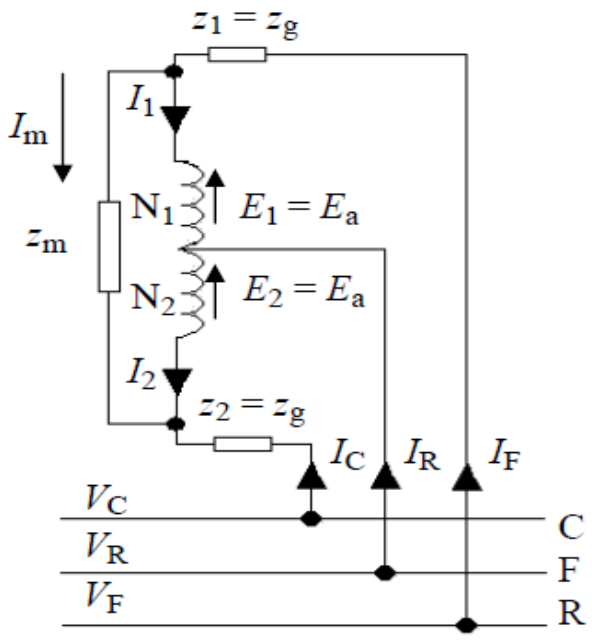

Z_1, Z_2 are AT's primary and secondary leakage impedances

Z_m is AT's magnetizing impedance

I_m is AT's magnetizing current

I_1 , I_2 are AT's primary and secondary current

E_1, E_2 are electromotive forces of AT's primary and secondary windings

N1, N2 are turns of the two windings

Figure 3.4: Equivalent circuit of an autotransformer [3]

Assume that $N_1 = N_2$ and $Z_1 = Z_2 = Z_g$, therefore

$$E_1 = E_2 = E_a = \frac{1}{2} Z_m I_m \quad 3.47$$

$$I_m = \frac{1}{2}(I_F - I_C) \quad 3.48$$

$$I_C + I_R + I_F = 0 \quad 3.49$$

$$V_R - V_C = E_a - Z_g I_C \quad 3.50$$

$$V_F - V_R = E_a + Z_g I_F \quad 3.51$$

From equations 3.48 and 3.49

$$I_C = -I_m - \frac{1}{2} I_R \quad 3.52$$

$$I_F = I_m - \frac{1}{2} I_R \quad 3.53$$

From equations 3.50 and 3.51

$$V_F - V_C = 2E_a + Z_g(I_F - I_C) = Z_m I_m + 2Z_g(I_F - I_C) = I_m(Z_m + 2Z_g) \quad 3.54$$

$$V_C + V_F - 2V_R = Z_g(I_F + I_C) = -\frac{1}{2} Z_g I_R \quad 3.55$$

Substitute equation 3.52 into 3.53, equation 3.54 into 3.55

$$I_C = \left(\frac{1}{2Z_g} - \frac{1}{Z_m + 2Z_g}\right) V_C - \frac{1}{Z_g} V_R + \left(\frac{1}{2Z_g} + \frac{1}{Z_m + 2Z_g}\right) V_F \quad 3.56$$

$$I_R = -\frac{1}{Z_g} V_C + \frac{2}{Z_g} V_R - \frac{1}{Z_g} V_F \quad 3.57$$

$$I_F = \left(\frac{1}{2Z_g} - \frac{1}{Z_m + 2Z_g}\right) V_C - \frac{1}{Z_g} V_R + \left(\frac{1}{2Z_g} + \frac{1}{Z_m + 2Z_g}\right) V_F \quad 3.58$$

Thus,

$$Y_{AT} = \begin{bmatrix} \frac{1}{2Z_g} - \frac{1}{Z_m + 2Z_g} & -\frac{1}{Z_g} & \frac{1}{2Z_g} + \frac{1}{Z_m + 2Z_g} \\ -\frac{1}{Z_g} & \frac{2}{Z_g} & -\frac{1}{Z_g} \\ \frac{1}{2Z_g} - \frac{1}{Z_m + 2Z_g} & -\frac{1}{Z_g} & \frac{1}{2Z_g} + \frac{1}{Z_m + 2Z_g} \end{bmatrix} \quad 3.59$$

$$\begin{bmatrix} I_C \\ I_R \\ I_F \end{bmatrix} = Y_{AT} \begin{bmatrix} V_C \\ V_R \\ V_F \end{bmatrix} \quad 3.60$$

If we assume the circuit which connects the magnetizing impedance (Z_m) is open, then $Z_m \to \infty$, meanwhile the admittance matrix become:

$$Y_{AT} = \begin{bmatrix} \frac{1}{2Z_g} & -\frac{1}{Z_g} & \frac{1}{2Z_g} \\ -\frac{1}{Z_g} & \frac{2}{Z_g} & -\frac{1}{Z_g} \\ \frac{1}{2Z_g} & -\frac{1}{Z_g} & \frac{1}{2Z_g} \end{bmatrix} \quad 3.61$$

3.6.1 Admittance Matrix of the Autotransformer

Autotransformer components are modeled by their equivalent circuits in terms of inductance, and resistance. The magnetizing impedance, Z_m, is assumed infinite $Z_1 = Z_2$ because the two windings are similar. An earthing resistance,Z_e, is assumed form the center-tap to remote earth. The assumed ratings of the AT are: 50/25 kV, 10 MVA, with 1.2 % impedance and an X/R ratio of 6.

The base impedance (Z_{base}) of the transformer can be calculated as:

$$Z_{base} = \frac{V_{rated}^2}{RatedMVA} \quad 3.62$$

Then

$$Z_{base} = \frac{25^2}{10} = 62.5\Omega$$

As stated earlier the percent impedance of a transformer is a measure of the ability of a transformer to maintain its rated voltage with a varying load and is determined by the construction of the core and physical spacing between the primary and secondary windings. Typical values range from 1 to 5% for small transformers. The lower the value, the better the regulation. Percentage impedance also determines the maximum fault current that the transformer can deliver.

Therefore, autotransformer impedance is:

$$Z_{AT} = Z_{base2} \times {}^{\%Z}/_{100} \quad 3.63$$

$$Z_{AT} = 62.5\Omega \times 0.012 = 0.75\Omega$$

$$\frac{X}{R} = 6$$

Then

$$X = 6R$$

Using right angle rule

$$Z_{AT}{}^2 = (6R)^2 + R^2 = 37R^2$$

$$(0.75\Omega)^2 = 37R^2$$

$$0.5625\,\Omega^2 = 37R^2$$

$$\sqrt{\frac{0.5625}{37}} = R = 0.123\Omega$$

Where

$$X = 6 \times 0.123\Omega = 0.7397\Omega$$

Then

The equivalent impedance of the transformer referring to the secondary side is:

$$Z_{eq} = 0.123 + 0.7397i\Omega \quad 3.64$$

Then $Z_1 = Z_2$

$$Z_1 = Z_2 = \frac{Z_{eq}}{2} = \frac{0.123 + 0.7397i\Omega}{2} = 0.0615 + 0.36985i\,\Omega$$

Per unit value of the primary winding will be

$$Z_1(p.u) = \frac{Z_{eq}}{Z_{base}} = \frac{0.0615+0.36985i\Omega}{62.5\Omega} = 0.000984 + 0.00591i$$

The same for $Z_2(p.u) = 0.000984 + 0.00591i$

The following Y matrix representing the autotransformer is obtained:

```
[PsYmat]=Ps_Y_mat_with_Re (10000, 0.0615+0.36985i, 0)

PsYmat =

   0.2188 - 1.3155i  -0.4375 + 2.6310i   0.2188 - 1.3155i
  -0.4375 + 2.6310i   0.8750 - 5.2621i  -0.4375 + 2.6310i
   0.2188 - 1.3155i  -0.4375 + 2.6310i   0.2188 - 1.3155i
```

3.7 Impedance Calculation

In the previous sections major components of the traction power supply system were modeled and designed. The application of this design to physical systems requires detailed knowledge and computation of the actual impedance which makes up the traction network. A monumental paper describing the impedance of the overhead conductor with earth return was written in 1923 by Carson [27].This paper, with certain modifications has since served as the basis for transmission line impedance calculations in cases where current flows through the earth. In this section impedance calculation of the traction network using Carson line model will be performed.

3.7.1 Carson's Line

One of the primary purposes of performing the steady-state analysis of a distribution feeder is to determine the voltages at every node. Because these voltages are a function of the line voltage drops it is critical that the line impedances used are as exact as possible. In 1923 John Carson developed equations that would determine the self and mutual impedances of any number of overhead or underground conductors taking into account the effect of ground [49]. In recent years the application of Carson's equation has become the standard for the computation of line impedances. Because Carson's equation results in an infinite series, approximations have been made to ease in the computation of the impedances

If some conductors are earthed or the system is not balanced, the earth will carry a return current. This earth current will spread in the earth following the path of least resistance and obeying Maxwell's equations. To consider the effect of earth currents on inductance calculations, Carson [Carson] proposed to replace the earth by a set of "earth return" conductors located directly under

the overhead conductors as shown in figure 3.5. The theory of Carson's line is well established and can be found in many resources. This section is included for completeness and to explain the line modeling used in this thesis.

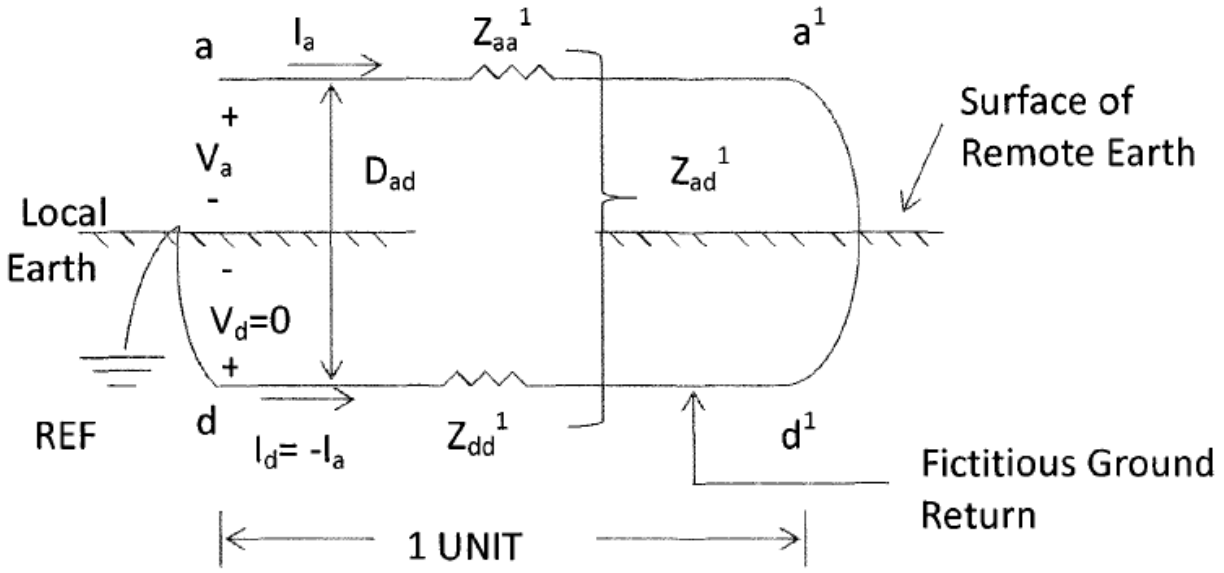

Figure 3.5: Carson line [29]

The conductor **a-a1** shown in figure 3.5 carries a current $\mathbf{I_a}$ with a return through circuit $\mathbf{d - d^1}$ beneath the surface of the earth. The earth is considered to have a uniform resistivity and to be semi-infinite. The current $\mathbf{I_a}$ in the ground spreads out over a large area. Wagner and Evans [9] show that Carson's line can be thought of as having a single realm conductor,$\mathbf{d - d^1}$, with self GMD equal to that of $\mathbf{a - a^1}$ and located at a distance $\mathbf{D_{ad}}$ below the overhead line, where $\mathbf{D_{ad}}$ is adjusted so that the inductance calculated with this configuration is equal to that measured by test.

The equations for Carson's line are,

$$\begin{bmatrix} V_{aa^1} \\ V_{dd^1} \end{bmatrix} = \begin{bmatrix} V_a - V_{a^1} \\ V_d - V_{d^1} \end{bmatrix} = \begin{bmatrix} Z_{aa^1} & Z_{ad^1} \\ Z_{ad^1} & Z_{dd^1} \end{bmatrix} \begin{bmatrix} I_a \\ -I_a \end{bmatrix} \quad 3.65$$

$$V_a = (Z_{aa^1} + Z_{dd^1} - 2Z_{ad^1})I_a = Z_{aa}I_a \quad 3.66$$

This last equation defines $\boldsymbol{Z_{aa}}$, where we clearly distinguish between $\mathbf{Z_{aa^1}}$ and $\mathbf{Z_{dd^1}}$
Thus

$$Z_{aa} \approx Z_{aa^1} + Z_{dd^1} - 2Z_{ad^1} \text{ ohm/unit length} \quad 3.67$$

Using the above equations and ignoring skin effect, we may write the self and mutual impedances of equation (3.65) as follows. The self-impedance of line ***a*** is

$$Z_{aa^1} = r_a + jwI_a = r_a + j\omega k(\ln({}^1/_{D_{sa}})) \text{ ohm/unit lenght} \quad 3.68$$

Similarly

$$Z_{dd^1} = r_d + j\omega k(\ln({}^1/_{D_{sa}})) \text{ ohm/unit lenght} \quad 3.69$$

Where $k = 2.10^{-7}$

Carson found that the earth resistance r_d is a function of frequency and he derived the empirical Formula

$$r_d = \pi^2.10^{-4}.f \text{ ohm/km} \quad 3.70$$

$$r_d = 9.869.10^{-4}.f \text{ ohm/km}$$

This has a value of 0.04934 ohms/km at 50 Hz. Finally, the mutual impedance is

$$Z_{ad^1} = j\omega m_{ad} = j\omega k(\ln({}^1/_{D_{sa}})) \text{ ohm/unit lenght} \quad 3.71$$

Combining (3.66), (3.67) and (3.69) as specified by the formula, we compute then impedance of wire **a** with earth return as

$$Z_{aa} = Z_{aa^1} + Z_{dd^1} - 2Z_{ad^1} = (r_d + r_a) + j2\omega k \ln\left({}^{D_{ad}}/_{r_o}\right) \Omega/L$$

$$\boldsymbol{\omega} = 2\pi f$$

$$Z_{aa} = (r_d + r_a) + j2\omega k \ln\left({}^{D_{ad}}/_{D_{sa}}\right) \Omega/\text{unit lenght}$$

$$Z_{aa} = r_a + \pi^2.10^{-4}.f + j4\pi.10^{-4}.f\,(0.25 + \ln(D_{ad}/r_o)) \quad 3.72$$

The self-impedance of a circuit with earth return depends upon the impedance of the earth which in turn fixes the value of $\mathbf{D_{ad}}$ **.** Wagner and Evans [10] discuss this problem in some detail and offer a physical explanation of Carson's original work.

The quantity $\mathbf{D_{ad}}$ is a function of both the earth resistivity **f** and the frequency and is defined by the relation

$$D_{ad} = 1.309125 \times \delta$$

$$D_{ad} = 658.87 \times \sqrt{\frac{\rho_e}{f}} \text{ m} \qquad 3.73$$

If no actual earth resistivity data is available, it is not uncommon to assume ρ_e to be 100 ohm-meter. The earth resistivity ρ_e depends on the nature of the soil and is commonly found in the literature.

The significance of this derivation is that the grounded configuration of Figure 3.5 can be replaced with a line above an earth with infinite conductivity.

Skin effect, the derivations of R and X above assume uniform current density through the cross section of the conductor. Uniform current density occurs only when the frequency is zero (direct current). As the frequency increases from zero, the current density increases near the conductor surface and decreases as the center of the conductor is approached. This phenomenon, known as *skin effect*, reduces the internal flux linkages, and lowers the internal inductance compared to the DC state. It also increases the resistance.

3.7.2 Main Assumption for the Impedance Calculation

Whether analytical techniques or commercial software are to be used, it is necessary to model the different components of the power supply system and perform simulation. Each of the 12 lines is modeled separately using Carson's theory. Mutual inductances between the different wires including those of the grounded conductors can be considered. The general concept of this approach will be described following the main assumptions below.

1. The supply source is treated as an ideal sinusoidal voltage source in series with impedance
2. The overhead power feeding system is treated individually in every section and all conductors are considered as parallel laid wires along the feeding length

3. The feeding length is relatively short when compared with the electric wavelength and thus the propagation effects along the conductors are neglected
4. Summation of all conductor currents including the earth-leakage current is equal to zero
5. There is mutual coupling between conductors of different feeding sections.
6. Distributed shunt capacitance between conductors are all neglected.

A group of m conductors results in the self and mutual impedance at each feeding section. In the autotransformer AC railway power feeding system described in this thesis, there are six main conductors to be considered.

1. **Catenary (C)**: parts of the overhead contact line system serving to establish contact with the current collector. To avoid errors the impedances of the messenger and the contact wire calculated independently in this thesis.
2. **Messenger (M)**: parts of the overhead contact line system used to support the contact wire.
3. **Rails (R)**: The two rails in the same track are also treated as an independent conductor. They are connected to autotransformers at the center tap.
4. **Feeder (F)**: Besides the catenary, another outer tap of the autotransformer is connected to the feeder wire.
5. **Static (S)**: Although there is a wire called “Earth wire” that is used for safety reasons and it is included for the calculation of the matrix impedance in this thesis for greater accuracy.

3.7.3 Conductor Arrangement

The conductor configuration or arrangement of the overhead line is based on the industry standards conductor clearances, in general, the following clearances need to be considered: ground, tracks, buildings, trees, conductors and structures of another line, other conductors on the same structure, the structure itself, guy wires and other equipment on the structure and the edge of the right of way.

According to IEC the minimum electrical clearances of the conductor must be maintained under all line loading and environmental conditions. Since the actual sag clearance of conductors on overhead contact line is seldom monitored, sufficient allowance for this clearance (safety buffer) must be included in the process of the initial design.

Minimum horizontal and vertical distances from energized conductor ("electrical clearances") to ground, other conductors, vehicles, and objects such as buildings, are defined based on three parameters. Clearances are defined based on the transmission line to ground voltage, the use of ground fault relaying, and the type of object or vehicle expected within proximity of the line. The IEC 270 Rules cover both vertical and horizontal clearances to the energized conductors.

The electric static clearance, which is the minimum distance required between the live parts of the overhead wire equipment and a structure or the earthed parts of the OHW equipment under 25 kV must be at the minimum of 320 mm as per IEC 270.

The minimum electrical clearance to earth or another conductor is 150 mm under adverse condition and the minimum clearance between 2 parallel wires in open overlaps is 250 mm but may be reduced to 150 mm absolute minimum under the worst case.

The following is derived minimum contact height for regulated wiring.

Rolling stock static height	4.42 m
Electrical clearance	0.15 m
Absolute minimum contact height	**4.57 m**
Allowance for overhead wiring dynamics	0.05 m
Allowance for vehicle bounce	0.05 m
Track vertical tolerance	0.05 m
Overhead wiring construction tolerance	0.05 m
Minimum design contact height	**4.75 m**

The standard contact height for a conductor system is usually higher than that derived above to allow for:

- Track maintenance
- Future upgrades such as larger rolling stock, or changes in infrastructure configurations.

The following is the standard contact height used in the design of the traction power supply system for the proposed railway line.

The average distance between the center line of the two tracks = 4.935 m
Gauge = 1.435m
Contact wire height above rail level at supports = 5.3 m
Messenger wire height above rail level at support = 6.45 m
Both contact and messenger wires are assumed to be located vertically above the track center
Negative feeder height above the rail level support =7.2 m
Negative feeder offset with respect to track center (towards outside) = 3.9175 m
Static (aerial) ground wire height above the rail level =6.0 m
Static (aerial) ground wire offset with respect to track center (towards outside) =3.2675 m

3.7.4 The physical data of conductors

3.7.4.1Environmental Conditions

In order to match both the mechanical and electrical characteristics of the overhead line conductor to the environmental conditions climatic details must first be collected and analyzed. The parameters required are temperature, wind, solar, rainfall, humidity, altitude, ice and snow, atmospheric pollution, soil, lightning, seismic factor, and general loadings. In this thesis, due to lack of information with regards to parameters mentioned above some assumptions are taken for the design.

3.7.4.2 Conductor Selection

The selection of the conductor size for the traction power supply system voltage level has taken into account the following technical and economic criteria:

1. The maximum power transfer capability.

2. The conductor cross-sectional area, which is directly related with the initial capital cost and the capitalized cost of the losses.

3. The conductor sizes, which conform to standards already used elsewhere on the network in order to minimize spares holdings and introduce a level of standardization.

4. The conductor thermal capacity.

5. The conductor diameter or bundle size, to meets recognized international standards for radio interference and corona discharge.

6. Conforms to environmental conditions and constructional methods understood in the country.

3.7.4.3 Types of Conductors

The international standards covering most conductor types are IEC 61089 (which supersedes IEC 207, 208, 209 and 210) and EN 50182 and 50183. For all negative feeder, earth wire and messenger wire both aluminum conductor steel reinforced (ACSR) and all aluminum alloy conductor (AAAC) may be considered. Aluminum conductor alloy reinforced (ACAR) and all aluminum alloy conductors' steel reinforced (AACSR) are less common than AAAC and all such conductors may be more expensive than ACSR. Historically ACSR has been widely used because of its mechanical strength, the widespread manufacturing capacity and cost effectiveness. For all but local distribution, copper based overhead lines are more costly because of the copper conductor material costs. Hard Copper wires are used for the overhead contact lines, which has a very high strength, corrosion resistance and is able to withstand desert conditions under sand blasting. All aluminum conductors are also employed at local distribution voltage levels. The types conductor used for the design of the catenary system are given in table 3.1 below.

Table 3.1: material used for the power supply line

Application	Material	Composition No of strands/DIA(mm)	Over all DIA(mm)	Resistance (ohm/km)
Contact wire	H.D copper	Solid	12.3	0.1695
Messenger	AWAC	Alumweld6/2.42 Aluminum 31/2.42	16.9	0.1903
Earth wire	ACSR	Steel 7/2.89 Aluminum 16/2.57	16.3	0.2143
Feeder	ACSR	Steel 7/2.89 Aluminum 26/3.72	23.5	0.1027
Rail	Steel		146	0.0240

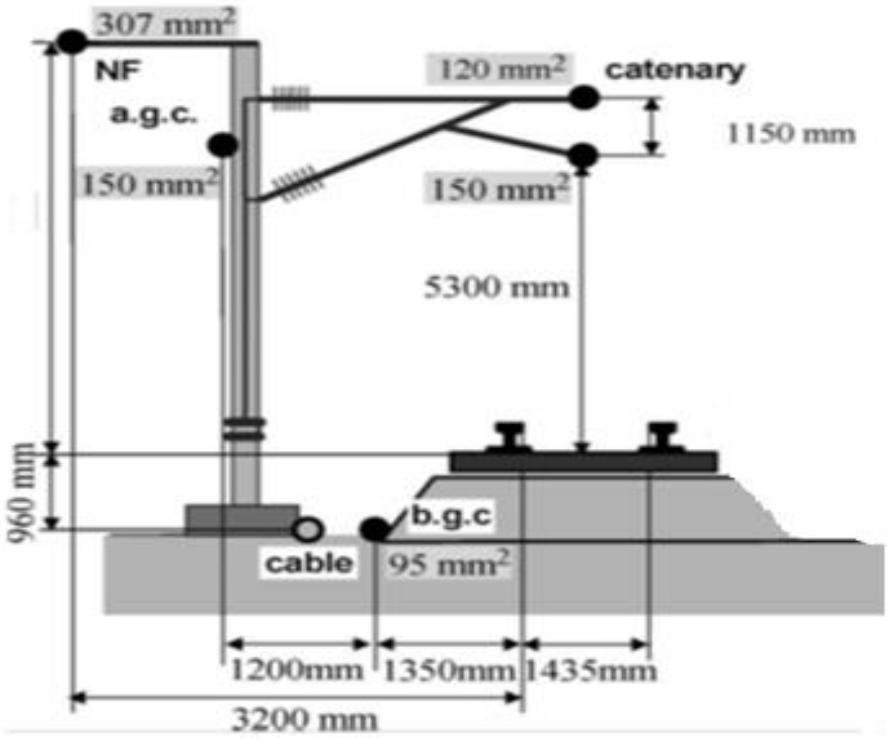

Figure 3.6: Conductors arrangement for the single track [29]

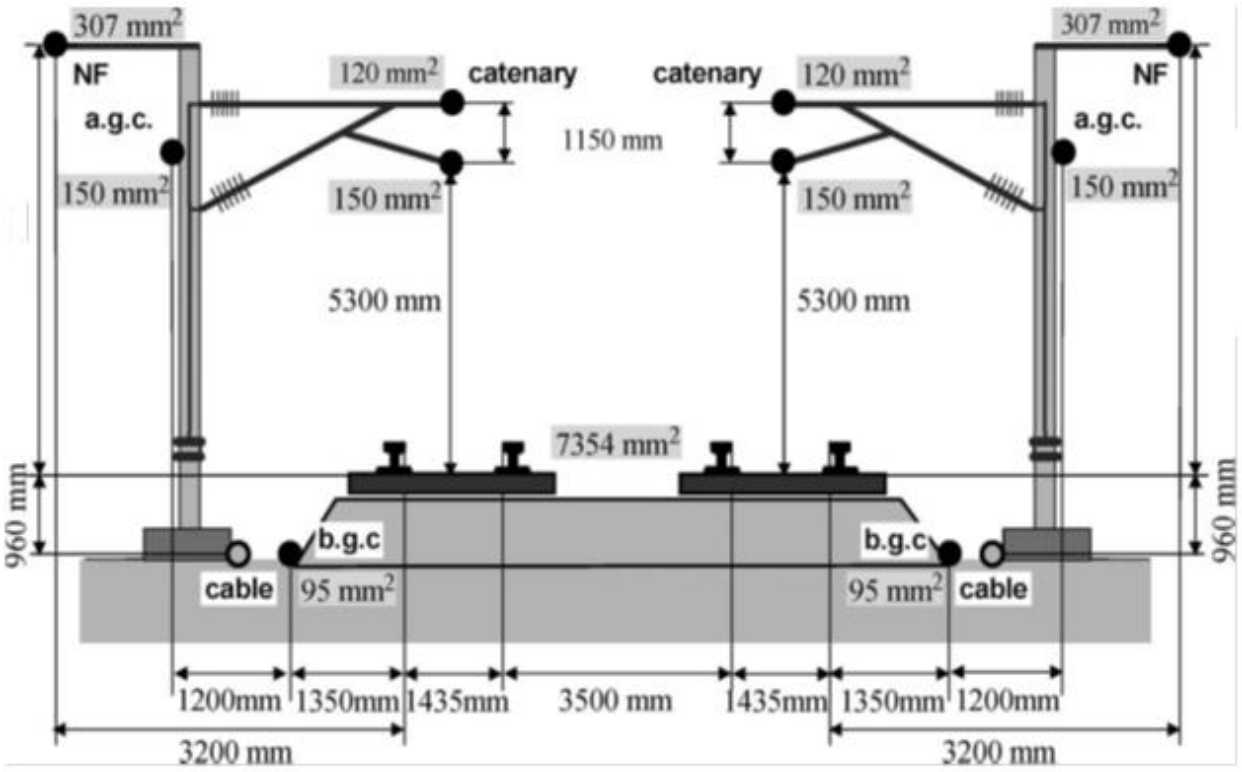

Figure 3.7: conductor arrangement in double track [29]

3.7.5 Full Impedance Matrices

A catenary system is a static power plant that has electrical parameters distributed along its length. The basic parameters of the line are conductor series impedance and shunt admittance. Each conductor has a self-impedance and there is mutual impedance between any two conductors. The impedance generally consists of a resistance and a reactance. The shunt admittance consists of the conductor's conductance to ground and the susceptance between conductors and the conductance of the air path to earth represents the leakage current along the line insulators due to corona. This is negligibly small and is normally ignored in this research.

Practical calculations of multi-conductor line parameters with series impedance expressed in Pu length (e.g. Ω /km). These parameters are then used to form the line series impedance matrices. The calculations use the method of image conductors, assumes that the earth is a plane at a uniform zero potential and that the conductor radii are much smaller than the spacing's among the conductors.

The self and mutual impedances depend on the conductor material as shown in table 3.1, construction, tower or line physical dimensions or geometry, and on the earth's resistivity. Figure 3.2 and figure 3.3 shows the overhead contact line tower physical dimensions and spacing's of conductors above the earth's surface including the rails for both single and double track railway line respectively for the calculation of line electrical parameters.

The fundamental theories used in the calculations of resistance and inductance parameters of overhead lines are extensively covered in section 3.7 above. The steps used in the calculation of line parameters are presented below.

3.7.5.1 Distances between Conductors (D_{sa})

The distance between each conductor D_{sa} has to be calculated in order to find the impedance of the system. As an example the following four figures below shows how these conductor distances are solved.

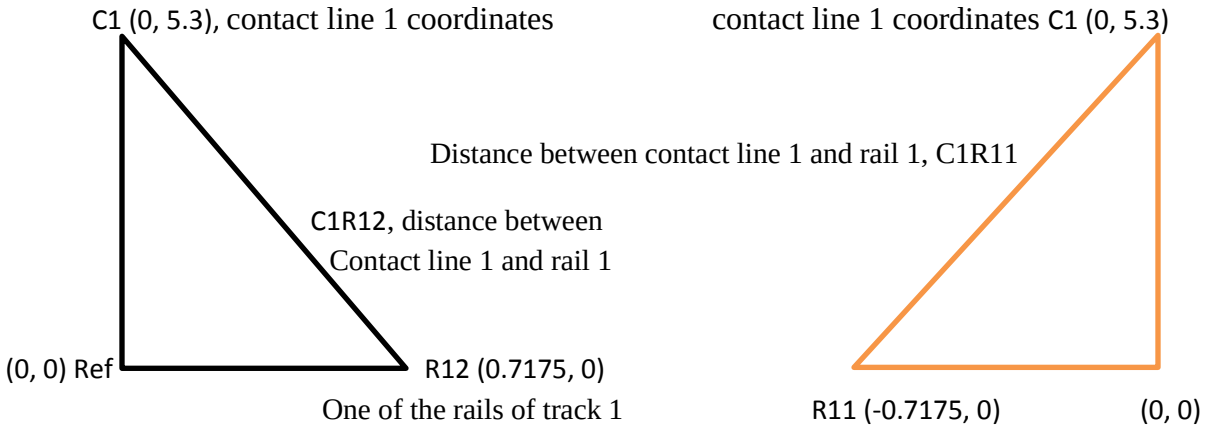

$$C1R1^2 = R12^2 + C1^2$$

$$C1R1^2 = (0.7175)^2 + (5.3)^2$$

$$C1R1 = 5.3483$$

$$C1R11^2 = R11^2 + C1^2$$

$$C1R11^2 = (-0.7175)^2 + (5.3)^2$$

$$C1R11 = 5.3483$$

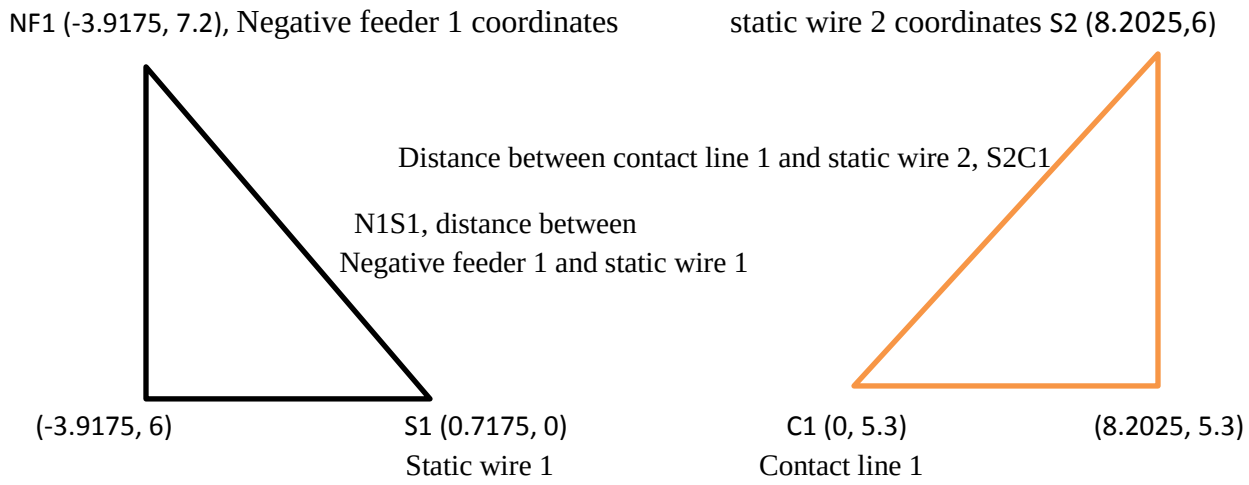

$$N1S1^2 = \left(-3.2675 - (-3.9175)\right)^2 + (7.2 - 6)^2$$

$$N1S1^2 = (0.65)^2 + (1.2)^2$$

$$N1S1 = 1.3647$$

$$S2C1^2 = (8.2025 - (0))^2 + (6 - 5.3)^2$$

$$S2C1^2 = (8.2025)^2 + (0.7)^2$$

$$S2C1 = 8.2332$$

Figure 3.8: Show how conductor distance solved

The following table is a matrix showing the various distances in meter between the conductors of the system based on figure 3.6 conductors arrangement for the single track.

Table 3.2: Distances in meter between the conductors of the system for single track based on figure 3.6 conductors arrangements

	C1	M1	F1	R11	R12	s1
C1	0.0064	1.1500	4.3539	5.3483	5.3483	3.3411
M1	1.1500	0.0045	3.9886	6.4897	6.4897	3.2983
F1	4.3539	3.9886	0.0036	7.8791	8.5628	1.3647
R11	5.3483	6.4897	7.8790	0.0024	1.4350	6.5194
R12	5.3483	6.4897	8.5629	1.4350	0.0025	7.2028
S1	3.3411	3.2983	1.3647	6.5194	7.2028	0.0034

The following table is a matrix showing the various distances in meter between the conductors of the system based on figure 3.7 conductor arrangements in double track.

Table 3.3: Distances in meter between the conductors of the system for double track based on figure 3.7 configuration

	C1	M1	F1	C2	M2	F2	R11	R12	s1	R21	R22	S2
C1	0.0064	1.1500	4.3539	4.9350	5.0672	9.0540	5.3483	5.3483	3.3411	6.7732	7.7486	8.2332
M1	1.1500	0.0045	3.9886	5.0622	4.9350	8.8842	6.4897	6.4897	3.2983	8.1213	8.5763	8.2148
F1	4.3539	3.9886	0.0036	9.0540	8.8842	12.770	7.8791	8.5628	1.3647	10.864	11.976	12.179
C2	4.9350	5.0672	9.0540	0.0054	1.1500	4.3539	6.7732	7.7486	8.2323	5.3483	5.3483	3.3411
M2	5.0672	4.9350	8.8842	1.1500	0.0044	3.9886	8.1213	8.5763	8.2148	6.4897	6.4897	3.2983
F2	9.0540	8.8842	12.770	4.3539	3.9886	0.0034	10.864	11.976	12.179	7.8791	8.5628	1.3647
R11	5.3483	6.4897	7.8790	6.7732	8.1213	10.864	0.0024	1.4350	6.5194	4.9350	6.3700	9.5929
R12	5.3483	6.4897	8.5629	7.7486	8.5763	11.976	1.4350	0.0025	7.2028	3.5000	4.9350	10.750
S1	3.3411	3.2983	1.3647	8.2323	8.2148	12.179	6.5194	7.2028	0.0034	9.5929	10.750	11.470
R21	6.7732	8.1213	10.864	5.3483	6.4897	7.8791	4.9350	3.5000	9.5929	0.0024	1.4350	6.5194
R22	7.7486	8.5763	11.976	5.3483	6.4897	8.5628	6.3700	4.9350	10.750	1.4350	0.0026	7.2028
S2	8.2332	8.2148	12.179	3.3411	3.2983	1.3647	9.5929	10.750	11.470	6.5194	7.2028	0.0022

3.5.7.2 Solving Self and Mutual Impedance of the Line

As explained earlier in section 3.7.1 the equations to solve the self and mutual impedance of the overhead catenary system assumes infinitely long and perfectly horizontal conductors above a homogeneous conducting earth having a uniform resistivity ρ_e (m) and a unit relative permeability. If no actual earth resistivity data is available, it is not uncommon to assume ρ to be 100 ohm-meter.

$$\rho_e = 100\,\Omega/\mathrm{m}$$

$$f = 50\ \mathrm{Hz}$$

δ is skin depth or depth of penetration into the conductor and is given by:

$$\delta = 503.292 \times \sqrt{\frac{\rho_c}{f\mu_r}} \qquad 3.74$$

Using the skin depth δ of equation (3.74) and an earth relative permeability of unity, the effect of earth return path is defined as an equivalent conductor at a depth given by:

$$D_{ad} = 1.309125 \times \delta \qquad 3.75$$

$$D_{ad} = 658.87 \times \sqrt{\frac{\rho_e}{f}}$$

$$D_{ad} = 658.87\sqrt{\frac{\rho_e}{f}}\ m = 658.87\sqrt{\frac{100}{50}} = 931.783m$$

$$r_d = 9.869.10^{-4}.f\,\Omega/km \qquad 3.76$$

$$r_d = 9.869 \times 0.0001 \times 50 \quad \Omega/km = 0.0493\,\Omega/km$$

3.7.5.1.1 Self-Impedance of the Line

To solve the self-impedance of the system the proximity effect between conductors is neglected. Using figure 3.2, the series voltage drop in each conductor due to current flowing in the conductor itself and currents flowing in all other conductors in the same direction is given by:

$$Z_{aa} = r_a + 9.869.10^{-4}.f + j4\pi.10^{-4}.f(0.25 + \ln(D_{ad}/r_o) \qquad 3.77$$

Where r_o is the radius of the conductor in meter and Z_{aa} is the impedance expressed in Ω /km.

Self-impedance of contact wire with radius of $r_o = 0.00615m$ and the conductor resistance of R=0.1695Ω/km

$$Z_{cc} = 0.1695\,\Omega/km + 0.0493 + j4\pi.10^{-4}.f(0.25 + \ln(931.783/0.00615)$$

$$Z_{cc} = 0.1695\,\Omega/km + 0.0493 + j0.06283(0.25 + \ln(931.783/0.00615)$$

$$\mathbf{Z_{cc} = 0.2188 + j0.7652\ \Omega/km}$$

Where subscript cc represents the contact line conductor

Messenger wire with radius of $r_o = 0.00845m$ and the conductor resistance of R=0.1903Ω/km

$$Z_{mm} = 0.1695\,\Omega/km + 0.0493 + j4\pi.10^{-4}.f(0.25 + \ln(931.783/0.00845)$$

$$Z_{mm} = 0.1903\,\Omega/km + 0.0493 + j0.06283(0.25 + \ln(931.783/0.00845)$$

$$\mathbf{Z_{mm} = 0.2396488 + j0.7452\ \Omega/km}$$

Where subscript mm represents the messenger wire conductor

Negative feeder wire with radius of $r_o = 0.01175$m and the conductor resistance of R=0.1027 Ω/km

$$Z_{FF} = 0.1027\,\Omega/km + 0.0493 + j4\pi.10^{-4}.f(0.25 + \ln(931.783/0.01175)$$

$$Z_{FF} = 0.1027\,\Omega/km + 0.0493 + j0.06283(0.25 + \ln(931.783/0.01175)$$

$$\mathbf{Z_{FF} = 0.1520 + j0.7245\ \Omega/km}$$

Where subscript FF represents the negative feeder conductor

Static wire with radius of $r_o = 0.00815$m and the conductor resistance of R=0.2143 Ω/km

$$Z_{SS} = 0.2143\,\Omega/km + 0.0493 + j4\pi.10^{-4}.f(0.25 + \ln(931.783/0.00815)$$

$$Z_{SS} = 0.1027\,\Omega/km + 0.0493 + j0.06283(0.25 + \ln(931.783/0.00815)$$

$$\mathbf{Z_{SS} = 0.2636 + j0.7632\ \Omega/km}$$

Where subscript ss represents the static wire conductor

Rail with radius of $r_o = 0.0730$m and the conductor resistance of R=0.0240 Ω/km

$$Z_{RR} = 0.0240\,\Omega/km + 0.0493 + j4\pi.10^{-4}.f(0.25 + \ln(931.783/0.0730)$$

$$Z_{RR} = 0.0240\,\Omega/km + 0.0493 + j0.06283(0.25 + \ln(931.783/0.0730)$$

$$\mathbf{Z_{RR} = 0.07334 + j0.609744\ \Omega/km}$$

Where subscript RR represents the static wire conductor.

3.7.5.1.2 Mutual Impedance of the Line

In this section the mutual impedance of the traction catenary system is solved but only some of them are presented here, the mutual impedance of the conductors which is not seen here can be found in appendix B.

The mutual impedance between conductor a and conductor d is given by:

$$Z_{ad^1} = 9.869.10^{-4}.f + j4\pi.10^{-4}.f\ln(D_{ad}/D_{sa}) \qquad 3.78$$

D_{sa} = the distance between the conductors

D_{ad} = equivalent conductor at depth

Mutual impedance between the contact wire and the messenger wire

$$Z_{C1m1} = 9.869.10^{-4}.f + j4\pi.10^{-4}\ln(D_{ad}/D_{sa})$$

$$Z_{C1m1} = 0.0493 + j0.06283\ln(931.783/1.150)$$

$$\mathbf{Z_{C1m1} = Z_{C2m2} = 0.0493 + j0.4208\ \Omega/km}$$

Mutual impedance between the contact wire and the negative feeder wire

$$Z_{C1F1} = 9.869.10^{-4}.f + j4\pi.10^{-4}\ln(D_{ad}/D_{sa})$$

$$Z_{C1F1} = 0.0493 + j0.06283\ln(931.783/4.3539)$$

$$\mathbf{Z_{C1F1} = Z_{C2F2} = 0.0493 + j0.3371\ \Omega/km}$$

Mutual impedance between the contact wire and the static wire

$$Z_{C1S1} = 9.869.10^{-4}.f + j4\pi.10^{-4}\ln(D_{ad}/D_{sa})$$

$$Z_{C1S1} = 0.0493 + j0.06283\ln(931.783/4.3539)$$

$$\mathbf{Z_{C1S1} = Z_{C2S2} = 0.0493 + j0.3371\ \Omega/km}$$

Mutual impedance between the contact wire and the Rail line

$$Z_{C1R11} = 9.869.10^{-4}.f + j4\pi.10^{-4}\ln(D_{ad}/D_{sa})$$

$$Z_{C1R11} = 0.0493 + j0.06283\ln(931.783/5.3483)$$

$$\mathbf{Z_{C1R11} = Z_{C1R12} = 0.0493 + j0.3242\ \Omega/km}$$

$$\mathbf{Z_{C1R11} = Z_{C1R12} = Z_{C2R21} = Z_{C2R22}}$$

The following is a matrix showing the various impedances in Ω/km between the conductors of the system using Carson line based on the single track configuration as shown in figure 3.6.

Table 3.4: six by six Z-matrix for the single track

	C1	M1	F1	R11	R12	S1
C1	**0.2188+j0.7652**	0.0493+j0.4208	0.0493+j0.3371	0.0493+j0.3242	0.04934+j0.3242	0.0493+j0.3538
M1	0.0493+j0.4208	**0.2396+j0.7452**	0.0493+j0.3426	0.0493+j0.3120	0.0493+j0.3120	0.0493+j0.3546
F1	0.0493+j0.3371	0.0493+j0.3426	**0.1520+j0.7245**	0.0493+j0.2998	0.0493+j0.2946	0.0493+j0.4100
R11	0.0493+j0.3242	0.0493+j0.3120	0.0493+j0.2998	**0.0733+j0.6097**	0.0493+j0.4069	0.0493+j0.3118
R12	0.0493+j0.3242	0.0493+j0.3120	0.0493+j0.2946	0.0493+j0.4069	**0.0733+j0.6097**	0.0493+j0.3055
S1	0.0493+j0.3538	0.0493+j0.3546	0.0493+j0.4100	0.0493+j0.3118	0.0493+j0.3055	**0.2636+j0.7632**

The following is a matrix showing various impedances in Ω/km between the conductors of the system using Carson line based on the double track configuration as shown in figure 3.7.

Table 3.5: Twelve by Twelve Z-matrix for the double track

	C1	M1	F1	C2	M2	F2
C1	**0.2188+j0.7652**	0.0493+j0.4208	0.0493+j0.3371	0.0493+j0.3293	0.0493+j0.3276	0.0493+j0.2911
M1	0.0493+j0.4208	**0.2396+j0.7452**	0.0493+j0.3426	0.0493+j0.3276	0.0493+j0.3293	0.0493+j0.2923
F1	0.0493+j0.3371	0.0493+j0.3426	**0.1520+j0.7245**	0.0493+j0.2911	0.0493+j0.2923	0.0493+j0.2695
C2	0.0493+j0.3293	0.0493+j0.3276	0.0493+j0.2911	**0.2188+j0.7652**	0.0493+j0.4208	0.0493+j0.3371
M2	0.0493+j0.3276	0.0493+j0.3293	0.0493+j0.2923	0.0493+j0.4208	**0.2396+j0.7452**	0.0493+j0.3426
F2	0.0493+j0.2911	0.0493+j0.2923	0.0493+j0.2695	0.0493+j0.3371	0.0493+j0.3426	**0.1520+j0.7245**
R11	0.0493+j0.3242	0.0493+j0.3120	0.0493+j0.2998	0.0493+j0.3094	0.0493+j0.2979	0.0493+j0.2797
R12	0.0493+j0.3242	0.0493+j0.3120	0.0493+j0.2946	0.0493+j0.3009	0.0493+j0.2945	0.0493+j0.2736
S1	0.0493+j0.3538	0.0493+j0.3546	0.0493+j0.4100	0.0493+j0.2971	0.0493+j0.2973	0.0493+j0.2726
R21	0.0493+j0.3093	0.0493+j0.2979	0.0493+j0.2797	0.04934+j0.3242	0.0493+j0.3120	0.0493+j0.2998
R22	0.0493+j0.3009	0.0493+j0.2945	0.0493+j0.2736	0.04934+j0.3242	0.0493+j0.3120	0.0493+j0.2946
S2	0.0493+j0.2971	0.0493+j0.2973	0.0493+j0.2726	0.04934+j0.3538	0.0493+j0.3546	0.0493+j0.4100
	R11	R12	S1	R21	R22	S2
$C1$	0.0493+j0.3242	0.0493+j0.3242	0.0493+j0.3538	0.0493+j0.3093	0.0493+j0.3009	0.0493+j0.2971
$M1$	0.0493+j0.3120	0.0493+j0.3120	0.0493+j0.3546	0.0493+j0.2979	0.0493+j0.2945	0.0493+j0.2973

*F*1	0.0493+j0.2998	0.0493+j0.2946	0.0493+j0.4100	0.0493+j0.2797	0.0493+j0.2736	0.0493+j0.2726
C2	0.0493+j0.3093	0.0493+j0.3009	0.0493+j0.2971	0.04934+j0.3242	0.04934+j0.3242	0.0493+j0.3538
M2	0.0493+j0.2979	0.0493+j0.2945	0.0493+j0.2973	0.0493+j0.3120	0.0493+j0.3120	0.0493+j0.3546
F2	0.0493+j0.2797	0.0493+j0.2736	0.0493+j0.2726	0.0493+j0.2998	0.0493+j0.2946	0.0493+j0.4100
*R*11	**0.0733+j0.6097**	0.0493+j0.4069	0.0493+j0.3118	0.0493+j0.3293	0.0493+j0.3132	0.0493+j0.2875
R12	0.0493+j0.4069	**0.0733+j0.6097**	0.0493+j0.3055	0.0493+j0.3508	0.0493+j0.3293	0.0493+j0.2803
*S*1	0.0493+j0.3118	0.0493+j0.3055	**0.2636+j0.7632**	0.0493+j0.2875	0.0493+j0.2803	0.0493+j0.2763
R21	0.0493+j0.3293	0.0493+j0.3508	0.0493+j0.2875	**0.0733+j0.6097**	0.0493+j0.4069	0.0493+j0.3118
R22	0.0493+j0.3132	0.0493+j0.3293	0.0493+j0.2803	0.0493+j0.4069	**0.0733+j0.6097**	0.0493+j0.3055
S2	0.0493+j0.2875	0.0493+j0.2803	0.0493+j0.2763	0.0493+j0.3118	0.0493+j0.3055	**0.2636+j0.7632**

Table 3.4 and 3.5 shows the mutual and self-impedance of the transmission line conductor for both single and double track railway line configuration respectively. For the single track there are 6 self-impedance and 30 mutual impedance per kilometer and for the double track there are 12 self- impedance and 132 mutual impedance per kilometer. This impedance value will be used to model the catenary system in next chapter using MATLAB/Simulink mutual inductance element.

4 MODELING OF TRACTION POWER SUPPLY

In this chapter traction power supply system components will be modeled using MATALAB/ Simulink software.

4.1 INTRODUCTION

In the previous chapter we have designed different components of the traction power supply system, in this chapter based on results found in earlier chapter, modeling and integration of components using MATLAB/ Simulink software will be performed

4.2 LINE MODEL

In the autotransformer AC railway power feeding system described in this thesis, there are six main conductors to be considered. These are:

1. Contact wire
2. Messenger wire
3. Negative feeder
4. Rails and
5. Static wire

One interesting thing that can be seen in railway engineering is the use of the rail as a return conductor. For the single track, we have six conductors including the two rails and for the double track, twelve conductors including the four rails. To model the traction power supply line MATLAB/ Simulink mutual inductance element which is shown in the figure 4.1 below is used for both single and double track.

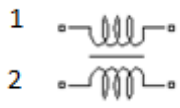

Figure 4.1: Mutual inductance element

The mutual inductance element shown above in figure 4.1 allows inserting winding 1 self-impedance (for example contact line impedance), winding 2 self-impedance (for example messenger wire impedance) and the mutual impedance (the mutual impedance of the contact line and the messenger wire) using block parameters shown below in figure 4.2.

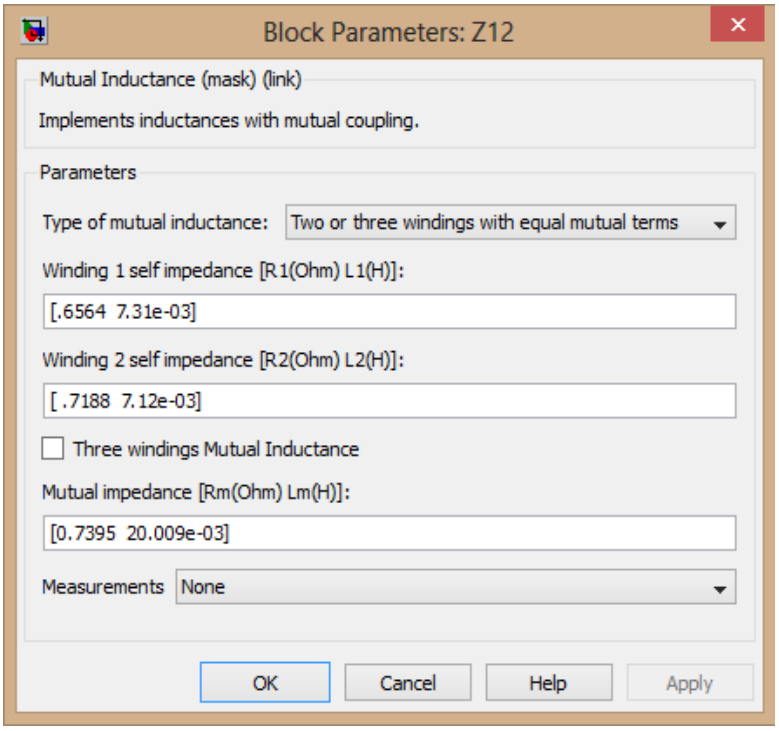

Figure 4.2: Mutual inductance block parameter

4.2.1 Single Track Line Model

Single track line (railway) is track having only a single pair of lines so that train can travel in only one direction at a time or a railway where trains travelling in both directions share the same track. As explained earlier for the single track there are six conductors, which give 36 full impedance matrixes, from which six of them are self-impedance and thirty of them are mutual impedance as presented in chapter 3.

For greater accuracy, each wire is modeled separately and no bundling of conductors was performed. To model the line in SimPower, the mutual inductance element is used. Figure 4.3

shows how this element is connected. For clarity, portions of the line model are shown enlarged in figures 4.4 and 4.5. The block parameters of the mutual impedance components are entered individually as shown in figure 4.2 and the numbers in parenthesis are real values which are taken from table 3.4 in chapter 3.

Winding 1 self-impedance (Example: contact line impedance), R and L:

(15 x 0.2188/5, 15 x 0.7652/314.159/5)

Winding 2 self-impedance (Example: messenger wire impedance), R and L:

(15 x 0.2396/5, 15 x 0.7452/314.159/5)

Mutual impedance (Example: mutual impedance of the contact wire and the messenger wire), R and L:

(15 x 0.0493, 15 x 0.4208/314.159)

The resistance and inductance values in parenthesis are multiplied by 15 because these values pertain to a section fifteen kilometer long and divided by 5, because each line or conductor is coupled to 5 other lines, which means there are 5 mutual impedances. The parameters of each individual's mutual impedance require a "self-impedance" parameter; hence, the total self-impedance of the line is divided by 5. The self-impedances (inductance) are divided by 314.159; because the given values (1.4459 for example) are the impedances per kilometer and converted to inductance by dividing 314.159($X_L = 2\pi fL = 2x3.14x50xL = 314.159 * L,\ then\ L = X_L/314.159$).Mathematical calculation can be found in Appendix B.

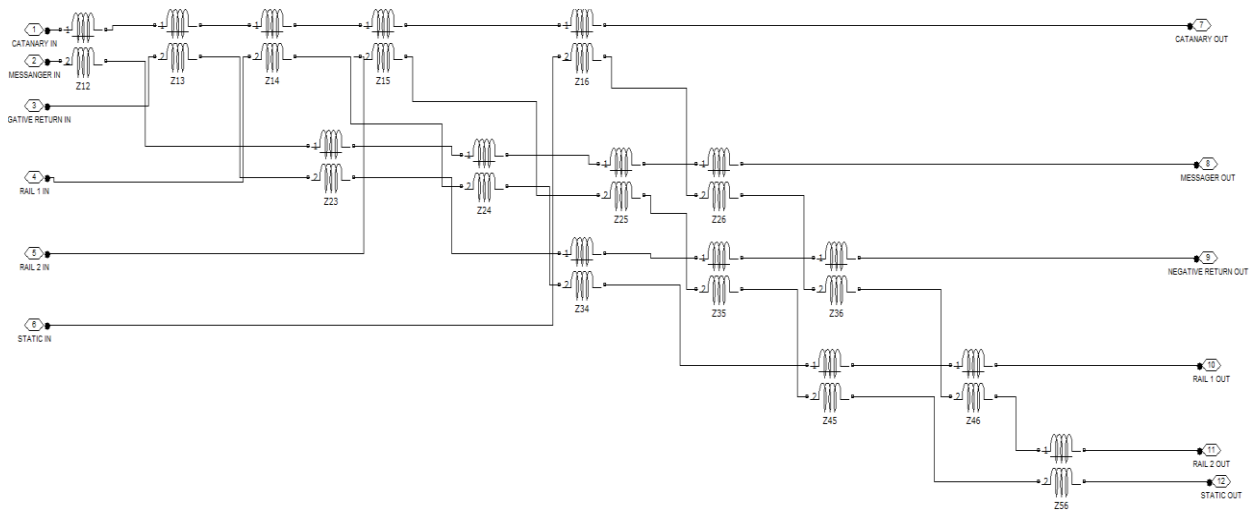

Figure 4.3: line model created using the mutual impedance element in SimPower

The two 25 kV (nominal) wires are to be connected to the catenary terminal of the AT, the three grounded wires are to be connected to the center tap of the AT, and the one feeder wires are to be connected to the -25 kV (nominal) of the AT. Therefore, the six input wires to the line diagram of figure 4.3 can be combined and form a set of three wires and the six output wires. These sets are appropriately called Catenary, Rail, and Feeder. If there are no trains in the section, the six wires can be represented by a line module having three inputs and three outputs as shown in figure 4.18. It should be emphasized that the lines in the module (within the box) are individually modeled and no bundling took place [20].

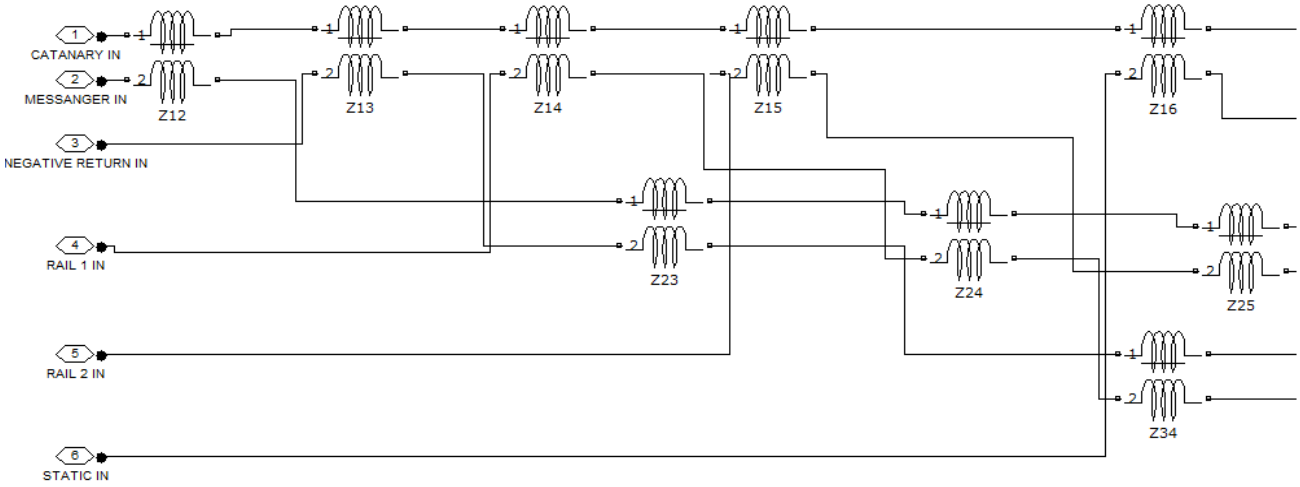

Figure 4.4: Input part of the line model

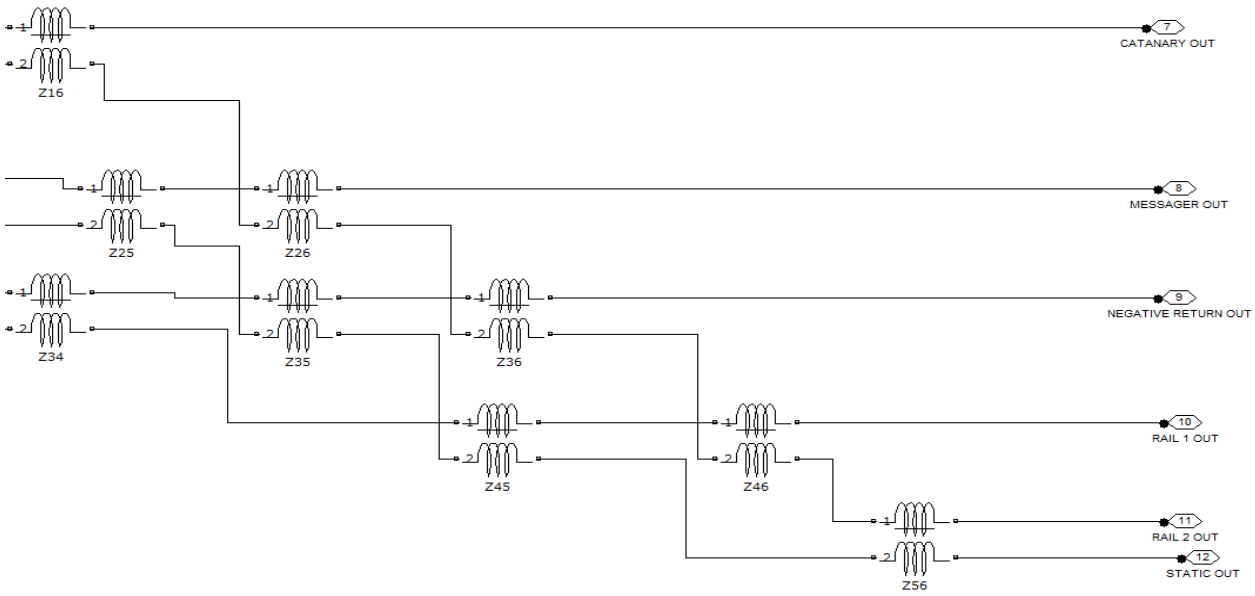

Figure 4.5: Output part of the single track line model

4.2.2 Double track line model

A double-track line usually involves running one track in each direction, compared to a single-track railway where trains in both directions share the same track.

For the double track line case, there are twelve conductors, which gives 144 full impedance matrix, from which twelve of them are self-impedance and one hundred twenty eight of them are mutual impedance as presented in chapter 3.

These are connected as shown in figure 4.6. For clarity, portions of the line model are shown enlarged in figures 4.7 and 4.8. The parameters of the mutual impedance components are entered individually and the numbers in parenthesis are real values which are taken from table 3.5.

Winding 1 self-impedance, R and L: **(4 x 0.2188/5, 4 x 0.7652/314.159/5)**

Winding 2 self-impedance, R and L: **(4 x 0.2396/5, 4 x 0.7452/314.159/5)**

Mutual impedance, R and L: **(4 x 0.0493, 4 x 0.4208/314.159)**

The resistance and inductance values in parenthesis are multiplied by 4 because these values pertain to a section fifteen kilometer long and divided by 11, because each line or conductor is coupled to 11 other lines, which means there are 11 mutual impedances. The parameters of each individual's mutual impedance require a "self-impedance" parameter; hence, the total self-impedance of the line is divided by 11. The self-impedances (inductance) are divided by 314.159; because the given values (1.4459 for example) are the impedances per kilometer and converted to inductance by dividing 314.159($X_L = 2\pi fL = 2x3.14x50xL = 314.159 * L$, $then\ L = X_L/314.159$).Mathematical calculation can be found in Appendix B.

The two 25 kV (nominal) wires are to be connected to the catenary terminal of the AT, the three grounded wires are to be connected to the center tap of the AT, and the one feeder wires are to be connected to the -25 kV (nominal) of the AT. Therefore, the twelve input wires to the line diagram of Figure 4.6 can be combined and form a set of three wires similarly the twelve output wires. These sets are appropriately called Catenary, Rail, and Feeder. If there are no trains in the section, the twelve wires can be represented by a line module having three inputs and three

outputs as shown in figure 4.19. It should be emphasized that the lines in the module (within the box) are individually modeled and no bundling took place.

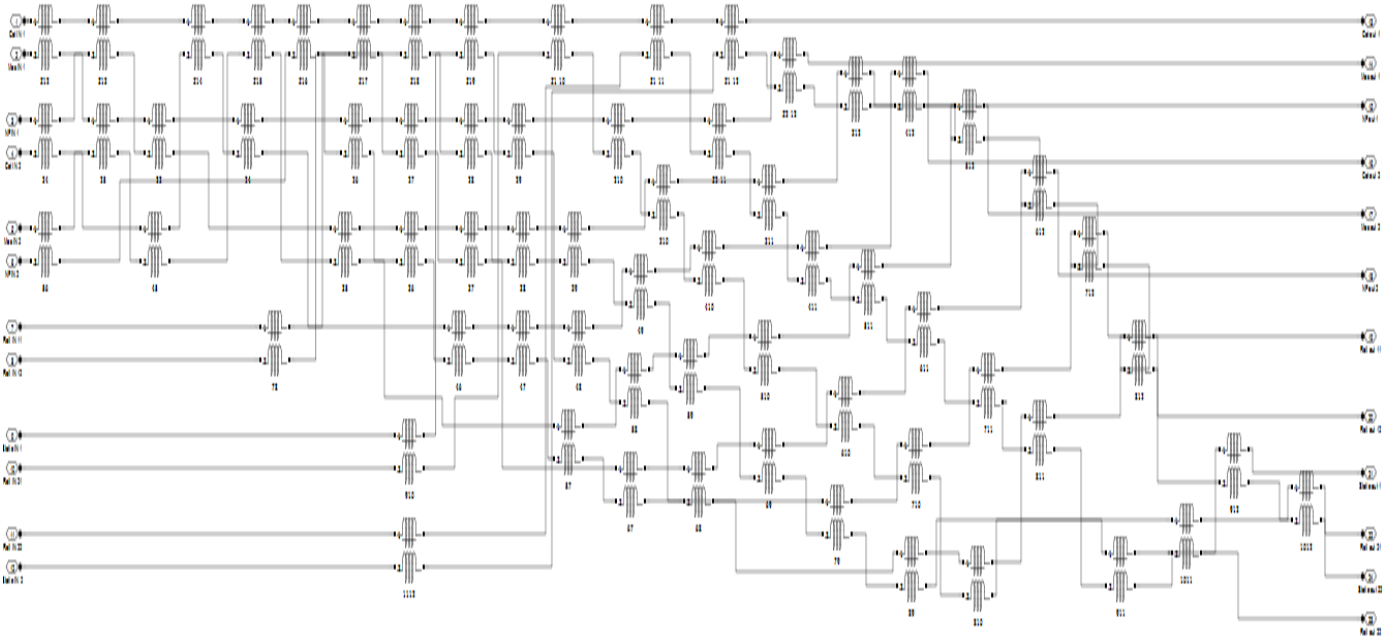

Figure 4.6: Double track line model created using the mutual impedance element

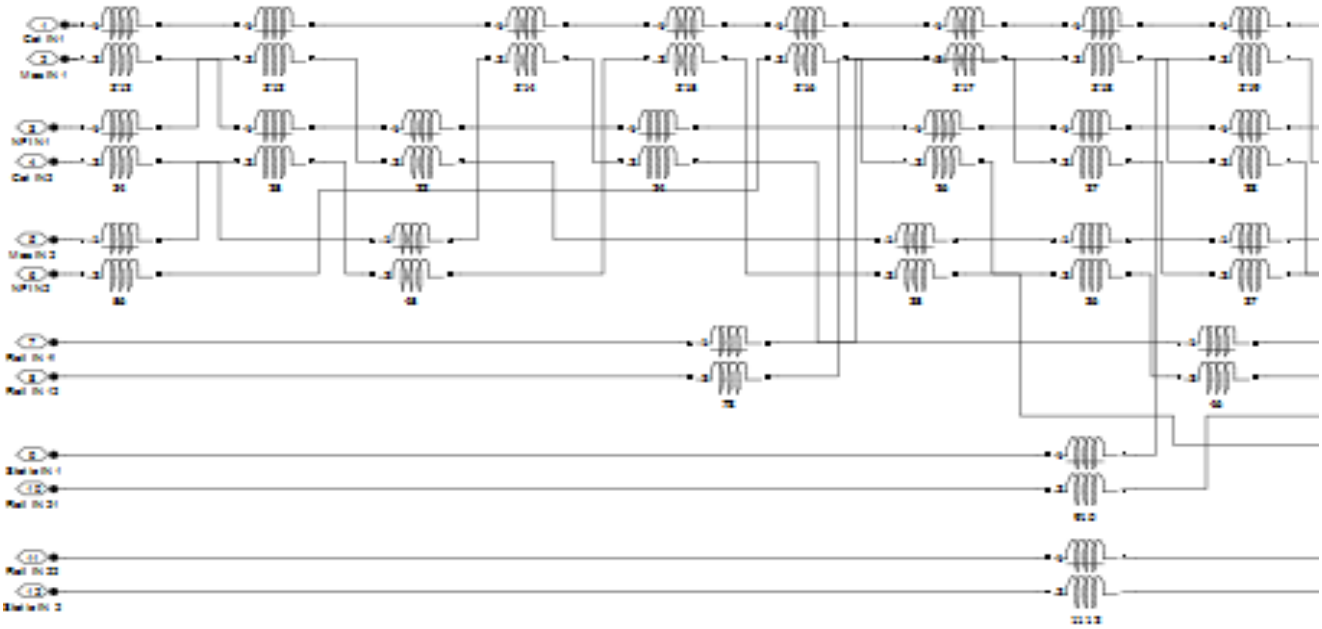

Figure 4.7: Input part of the double track line model

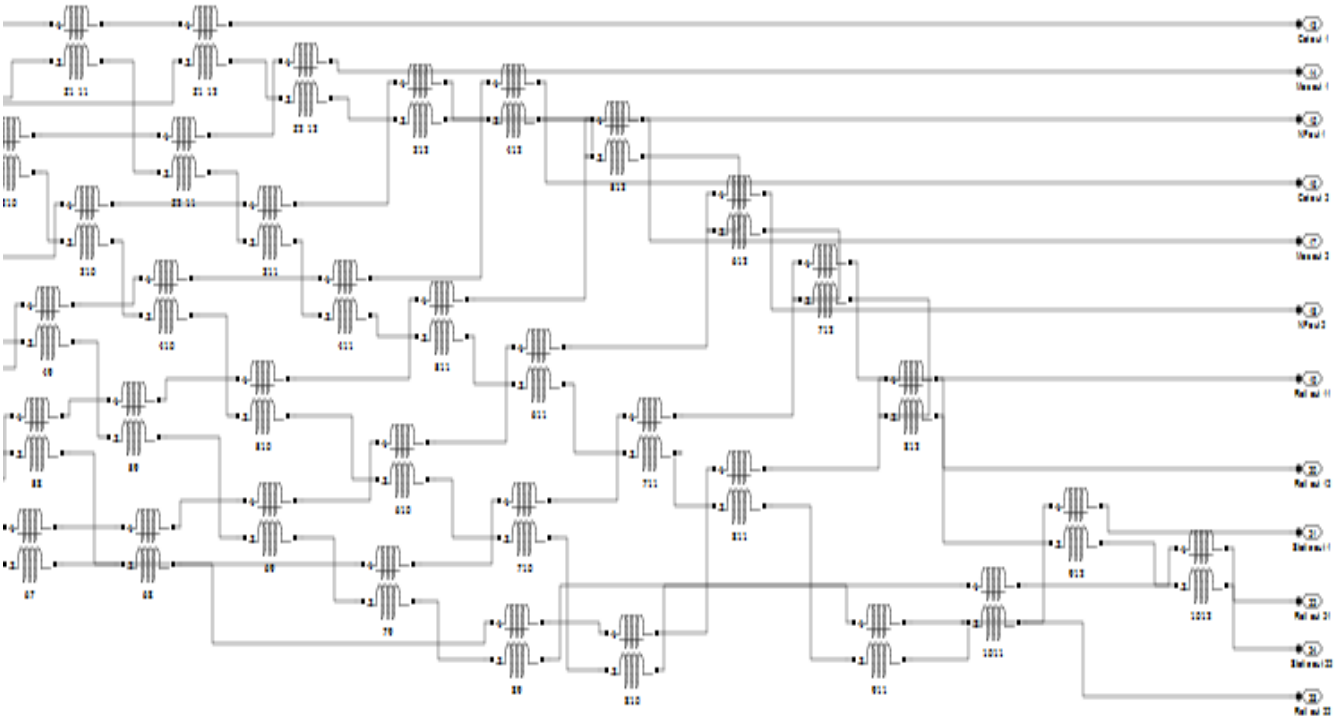

Figure 4.8: Output part of the double track line model

4.3 The Train Model

The train is modeled by a series RLC load. The parameters to be entered are shown in Figure 6.7.

Figure 4.9: Train model

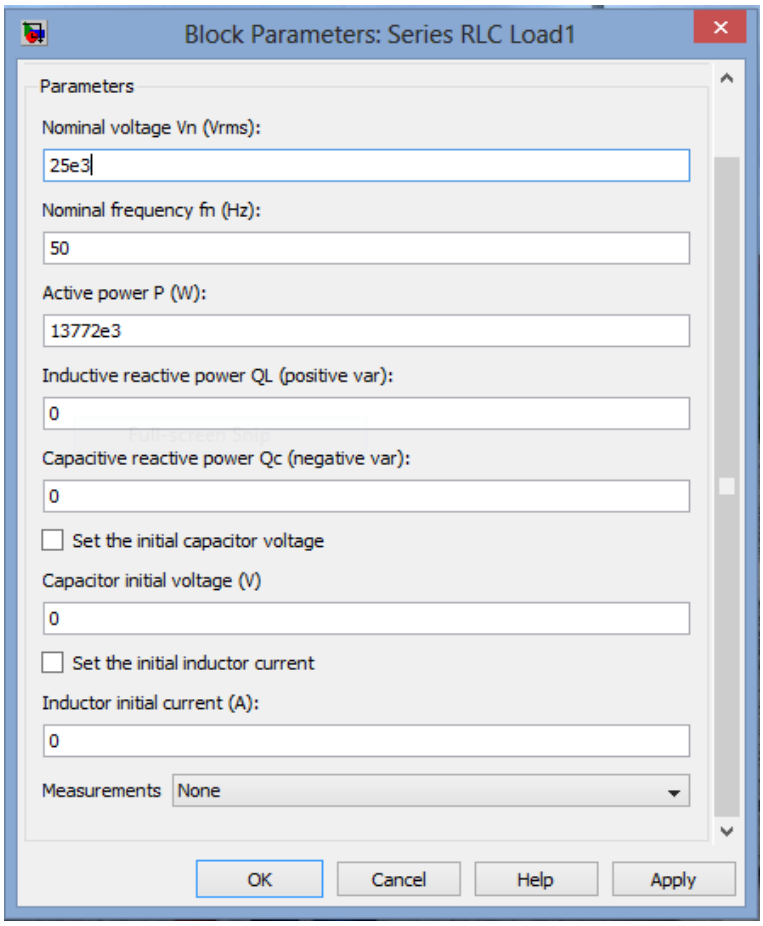

Figure 4.10: parameter window for the SimPower RLC load

4.4 The Measurements Module

Any current and voltage can be measured in a SimPower by simply inserting a current measurement block in series with the line. Any number of these current blocks can be combined in one module as shown in figure 4.12. This includes three current measurements blocks and shown in detail in figure 4.11. Voltages can be measured similarly by voltage measurement blocks to be inserted across the two points across which the voltage is to be measured.

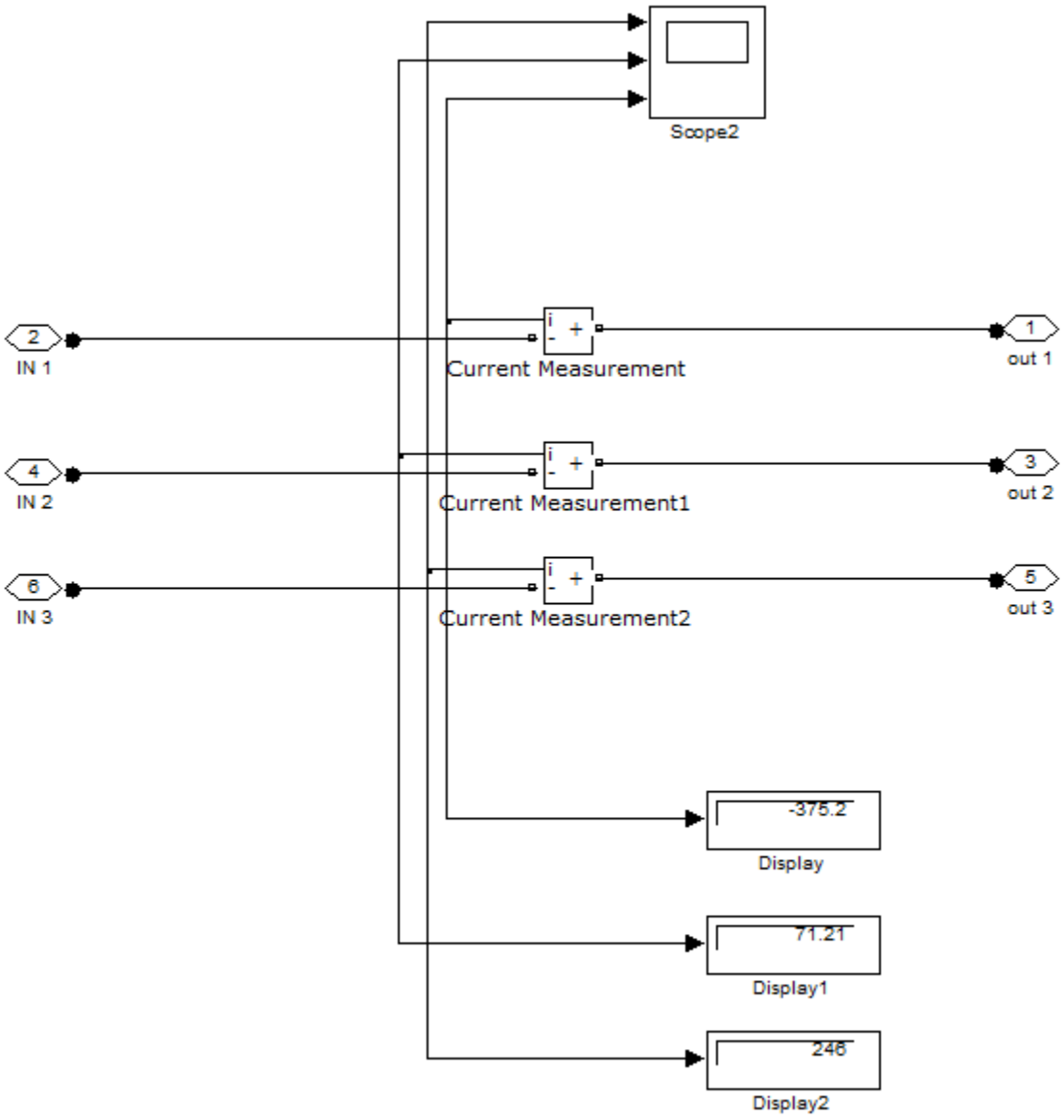

Figure 4.11: Current measurement blocks

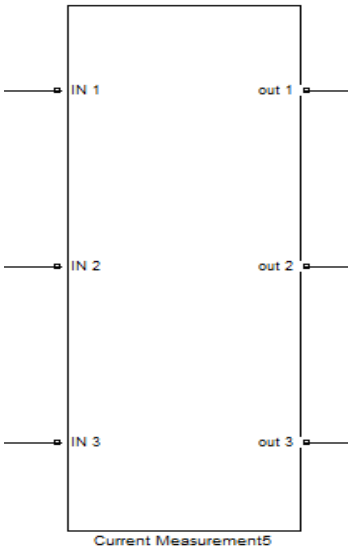

Figure 4.12: SimPower current measurement block

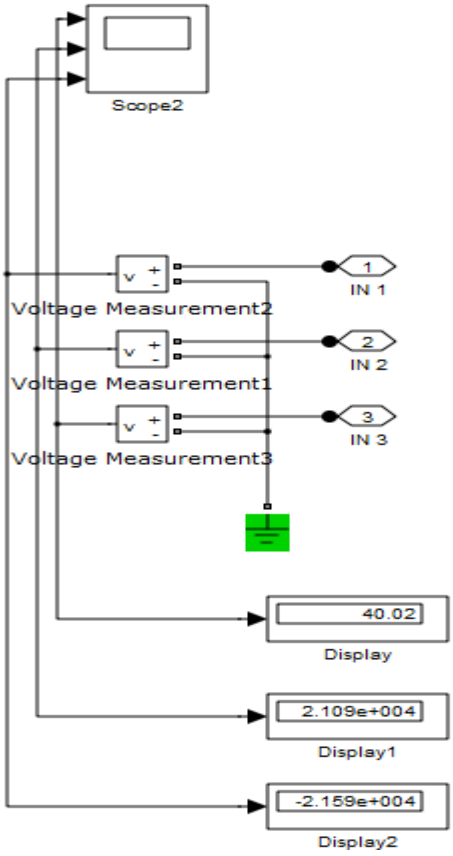

Figure 4.13: Voltage measurements

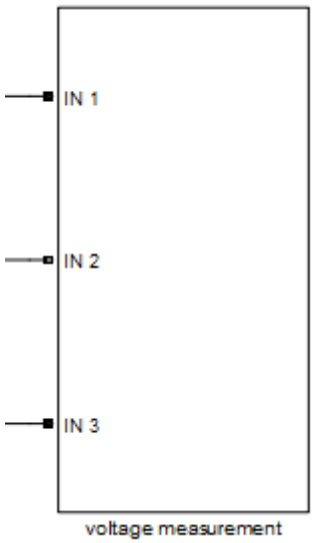

Figure 4.14: SimPower voltage measurement block

4.5 The Autotransformer Model

There is no autotransformer model in SimPower, therefore, a two-winding transformer is used and connected as an autotransformer [50]. This is shown in figure 4.15.

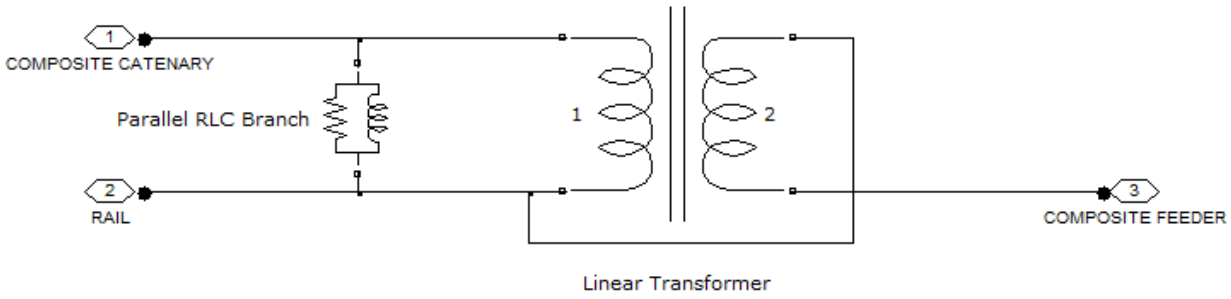

Figure 4.15: A SimPower two-winding transformer connected as an AT

The parameters requested for the two-winding transformer are entered as calculated in chapter three.

- Resistance (1e5 Ω)
- Inductance (1e5 H**)**
- Winding 1 parameters: (25e3 0.031 0.185)
- Winding 2 parameters: (25e3 0.031 0.185).

- Nominal power 10 MVA

Where e3, e5 are a matlab equivalent of 10^3 and 10^5 respectively. The shunt RL that appears in the transformer model is not used in our model and, therefore, arbitrary large values are entered.

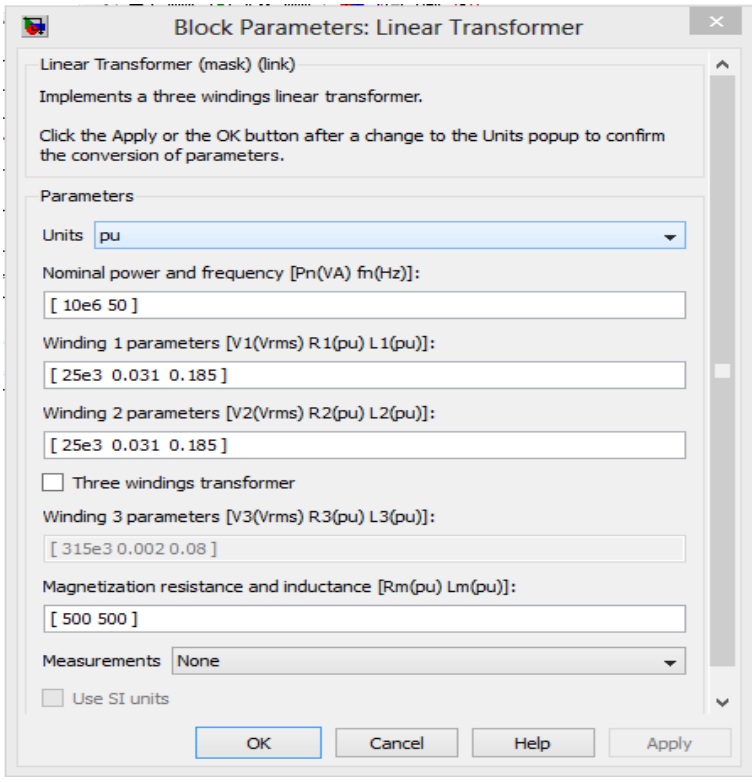

Figure 4.16: parameter window for SimPower linear transformer

4.6 Simulation of the Supply Substation

SimPower has models for different types of transformers including Zigzag, phase shifting, 3-phase, and Linear Transformer. The linear transformer appears closest to the substation transformer. It has three windings, a primary winding and two secondary windings. The two secondary windings can be connected at one end to form the center tap. Care should be taken when creating the center tap by connecting the LV end of one winding to the HV end of the other. The connected SimPower transformer to simulate the substation transformer is shown in figure 4.17. A detail explanation about linear transformer can be found in appendix C.

Typical data of the substation transformer are: primary voltage **132** kV; the no-load secondary voltage between the OCS and feeder is 55 kV with a grounded center tap; the MVA rating is 60 MVA, with 10% impedance and X/R ratio of 10. The calculated turn ratio is 132/55 = 2.4. The impedance of the primary will be assumed equal to that of the two secondary.

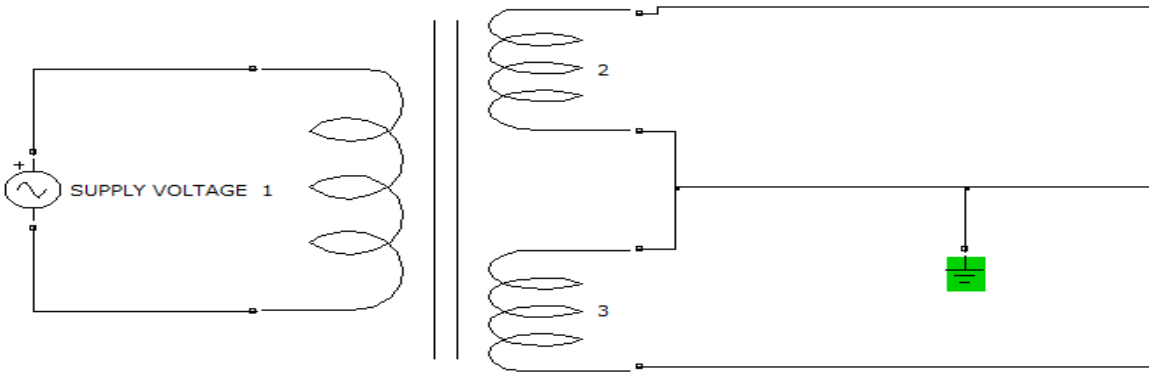

Figure 4.17: SimPower linear transformer connected to simulate a substation transformer

The following parameters must be entered in the description of this component; the values that are actually entered based on the previous paragraph are also shown in parenthesis:

Nominal power and frequency: (60e3 50 Hz)

Winding 1 parameters [V1(rms) R1(pu) L1(pu)]: (132e3 0.004975 0.04975)

Winding 2 parameters [V1(rms) R1(pu) L1(pu)]: (27.5e3 0.00124 0.0124)

Winding 3 parameters [V1(rms) R1(pu) L1(pu)]: (27.5e3 0.00124 0.0124)

Magnetizing resistance and reactance [Rm(pu) Lm(pu)]: (500 500)

The magnetizing impedance is usually neglected and arbitrary large values are entered in the last row.

The parameters of the other two windings are entered similarly.

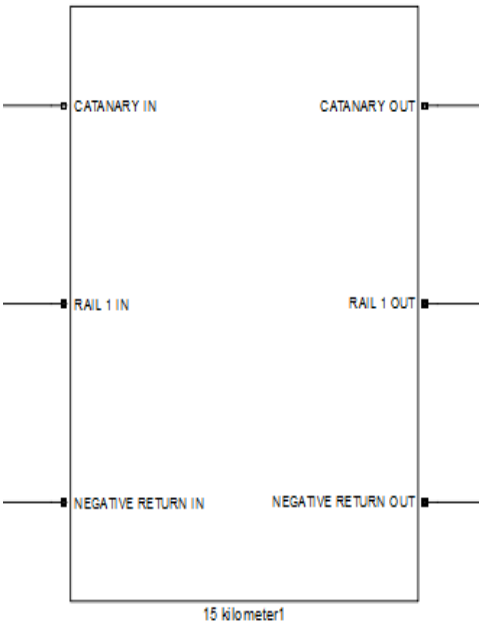

Figure 4.18: Line module with six wires forming three sets of wires

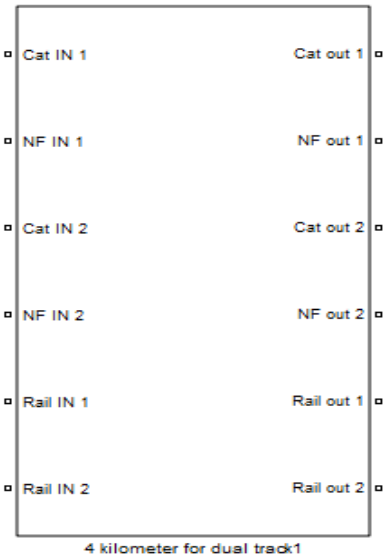

Figure 4.19: Line module with twelve wires forming three sets of wires

Here the number of input ports drawn on the Subsystem block's icon corresponds to the number of import blocks in the subsystem. Similarly, the number of output ports drawn on the block corresponds to the number of outport blocks in the subsystem.

4.7 Complete System Model

The complete system model as shown in figure 4.24 represents a sixty four kilometer long 2x25 kV autotransformer feeding system and is formed by integrating the following subsystem:

a) Substation transformer subsystem
b) Autotransformers subsystem
c) Overhead Catenary system subsystem
d) Train model
e) Measurements subsystem

For the sake of clarity the complete system model is divided into four parts and presented as shown in figures 4.20, 4.21, 4.22, and4.23.

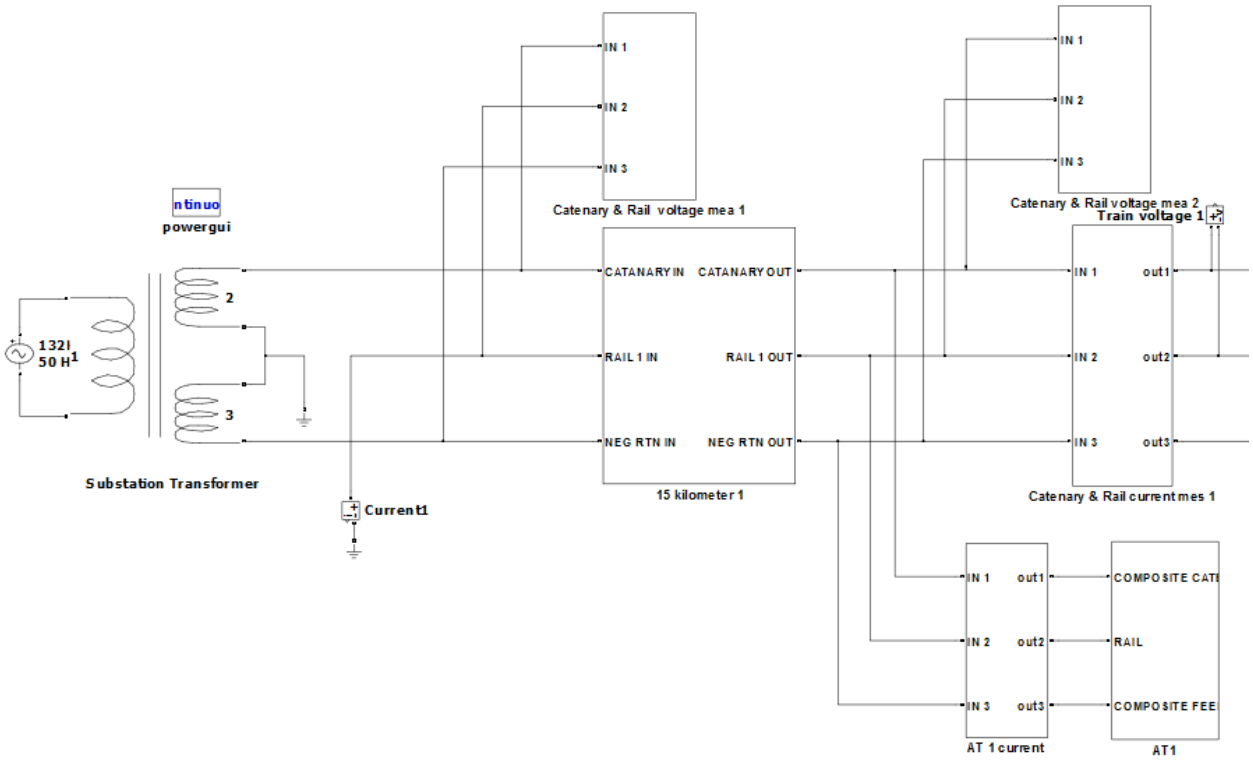

Figure 4.20: first part of the complete system

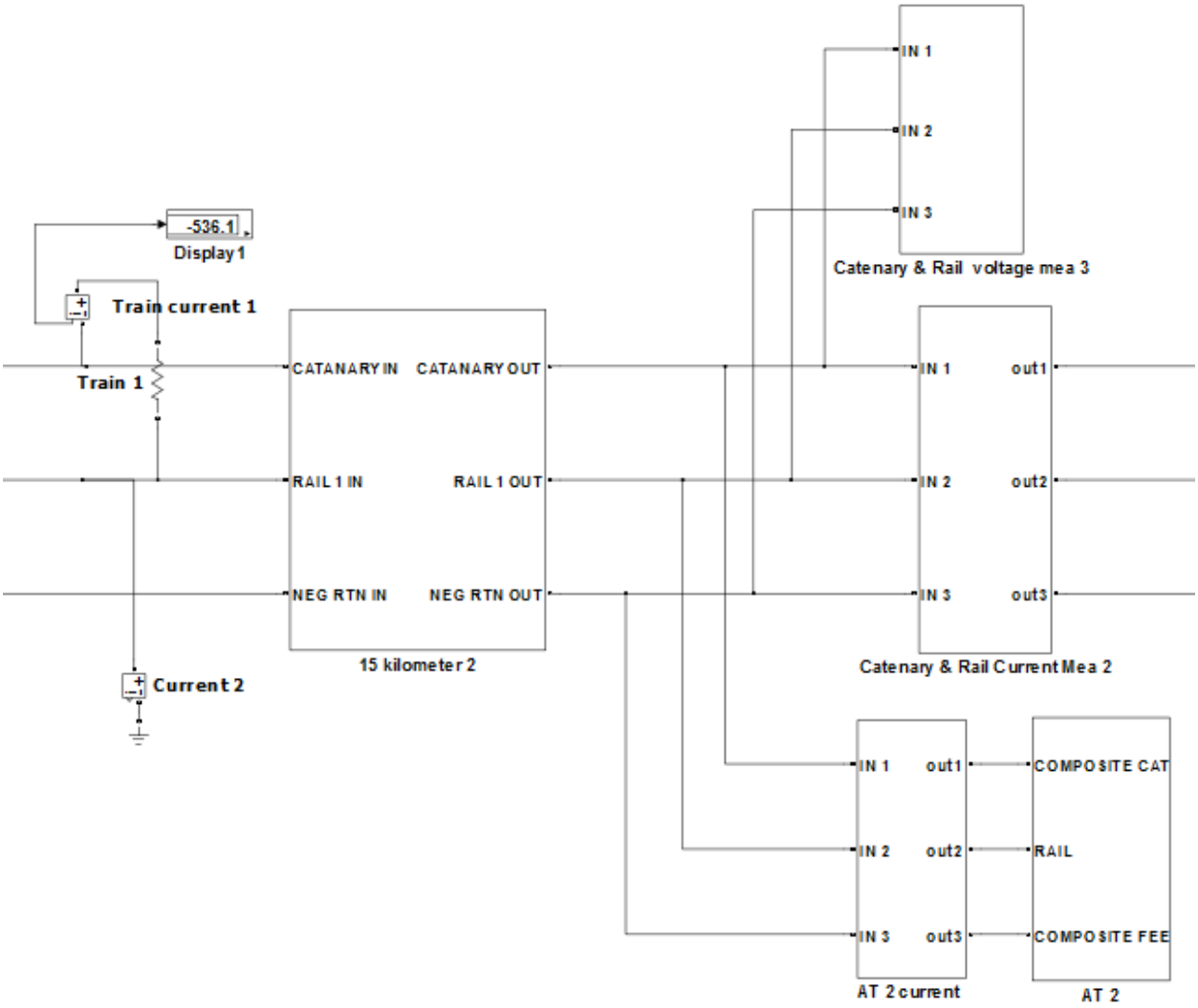

Figure 4.21: Second part of the complete system

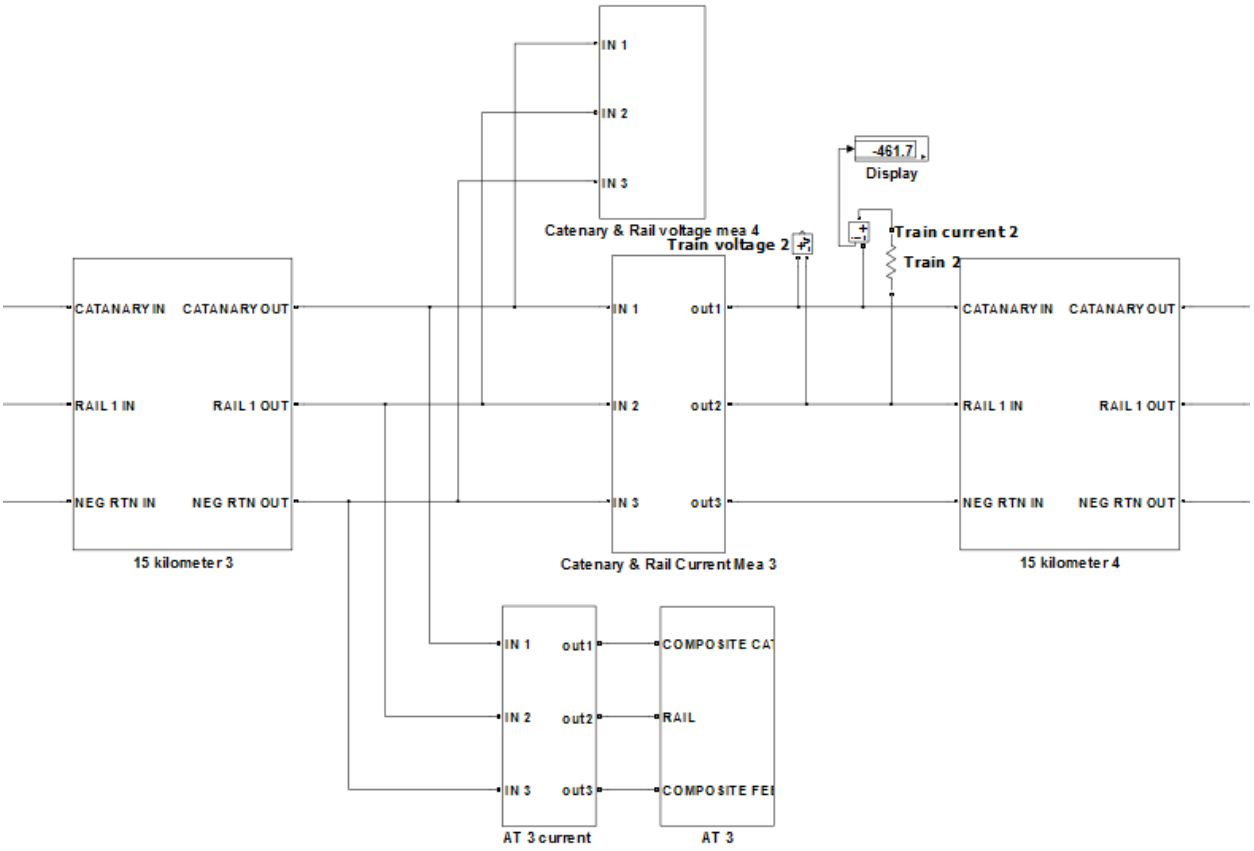

Figure 4.22: Third part of the complete system

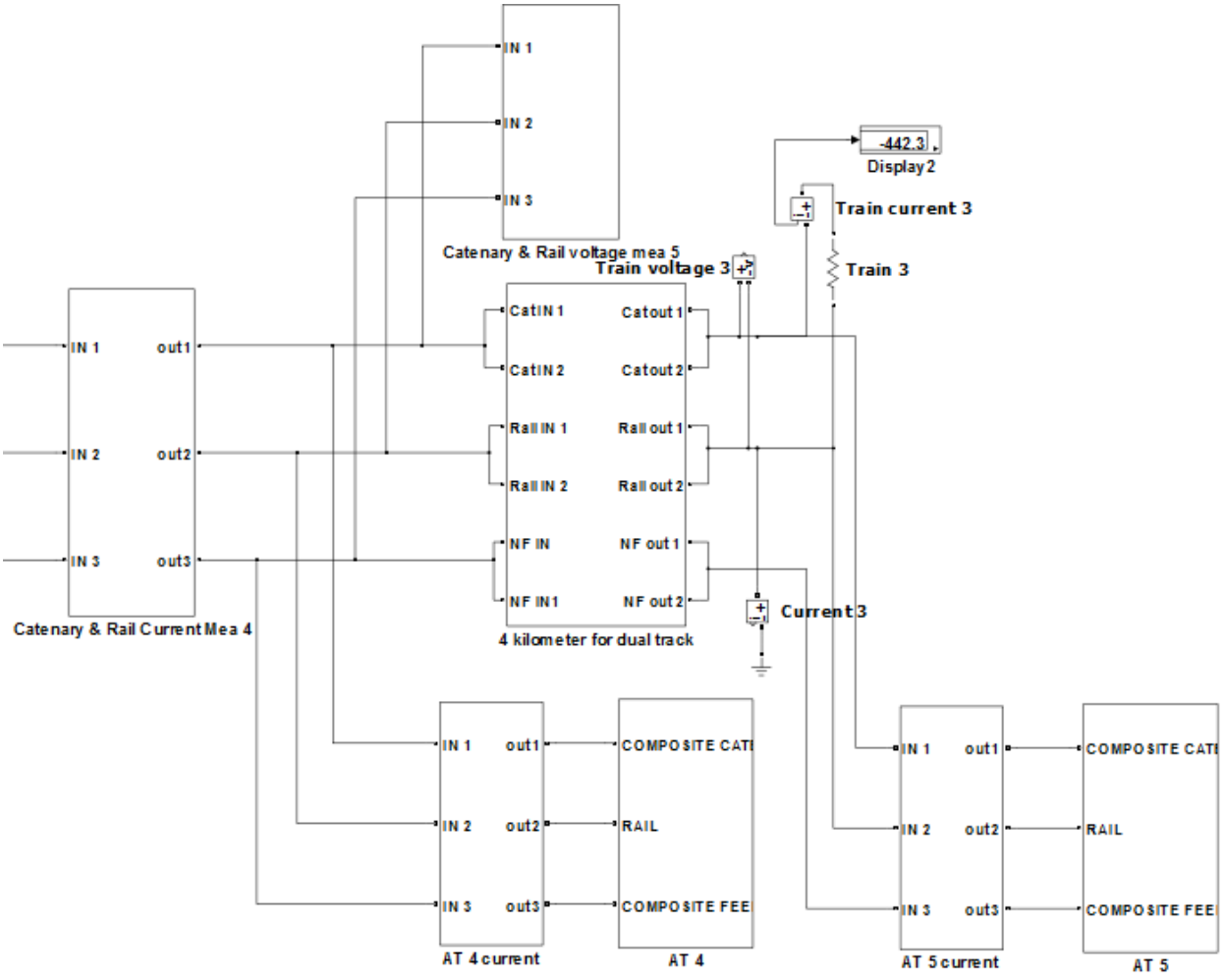

Figure 4.23: fourth part of the complete system

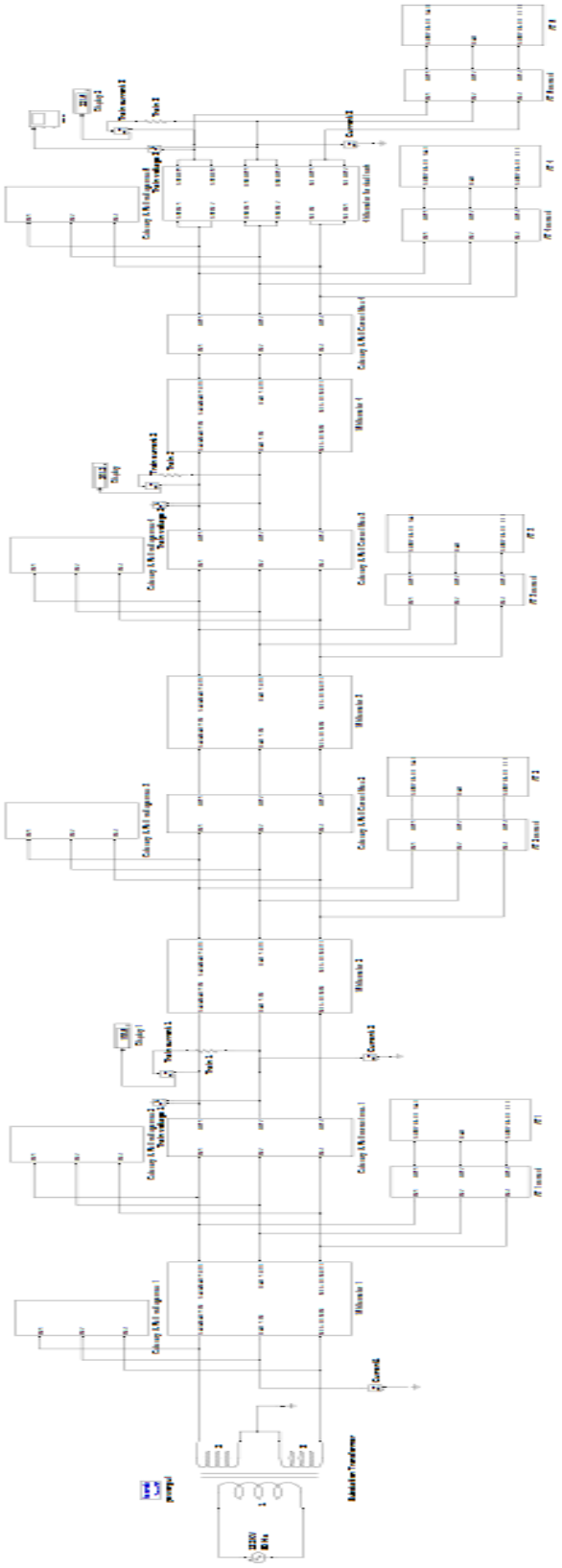

Figure 4.24: A block diagram of the complete system model

5 MATLAB Simulation and Discussion of Simulation Results

5.1 Introduction

The purpose of this simulation is to evaluate the designed autotransformer-fed power supply system for Modjo~Hawassa railway line corridors. Since voltage and current profile along the line are the most important parameters to evaluate the system performance, a computer-aided steady state load-flow simulation in terms of voltage and current were performed. In addition to that percentage voltage regulation was also employed to weigh the performance of the system.

The simulation of the traction power supply system is done using the Matlab /Simulink environment. SIMULINK® is a toolbox extension of the MATLAB program. It is a program for simulating static and dynamic systems. Simulink has the advantages of being capable of performing complex system simulations, graphical environment with visual real time programming and broad selection of toolboxes. The program is capable of solving both linear and nonlinear processes so it is perfectly suited to simulating traction power supply system.

The first step in simulating a traction power supply system is creating a model that represents components of a subsystem by using an existing blocks in the Simulink library or from those created by the user. The models presented in previous chapter are represented by their respective equivalent Simulink blocks. The second step is integrating those components of a subsystem and forming a system, in this case a traction power supply system, which have a total length of 64 kilometer including 60 kilometer single track and 4 kilometer double track railway model. In the developed model there are 26 subsystems. In this subsystem there are fifteen measurement modules, five autotransformer subsystem blocks, five overhead catenary subsystems and one substation power transformer block. Then the analysis is done for three different cases. The performance of the traction power system has been investigated by applying different headway distances on the trains and by increasing the number of train along the feeding section.

First , the study starts with the simple test of one train running in the feeding section with 5 ATs 15km apart. The supply voltage is 55kV (i.e. 2 x 27.5kV) and the feeding point is at one end of the section. In this case three different positions from the traction power substation were selected and analyzed. Followed by, the simulation of simultaneous operations of two

trains along the entire feeding section. For this case two different locations for each train were chosen.

Finally, the simulation is done with three coupled locomotives each having a maximum tractive effort of 441kN that able to haul full loaded freight trains. All the three train works cascaded together at the same time throughout the feeding section and also three carefully chosen spots were selected for the simulation. In all cases, the trains were all assumed to be identical. At the end of each case, simulation results obtained with respect to substation output voltage and current, train (pantograph) voltage and current, autotransformer voltage and current, will be discussed.

5.2 Simulink Model

A Simulink model of the traction power supply system can be found in chapter four figure 4.23, which is developed for three trains, the maximum possible number of traction load, which have a power consumption of 13.772 MVA. Each traction load is at its rated capacity and has a minimum spacing of 19 kilometer and a maximum of 49 kilometer between two consecutive trains.

5.3 Simulation parameters

The simulation parameters used in this thesis are based on the industry standards, literature reviews and some approximate calculation. Some methods for determining the parameters through calculation are given in the Appendix B and C. Summary of the simulation parameters can be found in appendix D.

5.4 Simulation Results and Discussions

The simulation of the model mentioned in section 4.2 or developed in chapter four figure 4.23 is done by using the above stated simulation parameters. In this section, results are presented in table format for the following cases, followed by discussion and also graphic results are given at the end of each case and the performance of the system is investigated by applying different headway distances on the trains and by increasing the number of train along the feeding section.

Case 1: when only one train is running across the entire feeding section and three specific positions (15, 45 and 64 km) from the traction power substation were chosen and made steady state load flow analysis one at a time.

Case 2: when two trains operates at the same time along the line. The locations of the train for this case are 15 and 45 km, and 15 and 64 km from the traction power substation, in other words the load flow analysis is performed based on two trains at a time.

Case 3: The simultaneous operations of three cascaded trains at different places (15, 45 and 64 km) from the traction power substation were selected and steady state load flow analysis is performed.

I. Case 1: single train

Table 5.1 and Table 5.2 show simulation result of voltages and currents respectively; Table 5.3 and Table 5.4 also present simulation result of autotransformer voltage and current. Accordingly, discussion is made based on the results.

Table 5.1: Simulation results of voltages at various distances from the traction substation for single train

Number of train	Distance in km	SS output voltage	Contact line voltage	Train 1 voltage	Train 2 voltage	Train 3 voltage	% voltage regulation
One train	15	54.832 kV	27.413 kV	26.676 kV	-	-	2.68 %
	45	54.764 kV	27.380 kV	-	25.47kV	-	6.97 %
	64	54.733 kV	27.365 kV	-	-	24.778kV	9.45 %

Table 5.2: Simulation results of currents at various distances from the traction substation for single train

Number of train	Train position in km	SS output Current(A)			Train 1 current(A)	Train 2 current(A)	Train 3 current(A)
one train	15	C	346.88	593.86	587.82	0	0
		N	246.98				
	45	C	338.85	567.14	0	561.28	0
		N	228.29				
	64	C	316.70	551.85	0	0	545.99
		N	235.15				

Table 5.1 shows that as the train moves away from the traction substation, the output voltage of the substation almost remains the same or the substation transformer voltage drop increases very slightly as the train moves from the feeding point to the other end, for instant, the voltage drop in the traction substation transformer increased by **0.18 %** comparing results of **train 1** position (15 km) with **train 3** position (64 km), which indicates that output voltage is more or less not affected by the train position. It can also be seen that the train voltage decreased from **26.67 kV** to **24.78 kV** as the train position changed from 15 km to 64 km along the feeding section, which shows that as the train distance increases relative to the traction substation, the impedance of the traction network lifts up which in turn leads to rises in voltage drop across the catenary system. In addition percentage voltage regulation of the overhead line increased from **2.68 % to 9.45 %**.

Table 5.2 also indicates the train current decreases when the distance from the substation increases, this is because as the trains distance increases, small amount of current flows in different circuits such as autotransformers that does not have train in between (theoretically this current should not flow into this autotransformers but practically that is not the case because it only works for ideal autotransformers) and cause the current to return to the substation via the return conductors and it is found that the train current decreases from **587.82 A to 545.99 A** along the feeding section.

Table 5.3: Simulation results of autotransformer voltages for the single train at a distance of 15 km and 64 km from the traction substation

Train position		AT 1	AT 2	AT 3	AT 4	AT 5
		Magnitude	Magnitude	Magnitude	Magnitude	Magnitude
15 km	**C**	26.67 kV	26.78 kV	26.85 kV	26.86 kV	26.87 kV
	R	0.000 V	66.22 V	0.000 V	6.87 V	0.000 V
	N	27.21 kV	27.02 kV	26.92 kV	26.89 kV	26.88 kV
64 km	**C**	26.69 kV	26.06 V	25.47 kV	24.87 kV	24.78 V
	R	0.000 V	29.96 V	0.00 V	23.47 V	0.00 V
	N	26.73 kV	26.16 V	25.67 kV	25.34 kV	25.366 kV

Table 5.4: Simulation results of autotransformer current for the single train at a distance of 15 km from the traction substation

	AT 1	AT 2	AT 3	AT 4	AT 5
	Magnitude(A)	Magnitude(A)	Magnitude(A)	Magnitude(A)	Magnitude(A)
C	78.71	35.13	15.42	6.45	5.91
R	158.6	71.44	31.97	13.9	12.83
N	79.93	36.31	16.56	7.52	6.95

Table 5.3 shows the autotransformer voltage is within the recommended ranges with the maximum and minimum value of **27.21 kV** and **24.78 kV** respectively. It is also recorded that **66.2 V** become the highest rail voltage through the feeding section, which is below the maximum permissible rail voltage according to European standards BS EN 50122-1 (IEC 62128-1) whereas the lowest value is **zero**.

Table 5.4 indicates that the sum of current in all autotransformers equals to **train 1 current** as shown in **table 5.2**, which is **583 A**, this is because, in autotransformer fed system the train is

always in between two paralleling or autotransformer stations, due to this, theoretically the train current distributed only between the two neighboring autotransformers depending on their distance from the train but practically this is not true, small amount of currents passes to the next autotransformers as shown in **table 5.4.**

From **Table 5.1**, **Table 5.2**, **Table 5.3 and Table 5.4** it is possible to conclude that the results of voltage and current obtained from the steady state simulation for a single train running at various positions from the traction substations confirms with EN 50163: 2004, BS EN 50122-1 (IEC 62128-1) and EN 50388:2012 standards, which reveals that our objective for this case is achieved successfully.

In the following section, selected graphic results for the above case, **case 1** is presented. Just looking at the graphs for all cases it is possible to say which case would have the highest or lowest currents or voltages. The simulation enables us to quantify this currents or voltages.

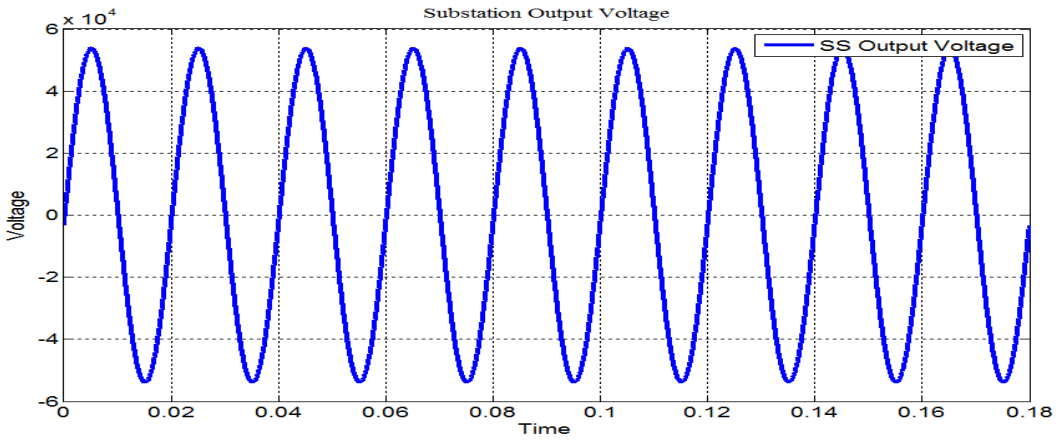

Figure 5.1: Substation Output Voltage when the train is at 15 km

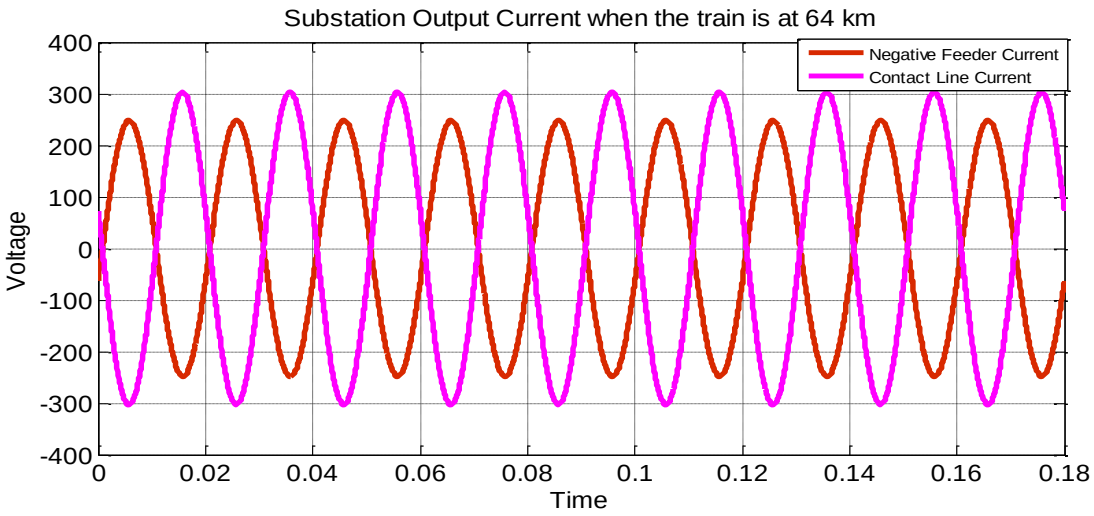

Figure 5.2: substation output voltage when the train is at 64 km

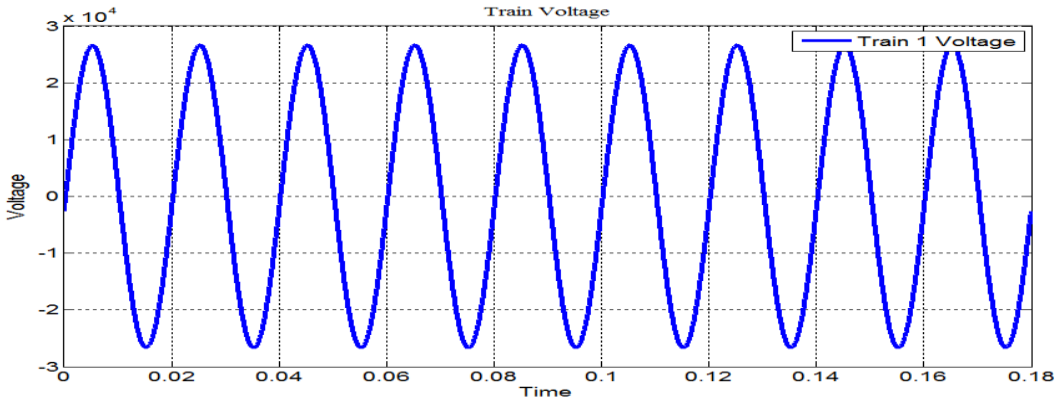

Figure 5.3: Train Voltage at 15 km

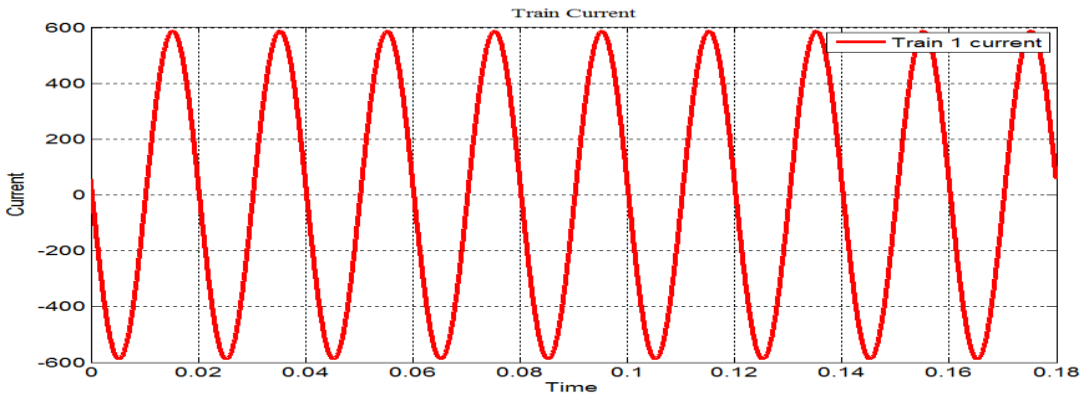

Figure 5.4: Train current at 15 km

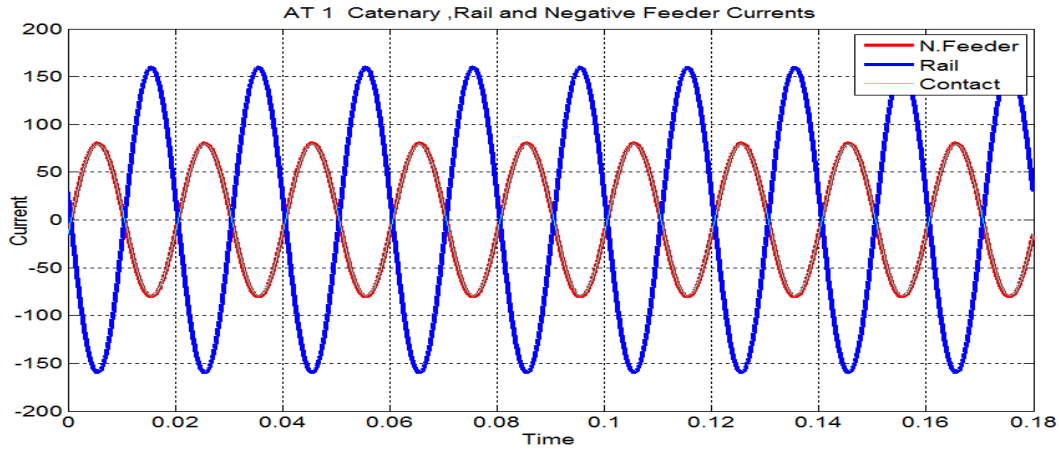

Figure 5.5: Autotransformer 1 currents

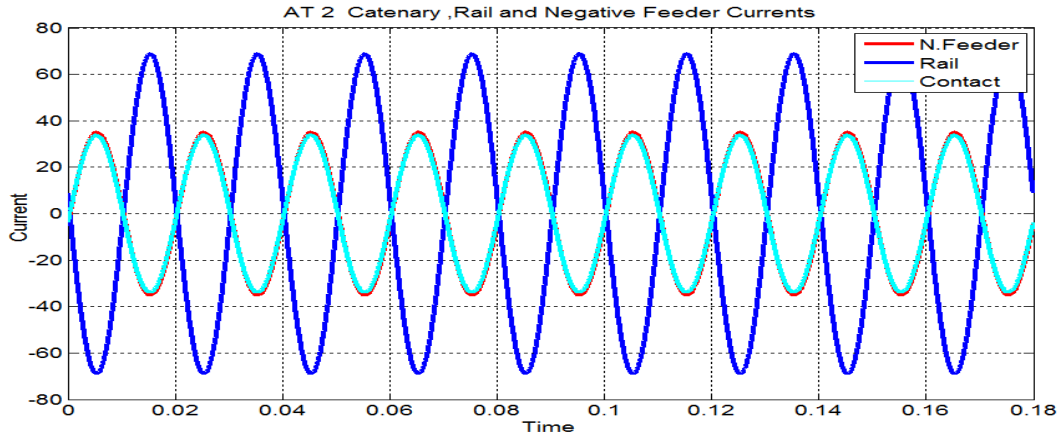

Figure 5.6: Autotransformer 2 currents

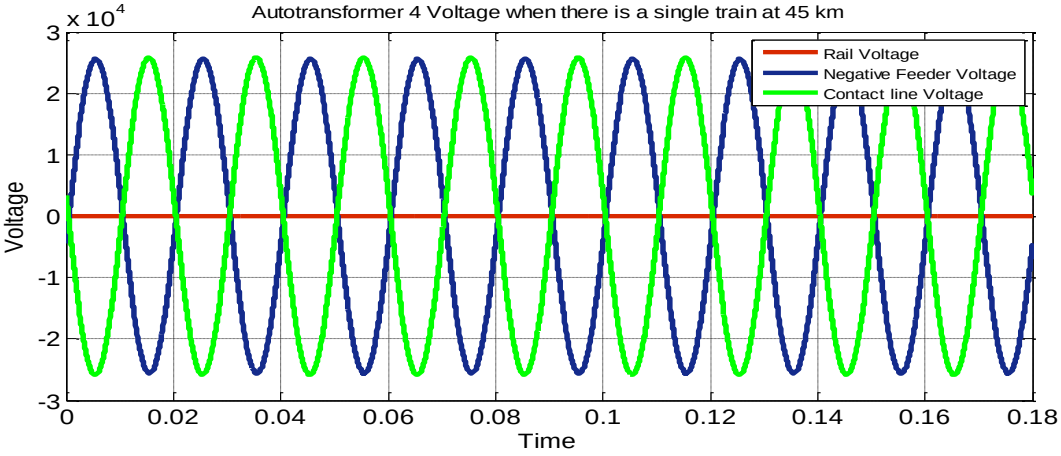

Figure 5.7: Autotransformer 4 voltage when the train is at 45 km

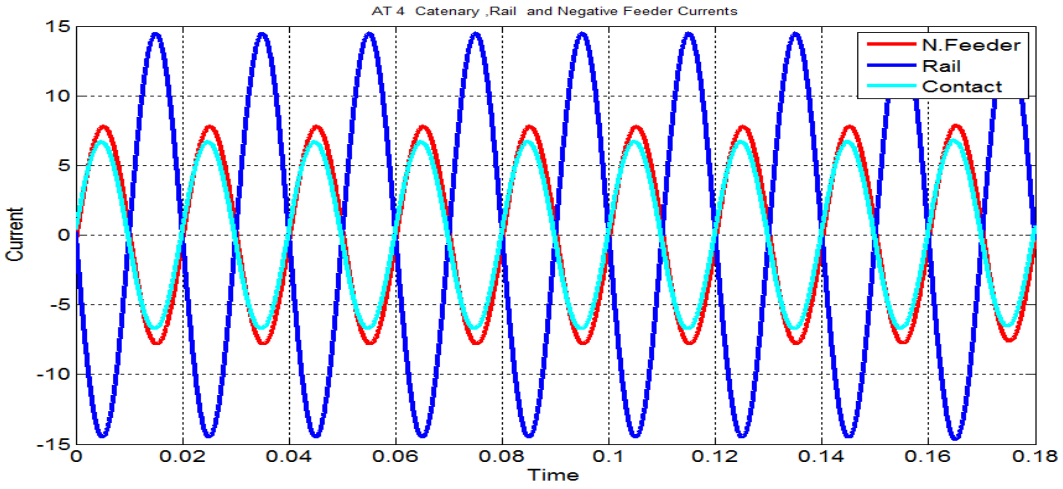

Figure 5.8: Autotransformer 4 currents

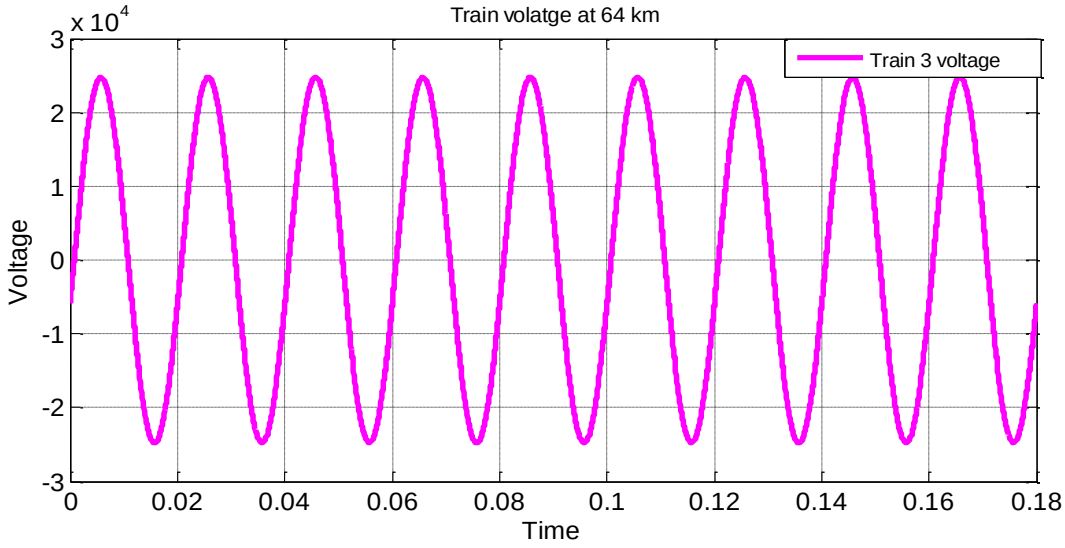

Figure 5.9: Train voltage when the locomotive is at 64 km

II. Case 2. Two trains

Simulation results of this case are illustrated in Table 5.5, Table 5.6 , Table 5.7 and Table 5.8, followed by discussions.

Table 5.3: Simulation results of voltages at various distances from the traction substation for two trains

Number of train	Distance in km	SS output voltage	SS output Contact line voltage	Train 1 voltage	Train 2 voltage	Train 3 voltage	% voltage regulation
Two train	15 & 45	54.53 kV	27.26 kV	25.85 kV	24.82 kV	-	8.95 %
	15 & 64	54.51 kV	27.25 kV	25.84 kV	_	24.18 kV	11.26 %
	45 & 64	54.37 kV	27.18 kV	-	23.24 kV	22.76 kV	14.50 %

Table 5.4: Simulation results of currents at various distances from the traction substation for two trains

Number of train	Distance in km	SS output Current(A)			Train 1 current(A)	Train 2 current(A)	Train 3 current(A)
Two train	15 & 45	C	758.96	1121.01	569.58	546.92	0
		N	362.05				
	15 & 64	C	736.41	1105.00	569.35	0	532.84
		N	368.59				
	45 & 64	C	596.95	1018.87	0	512.07	501.59
		N	421.92				

Table 5.5 tells that as the trains' runs away from the traction power substation; the substation outputs voltage still very nearly the same or decreases very slightly, for example the voltage drop in the traction substation transformer increased by **0.29 %** comparing results of **train 1** position (15 km) with **train 3** position (64 km) and the maximum voltage drop of the substation

transformer increased by **0.6 %** compared with **case 1**, which shows that the output voltage is not affected by both the number of trains and trains positions.

It can also be seen that the maximum (**25.85 kV**) and the minimum (**22.76 kV**) train voltage is reduced by **3.1 %** and **8.14 %** respectively as compare with **case 1** that have equal distance from the traction substation, this is because as the number of train increases, the current flowing through the traction catenary network increases, which leads to a higher voltage drop. Therefore, each train on the system is being affected by other trains and also each train affects all other trains on the system. For example in the previous case, **case 1**, the value of **train 1 voltage** is found to be **26.676 kV** at a distance of 15 km from the traction substation as shown in **table 5.1,** but **25.85 kV** for the same train at the same position from the traction substation for **case 2**. This voltage variation at the pantograph affects train performance. When the voltage decreases, the acceleration, and, therefore, the velocity and the location of the train are altered. Conversely, when the system presents high voltage to the train, the rolling stock can accelerate at full rate and reach the maximum operating speed in shorter time. Thus, it is possible to say that two identical trains consisting with identical stopping pattern will have different trip times, depending on the number of train on the feeding section. Moreover, this higher voltage drop or voltage variation across the line causes the percentage voltage regulation to rise from **8.95 %** to **14.50 %.**

Table 5.6 also clearly indicates that when the distance from the substation increases, the train current reduced, owing to the same reason as it is stated in **table 5.3** and it is found that the train current varies from **587.82 A to 545.99 A** along the feeding section.

Table 5.5: Simulation results of autotransformer current for two train at a distance of 15 km from the traction substation

	AT 1	**AT 2**	**AT 3**	**AT 4**	**AT 5**
	Magnitude(A)	Magnitude(A)	Magnitude (A)	Magnitude (A)	Magnitude (A)
C	92.19	71.41	105.93	45.07	42.06
R	185.58	143.94	212.98	91.21	85.17
N	93.39	72.54	107.05	46.14	43.11

Table 5.6: Simulation results of autotransformer voltage for the simultaneous operations of two trains at a distance of 15 km & 45 km and 45 km & 64 km from the traction substation

Train position		AT 1	AT 2	AT 3	AT 4	AT 5
		Magnitude	Magnitude	Magnitude	Magnitude	Magnitude
15 & 45 km	**C**	25.85 kV	25.35 kV	24.82 kV	25.19 kV	25.00 kV
	R	0.000 V	39.7 V	0.000 V	46.12 V	0.000 V
	N	26.48 kV	25.84 kV	25.44 kV	24.98 kV	25.16 kV
45 & 64 km	**C**	25.72 kV	24.39 kV	23.24 V	22.83 kV	22.76 kV
	R	0.000 V	77.30 V	0.000 V	42.84 V	0.000 V
	N	25.89 kV	24.82 kV	24.00 kV	23.46 kV	23.45 kV

Table 5.7 shows that as the train distance and number increases the autotransformer output voltage generally decreases because as the number of the train and its distance increases the autotransformer catenary to rail voltage decreases due to voltage drop along line, but it is within the recommended ranges specified by EN 50163: 2004 with the maximum and a minimum value of **26.48 kV** and **22.76 kV** respectively. It is also observed that **46.12 V** become the highest rail voltage through the feeding section, BS EN 50122-1 (IEC 62128-1) while the lowest value is zero.

Due to the same reason as it is mentioned for **Table 5.4**, the sum of the autotransformers currents equals with sum of train currents which is found at 15 km and 45 km from the traction substation. This can be clearly seen in **Table 5.8**.

From **Table 5.5**, **Table 5.6**, **Table 5.7 and Table 5.8** it is possible to conclude that the results of voltage and current obtained from the steady state simulation for two trains running at various positions from the traction substations confirms with EN 50163: 2004, BS EN 50122-1 (IEC 62128-1) and EN 50388:2012 Standards, which reveals that our objective for this case is also achieved successfully.

In the following section, selected graphic results for the above case, **case 2** is presented. Just looking at the graphs for all cases it is possible to say which case would have the highest or lowest voltages or currents. The simulation enables us to quantify this currents and voltages.

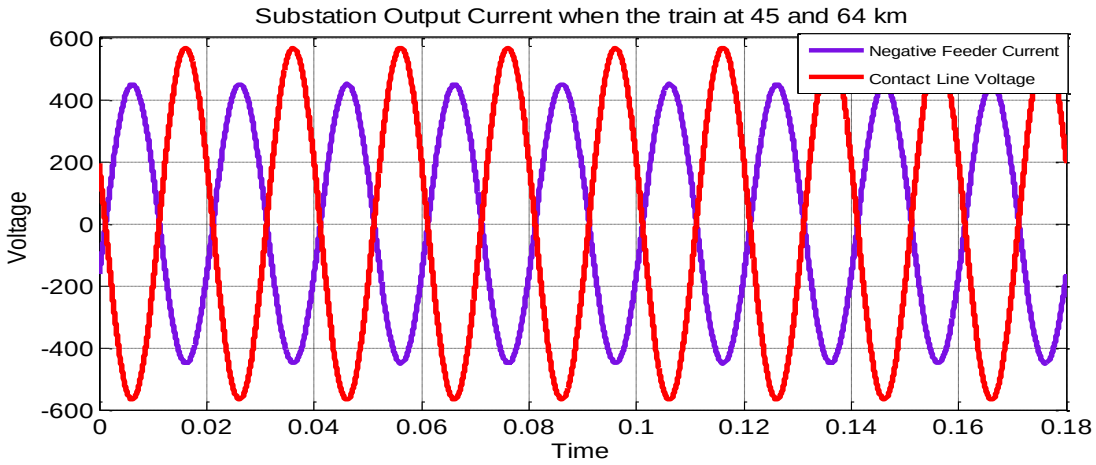

Figure 5.10: Substation Output Currents when the train is at 45 km and 64 km

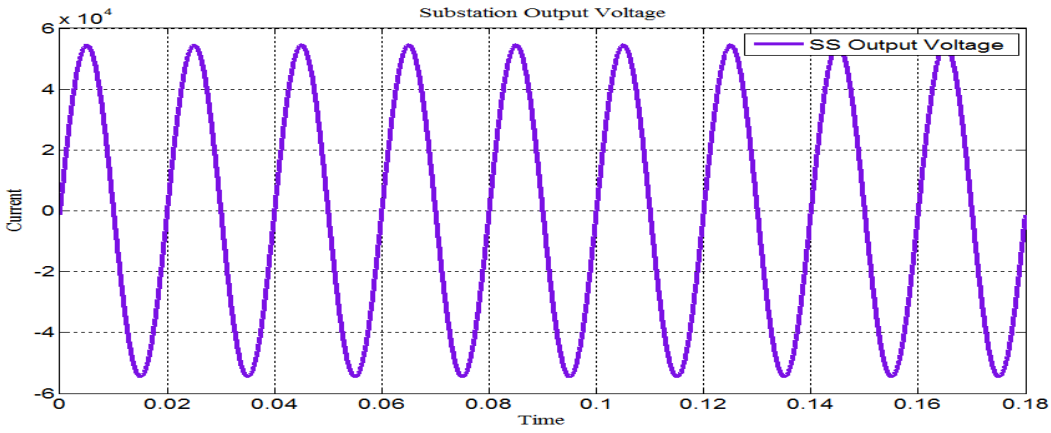

Figure 5.11: Substation Output Voltage when trains are at 15 km and 64 km

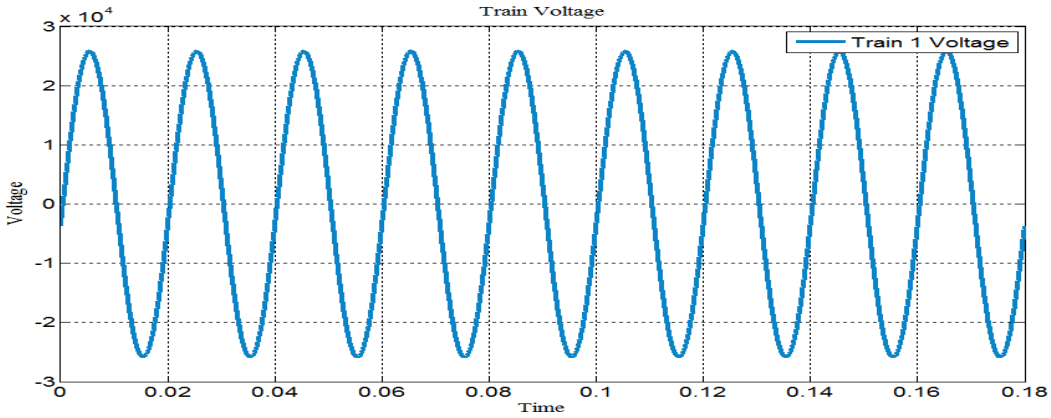

Figure 5.12: Train Voltage at 15 km

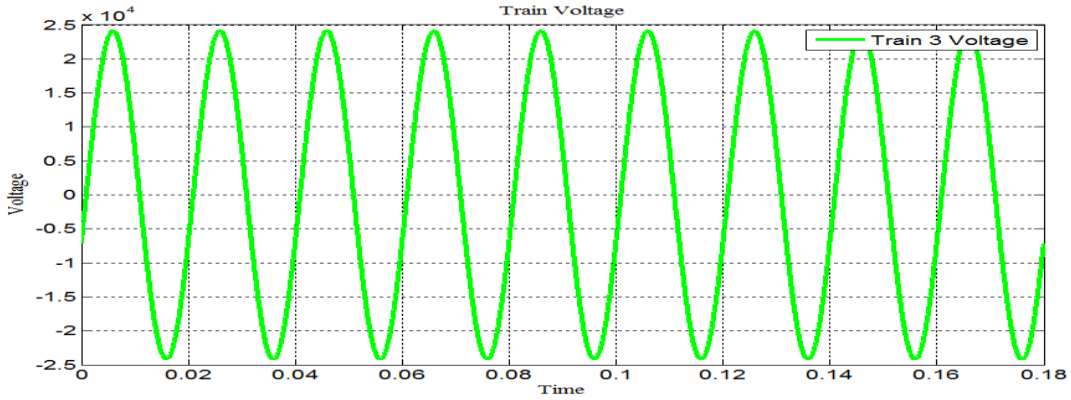

Figure 5.13: Train Voltage at 64 km

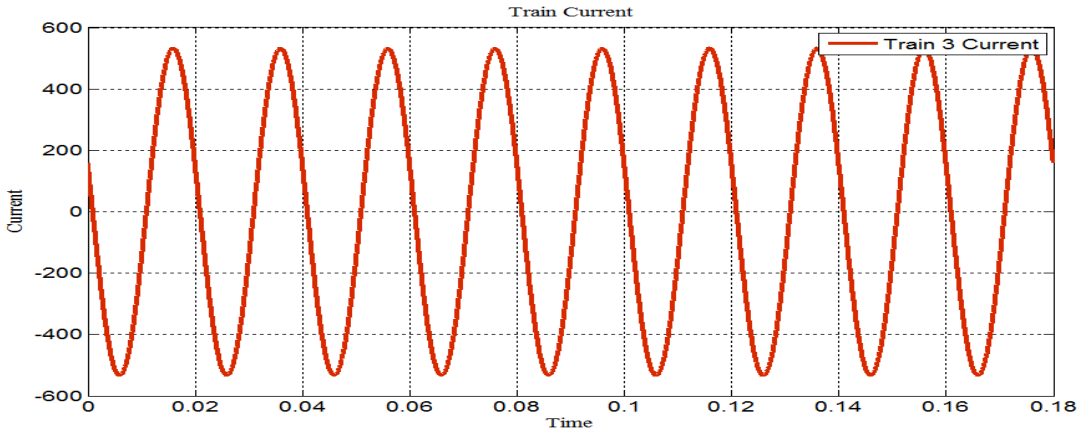

Figure 5.14: Train Currents at 64 km

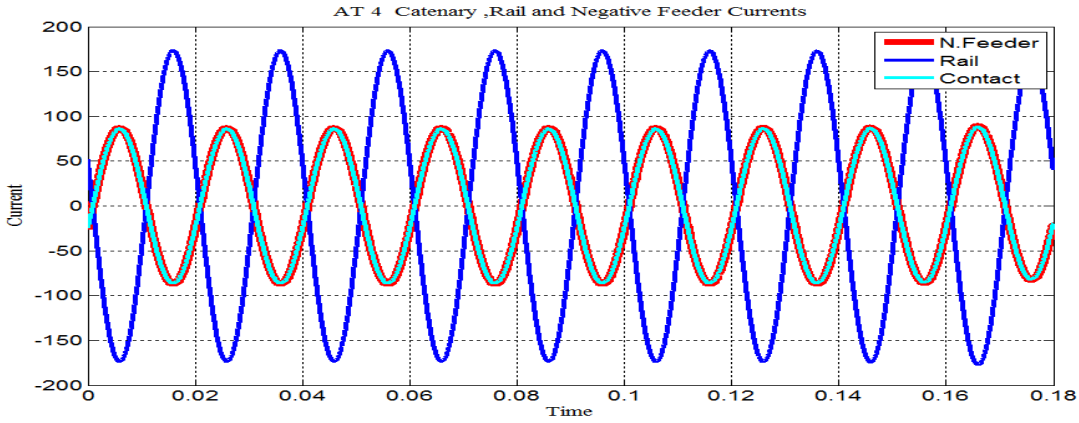

Figure 5.15: Autotransformer 4 currents

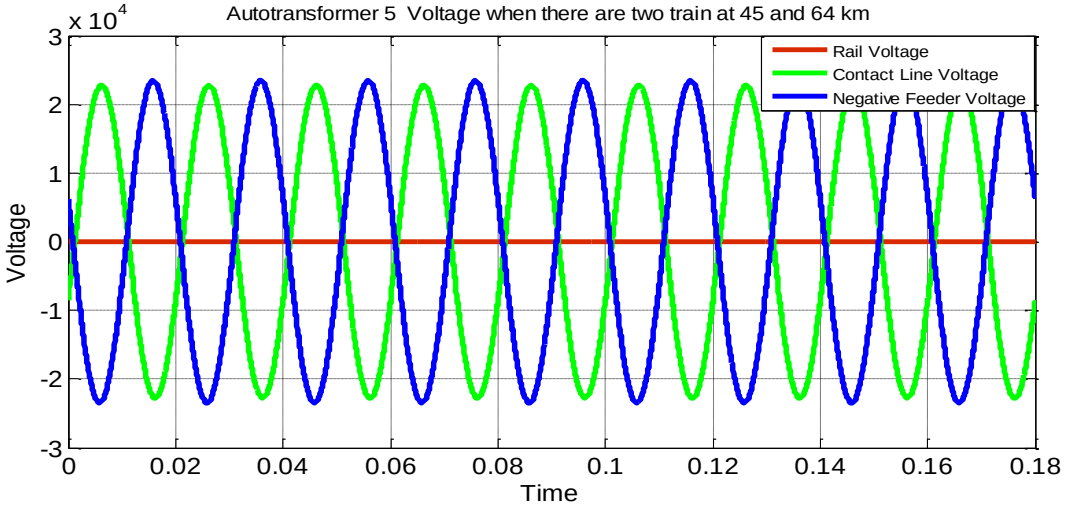

Figure 5.16: Autotransformer 5 Voltage when trains are at 45 km and 64 km

Table 5.7: Simulation results of voltages at various distances from the traction substation for three cascaded train

Number of train	Distance in km	SS output voltage	Contact line voltage	Train 1 voltage	Train 2 voltage	Train 3 voltage	% voltage regulation
Cascaded three train	15	54.21 kV	27.08 kV	24.65 kV	24.65 kV	24.65 kV	8.97%
	45	53.95 kV	26.96 kV	20.73 kV	20.73 kV	20.73 kV	23.1%
	64	53.91 kV	26.95 kV	19.82 kV	19.82 kV	19.82 kV	26.45%

Table 5.8: Simulation results of currents at various distances from the traction substation for three trains

Number of train	Distance In km	SS output current(A)			Train 1 current(A)	Train 2 current(A)	Train 3 current(A)
Three cascaded train	15	C	875.50	1635.90	543.21	543.21	543.21
		N	760.40				
	45	C	822.26	1375.71	456.72	456.72	456.72
		N	553.45				
	64	C	717.05	1249.31	414.63	414.63	414.63
		N	532.26				

Table 5.9: Simulation results of autotransformer current for three trains at a distance of 15 km from the traction substation

	AT 1	**AT 2**	**AT 3**	**AT 4**	**AT 5**
	Magnitude(A)	Magnitude(A)	Magnitude(A)	Magnitude(A)	Magnitude(A)
C	221.34	95.80	44.45	18.72	17.46
R	443.86	192.77	90.02	38.51	35.95
N	222.53	96.96	45.57	19.79	18.50

Table 5.10: Simulation results of autotransformer voltage for simultaneous operations of three cascaded trains at a distance of 15 km and 64 km from the traction substation

Trains position		**AT 1**	**AT 2**	**AT 3**	**AT 4**	**AT 5**
		Magnitude	Magnitude	Magnitude	Magnitude	Magnitude
15 km	**C**	24.65 kV	25.00 kV	25.21 kV	25.36 kV	25.29 kV
	R	0.00 V	87.12 V	0.00 V	19.46 V	0.00 V
	N	26.44 kV	25.78 kV	25.47 kV	25.28 kV	25.35 kV
64 km	**C**	24.70 kV	22.59 kV	21.48 kV	20.50 kV	19.82 kV
	R	0.00 V	68.47 V	0.00 V	53.51 V	0.00 V
	N	24.87 kV	23.03 kV	22.59 kV	19.03 kV	20.53 kV

Table 5.9 reveals that the substation output voltage approximately remain the same, when the trains move away from the traction substation. This indicate both the number of train and the position of the train does not affect the output voltage of the substation but the voltage drop at the traction substations is higher compared with **case 1** or **case 2**, at the same time, the minimum substation output voltage is below **54 kV** which is the lowest output voltage compared with remaining cases (case 1 and case 2) and the maximum voltage drop is **7.13 kV**, which is indeed the largest. This is because current required for three cascaded trains is much higher than that required for both single and two trains.

It can also be seen in **table 5.9** that the maximum voltage of the trains decreased by **7.59 %** and **4.64 %** while the minimum train voltage dropped by **20.01 %** and **12.91 %** compared with **case 1** and **case 2** respectively. This is due to the same details as it is pointed out in **table 5.1** and **table 5.5.** From this, it is possible to say that the voltage drop in the feeding circuit differs substantially depending upon the train positions and the numbers of trains in the same power-feeding section. Furthermore, the voltage regulation increased from **8.97 %** to **26.45** % .

Table 5.10 also clearly indicates that the train current decreases significantly as it moves away from the substation. Also the trains current which is found at 15 km position from the substation is **543.21 A** which is nearly equal to the nominal current but when the distance increases the current decreases sharply and reach **414.63 A** at the end of the feeding section. This is because some amount of currents flows to different circuits of the system, which reduces the amount of current which reaches to the current collecting devices or the pantograph. This shows the amount of current that reaches to the train depends on the distance of the train from the traction substation and also on the number of train along the feeding section. For example compared with **case 1** and **case 2** for the train which is found at a distance of 45 km from the traction substation the current decreased by **18.63 %** and **10.81 %** respectively. This indicates that both the number of trains and its position of the train affect the train current.

Table 5.11 also shows that as the train distance and number increases the autotransformer output voltage decreases. Compared with **case 1** and **case 2** the maximum voltage reduced by **7.45 %** and **3.96 %** respectively while the minimum voltage is decreased by **20.05 %** and **12.91%** consecutively. The maximum and the minimum AT voltages are within the recommended range

specified by European standards BS EN 50163: 2004. It is also indicated that the highest and the lowest value of the rail voltage is below the highest tolerance limit allowed by BS EN 50122-1 (IEC 62128-1).

In line for to the same reason as it is mentioned for **Table 5.4**, the sum of the autotransformers currents equals with sum of **train 1** current, **train 2** current and **train 3** current which are found at a distance of 15 km from the traction substation. This can be clearly seen in **Table 5.12**.

From **Table 5.9**, **Table 5.10**, **Table 5.11 and Table 5.12** it is possible to conclude that the results of voltage and current obtained from the steady state simulation for three Cascaded train running at various distance from the traction substations confirms with BS EN 50163: 2004, BS EN 50122-1 (IEC 62128-1) and EN 50388:2012 Standards, which reveals that our objective for this case is also achieved successfully.

In the following section, selected graphic results for the above case, **case 3** is presented. Just looking at the graphs for all cases it is possible to say which case would have the highest or lowest voltages or currents. The simulation enables us to quantify this currents or voltages.

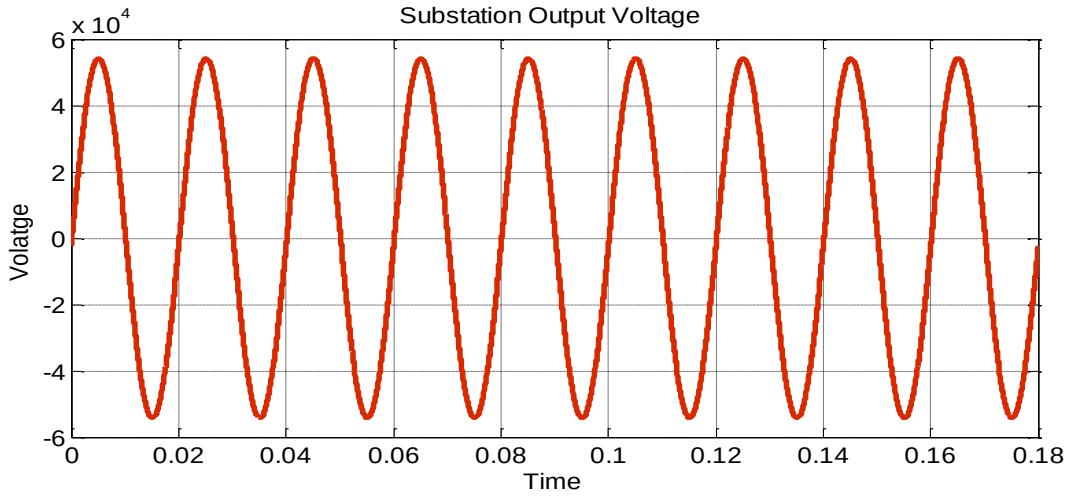

Figure 5.17: Substation output voltage when there are three cascaded train at 64 km

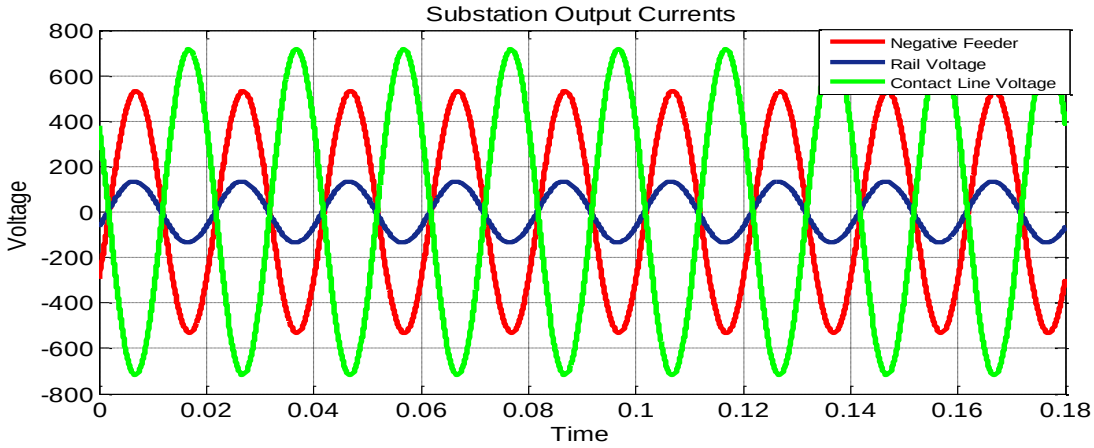

Figure 5.18: Substation output Current when there are three cascaded train at 64 km

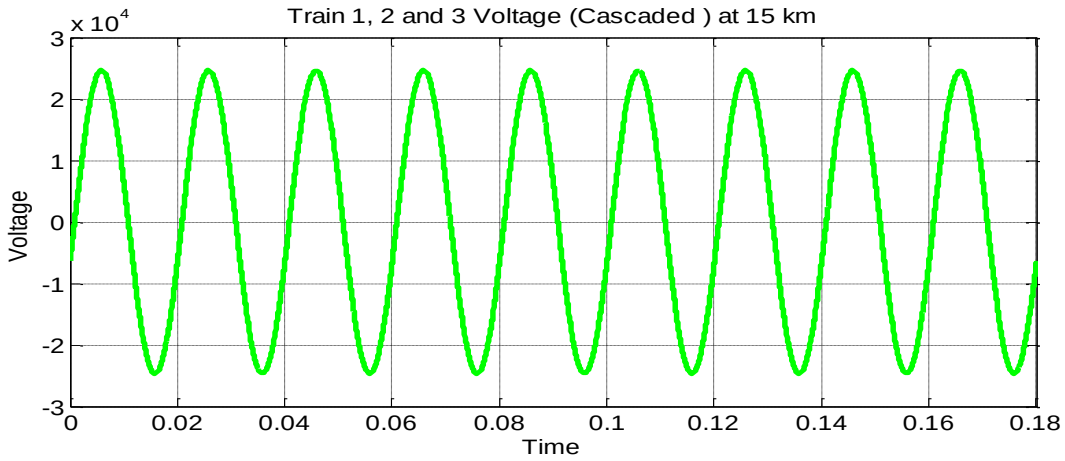

Figure 5.19: Voltages of the three cascaded trains at 15 km

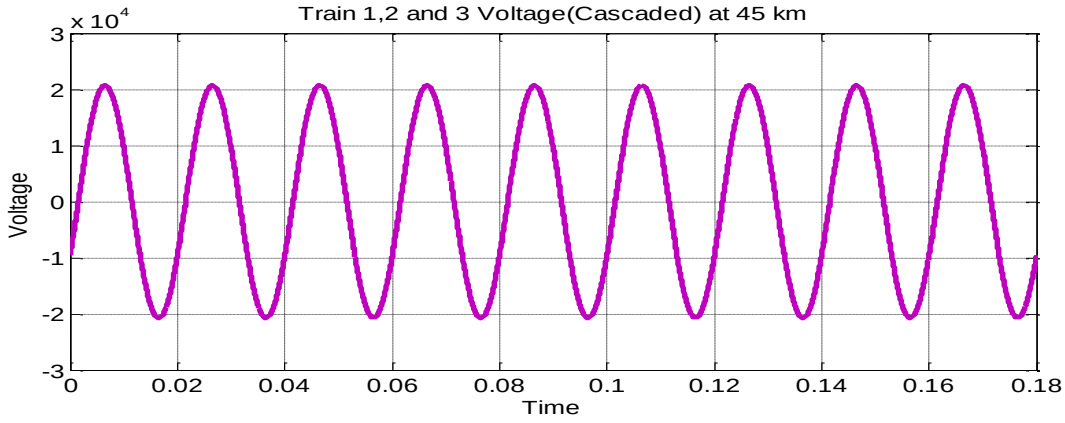

Figure 5.20: Voltages of the three cascaded trains at 15 km

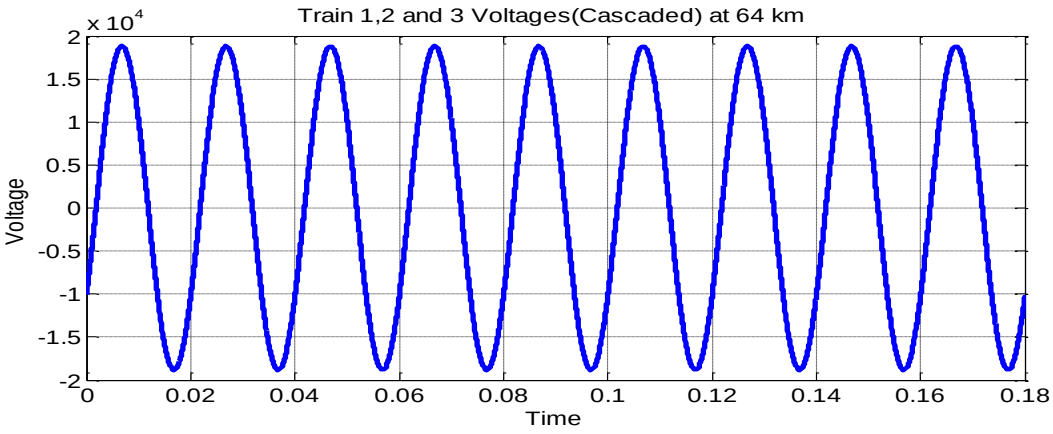

Figure 5.21: Voltages of the three cascaded trains at 64 km

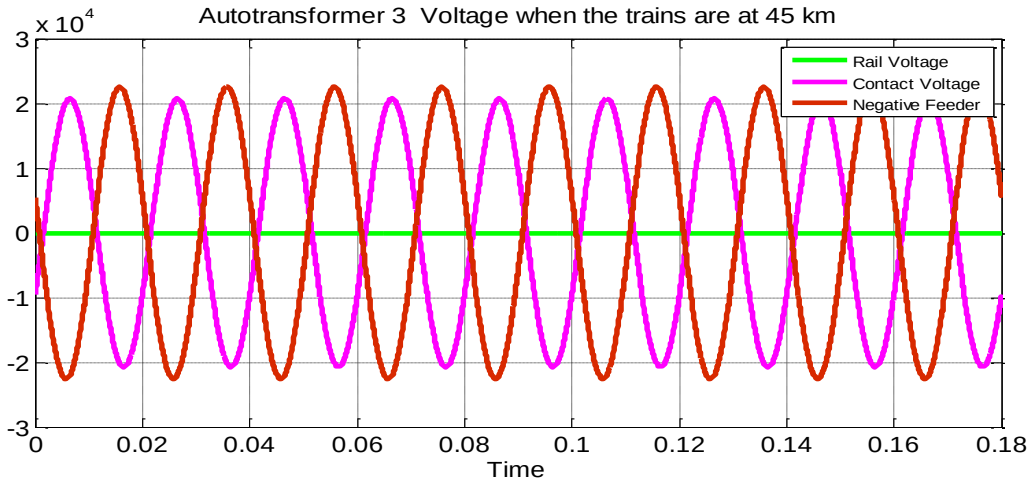

Figure 5.22: Autotransformer 5 Voltage when trains are at 45 km

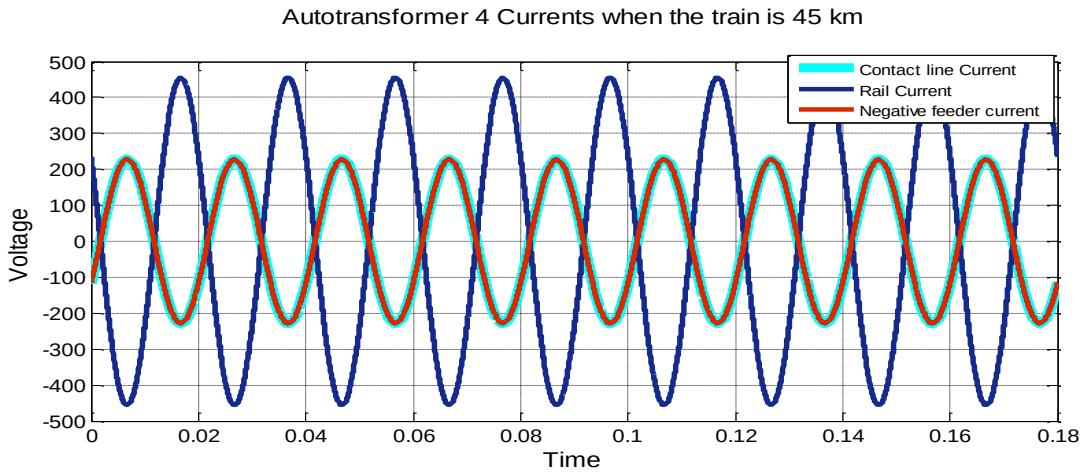

Figure 5.23: Autotransformer 4 current when trains are at 45 km

6 CONCLUSION, RECOMANDATION AND SUGGESTIONS FOR FUTURE WORK

In this chapter based on the results of the evaluation of designed traction power supply system, the following major conclusions are drawn. Moreover, useful recommendations are forwarded and the main areas of future work are suggested.

6.1 Conclusion

In this thesis, design and simulation of traction power supply system for the case of Modjo~Hawassa railway line has been studied. Traction power supply system was designed and modeled, simulations were performed using the Matlab /Simulink environment and discussions were made based on the simulation results obtained with respect to voltage, current and percentage voltage regulation.

A detailed literature survey of a traction power supply system and its major components such as traction power transformer, the transmission line or the catenary system, and the moving loads together with related issues such as power demands of the load, voltage fluctuations range, load flow and other main subjects were reviewed and presented to summarize the state of the art techniques that are correlated to the methods proposed in this research.

System designs for traction power supply system have been carried out. The design comprises four main sections. The first section is related to the power consumption of the locomotive considering the auxiliary power and the efficiency of the locomotive. This auxiliary power consumption takes into account train heating, and air condition. Moreover the electrical and mechanical losses between the pantograph and the motor are considered at the same time. The second section presented the calculation of the traction power transformer capacity based on the load current of the feeding section or the maximum effective feeder current which is mainly determined by traffic volume and line passing capacity conditions or train loading density which in turn related to the annual transportation. The third section is related to the design of traction substation power transformer and the autotransformer based on the ANSI/IEEE C37.010-1979

standard. The fourth section is presented the impedance calculation of the overhead line catenary system including the rail and the return conductor using the Carson transmission line equation.

Based on the design, a model for the major components of the traction power supply system such as the traction substation power transformer, autotransformers, the overhead catenary wire, rails, return conductor and the traction load using MATLAB/Simulink was developed and cascaded together to represent the traction power supply system .

In this research, the steady state load flow analysis for the traction power supply system have been made based on three different scenarios which are single train, two trains and three cascaded trains running along the feeding section at different position from the traction substation. Added to this, plots of waveform for all scenarios have provided for both current and voltage.

In this study, the current and voltage value in general, have been varied with distance of electric locomotive and the number of train across the line. From simulation results obtained in chapter 5, it can be conclude that the magnitude of the train voltage decreases with increase in distance of locomotive from the traction substation and also decreases with increasing the number of train along the feeding section. During simulation in worst-case scenario for voltage, **19.82 kV** was observed that is well above the lowest permanent voltage likely to remain indefinitely recommended by BS EN 50163: 2004, which is **19 kV**.

In worst-case scenario for current **414.63 A** was observed, which is well above the minimum recommended limit at any voltage in the range, as set out in EN 50388:2012 clause 7.2. In addition to this, the rail currents and voltages are within the recommended limit of BS EN 50122-1 (IEC 62128-1) in the worst-case scenario. Generally, in all considered scenarios for simulation, the traction power supply system values of currents and voltages waveform within the acceptable limits set by BS EN 50163:2004,EN 50388:2012 and BS EN 50122-1 (IEC 62128-1).

Finally, the simulation result shows the designed traction power supply system provided a significant operating margin. Minimum voltages and currents along the line having a single train or two trains or three cascaded trains at different locations from the traction substation are well

above industry standards. In account of all this result, it is possible to conclude that the objective for design and simulation of traction power supply system for the case of Modjo~Hawassa railway line have met.

6.2 Recommendation

- Due to lack of real information, the models developed take some approximation and datasheet from international railway standard. Thus, by considering the actual information we can improve the result obtained in this thesis.
- Regenerative braking can be considered. Regenerated energy is consumed by the other train in the same section; no damping resistor required.
- The model of a snapshot of the system can be used with little modifications to perform the more complex fault analysis and more detailed modeling of the system.

6.3 Suggestion for future work

- MATLAB/Simulink provides only a steady solution for a given train condition. In order to establish voltage and current profiles over time at certain points of the power network while trains are moving in the railway system, it is essential to integrate the MATLAB/Simulink to a train movement simulator taking into account the track geometry, signaling constraints, traction equipment behavior and civil engineering speed restrictions.

- The designed traction power supply system used in this thesis is to operate in normal feeding conditions. However, railway schemes are designed to operate in various emergency conditions such as short-circuits. The extension of the load flow analysis for such emergency conditions can be a further research.

REFERENCE

[1]. L. WOLFGANG, Railroad history, San Diego Railroad Museum, March 2002.

[2]. W.S. CHAN, "Whole system simulator for AC traction", PhD Thesis, University of Birmingham, UK, July 1988.

[3]. T. Kulworawanichpong, "Optimizing AC Electric Railway Power Flows with Power Electronics Control," PhD thesis, University of Birmingham, November 2003.

[4]. Steven Harrod, "Auto-transformer power supply system for electric railways", PhD Thesis, Sweden , September 2001.

[5]. F.F. Nouvion, "Railway electrification technology – Technical paper", Indian Railways International Seminar and Exhibition on Railway Electrification, 1985.

[6]. R.J. Hill, "Electric railway traction – Part 2 traction drives with three-phase induction motors", Power Engineering Journal, pp. 143-152, June 1994.

[7]. R.J. Hill, "Electric railway traction – Part 1 electric traction and DC traction motor drives", Power Engineering Journal, pp. 47-56, February 1994.

[8]. R.J. Hill, "Electric railway traction – Part 3 traction power supplies", Power Engineering Journal, pp. 275-286, December 1994.

[9]. R.W. Sturland, "Traction power supplies", GEC ALSTHOM Transmission & Distribution Projects Ltd, 2004.

[10]. C. F. Wagner and R. D. Evans, Symmetrical Components. New York: McGraw-Hill, 1933.

[11]. R.W. White, "AC supply systems and protection", Fourth Vocation School on Electric Traction Systems, IEE Power Division, April 1997.

[12]. C. Courtois, "Why the 2x25 kV alternative?", Half-day Colloquium on 50 kV Auto-transformer Traction Supply Systems – The French Experience, IEE Power Division, pp. 111-114, November 1993.

[13]. A. Mariscotti, P.Pozzobon, and M. Vanti, "Distribution of the Traction Return Current in AT Electric Railway Systems," IEEE Transactions on Power Delivery, vol. 20, no. 3, July 2005.

[14]. R. J. Hill, I. H. Cevik, "On-line Simulation of Voltage Regulation in Autotransformer-Fed AC Electric Railroad Traction Networks", IEEE Transactions on Vehicular. Technology, vol. 2, no. 3, August 1993.

[15]. J. R. Carson, "Wave propagation in overhead wires with ground return," Bell System Tech Journal, 1926.

[16]. J. D. Glover, M. S. Sarma, T. J. Overbye, Power Systems Analysis and Design, 4th ed.Thomson Engineering, May 2007.

[17]. G. Varju. Simplified method for calculating the equivalent impedance of an AT system. Technical report, Technical University of Budapest/Innotech Ltd, 1996.

[18]. T. K. Ho, Y. L. Chi, J. Wang, and K. K. Leung, "Load flow in electrified railway," in Proceedings of the second International Conference on Power Electronics, Machines and Drives, vol. 2, pp. 498 −503, 2004.

[19].Vinod Sibal, "Traction power supply system for California high speed train project", California, America, 2011.

[20] Belay Tibeb Mintesnot, "Modeling and Simulation of AC traction power Supply system" Msc thesis, Southwest Jiao tong University, November, 2013.

[21]. E. Pilo, L. Ruoco, and A. Fernandez. "Catenary and autotransformer coupled optimization for 2x25kV systems planning. In Computers in Railways X: Computer System Design and Operation in the Railway and Other Transit Systems", Prague, Czech Republic, 2006.

[22]. U. J. Shenoy, Senior Member, IEEE, K.G.Sheshadri, K. Parthasarathy, Senior Member, IEEE, H.P.Khincha, Senior Member, IEEE, D.Thukaram, Senior Member,IEEE,´´ MATLAB Based Modeling and Simulation of 25KV AC Railway Traction System-A Particular Reference to Loading and Fault Condition," 2009.

[23]. Abrahamsson, L., Kjellqvist, T. &Ostlund, S., HVDC Feeder Solution for Electric Railways. IET Power Electronics, 2012. Accepted for publication.

[24]. F.Shahnia and S.Tizghadam, "Power distribution system analysis of Rural electrified railways" University of Tabriz, Iran, 2005.

[25]. F. Kiessling, R. Piff, A. Schmieder, and E. Scheneider, "AC 25kV 50 Hz traction power supply of the Madrid-Seville line" in Contact Lines for Electrical Railways: Planning-Design-Implementation- Maintenance, SIEMENS, August 2009.

[26]. Alfonso Capasso and Marco Ciucciarelli "An integrated methodology for 2x25 KV 50Hz traction system calculation for evaluation of the regenerative braking effects in a high speed railway line" La Sapienza-University of Rome, Italy, 2010

[27]. C. J. Goodman, "Modeling and Simulation," in Professional Development Course on Railway Electrification Infrastructure and Systems, 2009.

[28]. J. D. Glover, A. Kusko, and S. M. Peeran, "Train Voltage Analysis for AC Railroad Electrification," IEEE Transactions on Industrial Applications, vol. IA-20, no.4, July/August 1984.

[29]. A. Mariscotti, P. Pozzobon, and M. Vanti, "Simplified Modeling of 2 x 25-kV AT Railway System for the Solution of Low Frequency and Large-Scale Problems," IEEE Transactions on Power Delivery, vol. 22, pp. 296 — 301, January 2007

[30]. Z.Shao, "Auto-transformer power supply system for electric railways", PhD Thesis, University of Birmingham, UK, November 1988

[31]. H. Bozkaya, "A comparative assessment of 50 kV auto-transformers and 25 kV boosters Transformer railway electrification systems", MPhil Thesis, University of Birmingham, UK, October 1987.

[32]. P. Lukaszewicz, Energy Consumption and Running Time for Trains. PhD thesis, Division of Railway Technology, KTH, Stockholm, Sweden, 2001.

[33]. Hill, R.J. and Cevik, I.H.: „On-line Simulation of Voltage Regulation in Autotransformer-fed AC Electric Railroad Traction Networks", IEEE Trans. on Vehicular Technology, vol. 42, no.3, pp.365-372, 1993.

[34]. A.J. Griffin, "Methods of improving the voltage regulation on 25 kV electrified railways", Int. Conf. On Main Line Electrification, September 1989, York, UK, pp. 252–259.

[35]. L. Abrahamsson and L. Söder, "Railway power supply investment decisions considering the voltage drops - assuming the future traffic to be known," in Intelligent System Applications to Power Systems, 2009.ISAP '09. 15th International Conference on, pp.1–6, 2009.

[37]. Jean-Marc Allenbach, Pierre Chapas, Michel Comte, and Roger Kaller, "Traction Electrique", Presses polytechniques et, universitaires romandes, 2008.

[38]. V. Galdi, C. J. Goodman, L. Ippolito and A. Piccolo, "AC locomotive: Traction equipment modeling", 3rd International Scientific Conference in Drives and Supply Systems for Modern Electric Traction, pp. 9-14, Warsaw, Poland, September 1997.

[39]. P.HIS and S.CHEN, "Electric load estimation techniques for high-speed railway (HSR) traction power system", IEEE trans. on Vehicular Technology, Vol.50, No.5, pp. 1260-1266, September 2001.

[40]. Mario A. Ríos and Gustavo Ramos, "Power System Modeling for Urban Massive Transportation Systems" Universidad de los Andes, Bogotá, D.C., Colombia, pp. 18, 2007.

[41]. Sebastian STICHEL and Mats BERG, Rail Vehicle Dynamics, KTH, 2012.

[42]. B.L theraja and A.K theraja "A text book of electrical technology", part 3, chapter 43, vo.1, New Delhi, 2005.

[43]. Denis Seimbill "Design of power supply system in DC electrified transit railways – Influence of the high voltage network", KTH Royal Institute of Technology, pp.9-10, Sweden 2014.

[44]. Y.Oura, Y.Mochinaga, and H.Nagasawa, "Railway electric power feeding system," Japan Railway & Transport Review, vol. 16, pp. 48–58, June 1998.

[45]. B.Boullanger, "Modeling and simulation of future railways," Master's thesis, Royal Institute of Technology (KTH), Mar. 2009.

[46]. P. M. Anderson, Analysis of Faulted Power Systems, Iowa State University Press, 1973.

[47]. Kiros Tesfay, "Traction Transformer Capacity", power point, Lecture 6, Addis Ababa Institute of Technology,Ethiopia,2014.

[48]. J. D. Glover, M. S. Sarma, T. J. Overbye, Power Systems Analysis and Design, 4th ed.Thomson Engineering, May 2007.

[49]. H. Roussel, C. Courtois, "High Speed Line Power Supply", EIS, pp. 109-119, July 1992.

[50]. Sanjay Y. Patel "Special Design Auto-Transformers" Smit Transformers, Ohio, September 2004.

[51]. T. K. Ho, Y. L. Chi, J. Whang, K. K. Leung, L. K. Siu, and C. T. Tse, "Probabilistic load flow in AC electrified railways," IEE Proc.-Electr. Power Appl., vol. 152, pp. 1003–1013, May 2005.

[52]. C. T. Tse, K. L. Chan, S. L. Ho, C. Y. Chung, S. C. Chow, and W. Y. Lo, "Effective Load flow Technique with Non-constant MVA Load for the Hong Kong Mass Transit Railway Urban Lies Power Distribution System," in Proceedings of the 4th International Conference on Advances in Power System Control, Operation and Management, Hong Kong, November 1997.

[53]. Jansson, N. Electrical Data for the Locomotive Types Rc4 and Rc6 (original title in Swedish). TrainTech. Solna : s.n., March 2004,Technical Report.

[54]. New current feeding system in the Swedish railway grid (original title in Swedish). Elbranschen 4/99, 1999.

[55] Piotr Lukaszewicz. The impact of variables on the energy usage and running times of trains analysis performed in the simulation software ERTS (original title in Swedish), Technical report, KTH, 2005.

[56] R. J. Hill. Electric railway traction, Part 7, Electromagnetic interference in traction systems, Power Engineering Journal, 259–266, December 1997.

APPENDIX A

MATLAB SCRIPT

A.1 MATLAB script to solve the source current and the admittance matrix

```
Z1=1.213+12.13i;                    % transformer primary winding impedance
Z2=0.250799+2.50799i;               % secondary winding impedance
a=2.4;                              % the transformer transformation ratio
Ze=0.1;                             % the earth resistance
Vo=132000;                          % The source voltage of the transformer
in(v)
zo=0;
z1prime=zo+Z1;                      % the primary circuit impedance of the
transformer including short circuit impedance
ZA=z1prime+6*Z2;                    % includes the primary and secondary
impedance of the transformer
ZB=6*Z2+24*Ze;                      %includes the secondary impedance and the
earth resistance
isource=[2.5*Vo/ZA 0 -2.5*Vo/ZA]'; % the source current
Zmatrix=[(ZA + ZB) 0 (-ZA+ZB); 1 1 1; (-ZA+ZB) 0 (ZA+ ZB)]; % the impedance
matrix of the system
Ystation=inv(Zmatrix);              % the admittance matrix of the system
Ystation=inv(Zmatrix)*[-24 24 0; 0 0 0;  0 24 -24];
```

A.2 MATLAB script to find the admittance matrix of the autotransformer

```
A Matlab script was written:
%this function generates the 3x3 Y matrix to model the autotransformer.
% I=YV The I vector is [Ic Ir If]' and the V_vector is [ve vr vf]'
%zm is the magneitzing impedance assumed between the C and the F wires.
%the equivalent impedance of the C-R and the F-R winding are assumed equal to
zg
%if zm is 1000 or greater it will be ignored( assumed open and the
magnetizing current neglected.
function[PsYmat]=Ps_Y_mat_with_Re(Zm,Zs,Re);
PsYmat = zeros(3,3);
Zm2Zs=4*Zm+2*Zs;
if(Zm<1000)
    PsYmat=[1/(2*Zs)+1/Zm2Zs -1/Zs 1/(2*Zs)-1/Zm2Zs;
        -1/Zs  2/Zs -1/Zs;
        1/(2*Zs)-1/Zm2Zs  -1/Zs  1/(2*Zs)+1/Zm2Zs];
else
     PsYmat=[1/(2*Zs) -1/Zs 1/(2*Zs);-1/Zs 2/Zs -1/Zs;1/(2*Zs)  -1/Zs
1/(2*Zs)];
end
```

A.3 MATLAB script for Resistance of the line

```
% Script to estimate the total resistance of Modjo~Hawassa Rail line
% Coefficients of Davis equation applied to Ethiopian rail system
  A = 23.45;                         % units are KN
  B = .510556;                       % units are KN s/m
```

```
C = 0.09425;                          % units are KN s-s2/m2
% Create a speed vector
V = 0:1:90;                          % speed in meters/second
% calculate Resistance (in KiloNewtons) according to modified Davis equation

             R = A + B * V + C * V.^2;

% Make a plot of total resistance vs. speed
Plot (V, R,'o--')
Xlabel (' Speed (m/s)')
Ylabel ('Resistance (kN)')
Title ('Resistance of Modjo~Hawassa Rail line')
```

A.4 MATLAB script for tractive force and the resistance force

```
A = 23.45;           % units are kN
B = 0.510556;        % units are kN s/m
C = 0.09425;           % units are kN s-s/m-m
V = 0:1:90;         % speed in meters/second
R = A + B * V + C * V.^2;
plot(V,R,'o--')
xlabel(' Speed (m/s)')
ylabel('Resistance (kN)')
title ('Resistance of Modjo~Hawassa Rail line')

% Coefficients of Davis equation applied to Modjo~Hawassa rail line

plot(V,R,'o--')
xlabel(' Speed (m/s)')
ylabel('Resistance (kN) or T (kN)')
title ('Resistance of Modjo~Hawassa Rail line ')
grid
hold on
% Calculate the Tractive Effort (T) profile
P = 13772000;                         % power (MW)
VE=V;
% velocity in m/s (needed in the TE equation)
Nu= 0.8;                             % efficiency
T = Nu*P./V/1000;                     % in kN
plot(VE,T,'^-r')
grid
```

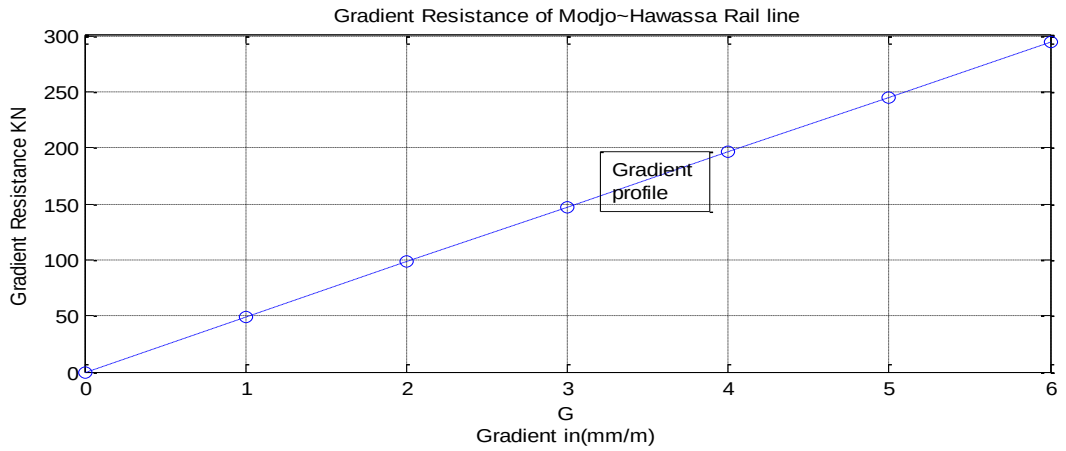

Figure A.1: Gradient resistance Vs Gradient profile

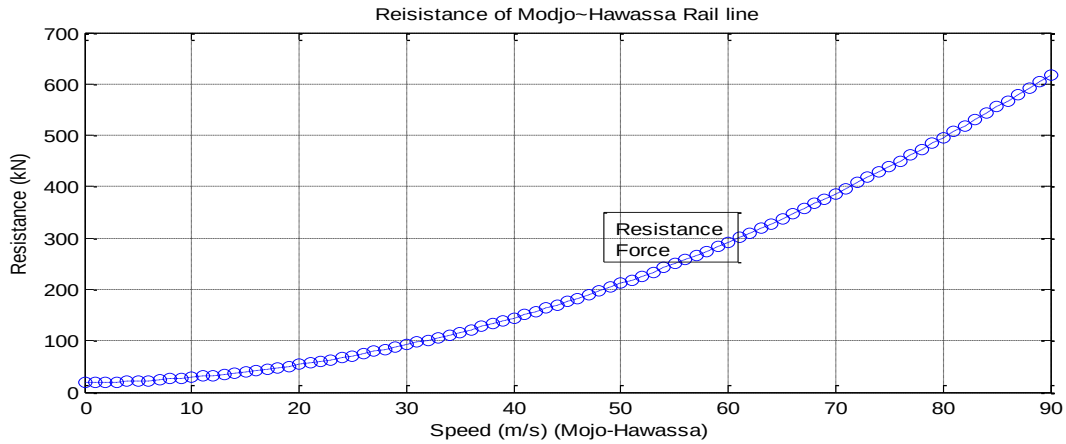

Figure A.2: Train resistance force Vs speed

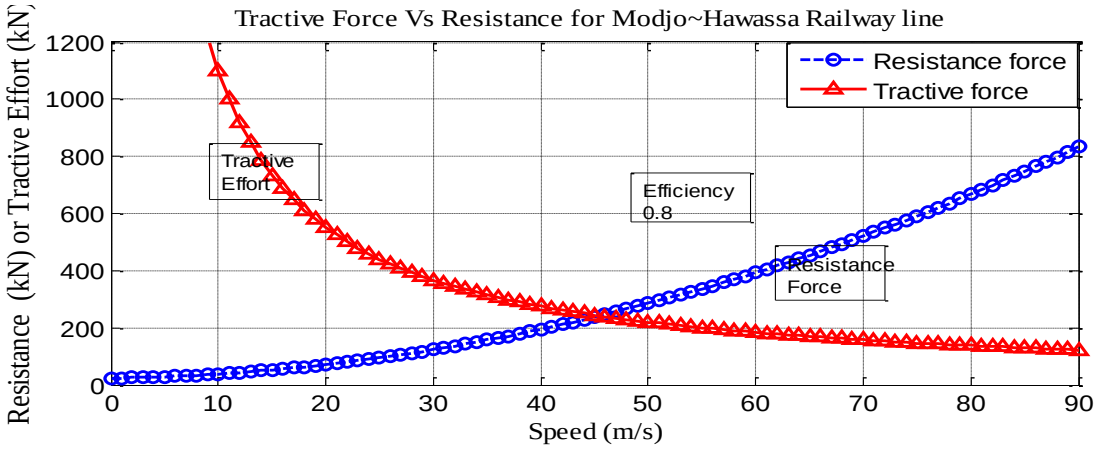

Figure A.3: Tractive effort vs speed diagram of a main line train

APPENDIX B

B.1 Solving self and mutual impedance of the line using carson equation

If no actual earth resistivity data is available, it is not uncommon to assume ρ to be 100 ohm-meter.

$$\rho_e = 100\,\Omega/\mathrm{m}$$

$$f = 50\ \mathrm{Hz}$$

δ Is skin depth or depth of penetration into the conductor and is given by

$$\delta = 503.292 \times \sqrt{\frac{\rho_c}{f\mu_r}} \qquad \text{B.1}$$

Using the skin depth δ of Equation (A) and an earth relative permeability of unity, the effect of earth return path is defined as an equivalent conductor at a depth given by:

$$D_{ad} = 1.309125 \times \delta \qquad \text{B.2}$$

$$D_{ad} = 658.87 \times \sqrt{\frac{\rho_e}{f}}$$

$$D_{ad} = 658.87\sqrt{\frac{\rho_e}{f}}\ \mathrm{m} = 658.87\sqrt{\frac{100}{50}} = 931.783\mathrm{m}$$

$$r_d = 9.869.10^{-4}.f\,\Omega/\mathrm{km} \qquad \text{B.3}$$

$$r_d = 9.869 \times 0.0001 \times 50 \quad \Omega/\mathrm{km} = 0.0493\,\Omega/\mathrm{km}$$

B.2 Self-impedance of the line using Carson formula

$$Z_{aa} = r_a + 9.869.10^{-4}.f + j4\pi.10^{-4}.f(0.25 + \ln(D_{ad}/r_o) \qquad \text{B.4}$$

Where $r_o = the\ radius\ of\ the\ conductor\ in\ meter$

The mutual impedance between conductor *a and* conductor *d is* given by

$$Z_{ad^1} = 9.869.10^{-4}.f + j4\pi.10^{-4}.f\ \ln(D_{ad}/D_{sa}) \qquad \text{B.5}$$

D_{sa} = the distance between the conductors

$$D_{ad} = \text{equivalent conductor at depth}$$

Self-impedance of Contact wire with radius of $r_o = 0.00615m$ and the conductor resistance of R=0.1695Ω/km

$$Z_{cc} = 0.1695\,\Omega/km + 0.0493 + j4\pi.10^{-4}.f(0.25 + \ln(931.783/0.00615)$$

$$Z_{cc} = 0.1695\,\Omega/km + 0.0493 + j0.06283(0.25 + \ln(931.783/0.00615)$$

$$Z_{cc} = 0.2188 + j0.7652\ \Omega/km$$

Messenger wire with radius of $r_o = 0.00845m$ and the conductor resistance of R=0.1903Ω/km

$$Z_{mm} = 0.1695\,\Omega/km + 0.0493 + j4\pi.10^{-4}.f(0.25 + \ln(931.783/0.00845)$$

$$Z_{mm} = 0.1903\,\Omega/km + 0.0493 + j0.06283(0.25 + \ln(931.783/0.00845)$$

$$Z_{mm} = 0.2396488 + j0.7452\,\Omega/km$$

Negative feeder wire with radius of $r_o = 0.01175m$ and the conductor resistance of R=0.1027 Ω/km

$$Z_{FF} = 0.1027\,\Omega/km + 0.0493 + j4\pi.10^{-4}.f(0.25 + \ln(931.783/0.01175)$$

$$Z_{FF} = 0.1027\,\Omega/km + 0.0493 + j0.06283(0.25 + \ln(931.783/0.01175)$$

$$Z_{FF} = 0.1520 + j0.7245\,\Omega/km$$

Static wire with radius of $r_o = 0.00815m$ and the conductor resistance of R=0.2143 Ω/km

$$Z_{SS} = 0.2143\,\Omega/km + 0.0493 + j4\pi.10^{-4}.f(0.25 + \ln(931.783/0.00815)$$

$$Z_{SS} = 0.1027\,\Omega/km + 0.0493 + j0.06283(0.25 + \ln(931.783/0.00815)$$

$$Z_{SS} = 0.2636 + j0.7632\,\Omega/km$$

Rail with radius of $r_o = 0.0730m$ and the conductor resistance of

R=0.0240 Ω/km

$$Z_{RR} = 0.0240\,\Omega/km + 0.0493 + j4\pi.10^{-4}.f(0.25 + \ln(931.783/0.0730)$$

$$Z_{RR} = 0.0240\,\Omega/km + 0.0493 + j0.06283(0.25 + \ln(931.783/0.0730)$$

$$Z_{RR} = 0.07334 + j0.609744\,\Omega/km$$

B.3 Mutual impedance using Carson formula

Mutual impedance between the contact wire and the messenger wire

$$Z_{C1m1} = 9.869.10^{-4}.f + j4\pi.10^{-4}\ln(D_{ad}/D_{sa})$$

$$Z_{C1m1} = 0.0493 + j0.06283\ln(931.783/1.150)$$

$$Z_{C1m1} = Z_{C2m2} = 0.0493 + j0.4208$$

Mutual impedance between the contact wire and the negative feeder wire

$$Z_{C1F1} = 9.869.10^{-4}.f + j4\pi.10^{-4}\ln(D_{ad}/D_{sa})$$

$$Z_{C1F1} = 0.0493 + j0.06283\ln(931.783/4.3539)$$

$$Z_{C1F1} = Z_{C2F2} = 0.0493 + j0.3371\ \Omega/km$$

Mutual impedance between the contact wire and the static wire

$$Z_{C1S1} = 9.869.10^{-4}.f + j4\pi.10^{-4}\ln(D_{ad}/D_{sa})$$

$$Z_{C1S1} = 0.0493 + j0.06283\ln(931.783/4.3539)$$

$$Z_{C1S1} = Z_{C2S2} = 0.0493 + j0.3371\ \Omega/km$$

Mutual impedance between the contact wire and the Rail line

$$Z_{C1R11} = 9.869.10^{-4}.f + j4\pi.10^{-4}\ln(D_{ad}/D_{sa})$$

$$Z_{C1R11} = 0.0493 + j0.06283\ln(931.783/5.3483)$$

$$Z_{C1R11} = Z_{C1R12} = 0.0493 + j0.3242\ \Omega/km$$

$$Z_{C1R11} = Z_{C1R12} = Z_{C2R21} = Z_{C2R22}$$

Mutual impedance between the messenger wire and the negative feeder

$$Z_{m1nF1} = 9.869.10^{-4}.f + j4\pi.10^{-4}\ln(D_{ad}/D_{sa})$$

$$Z_{m1nF1} = 0.0493 + j0.06283\ln(931.783/3.9886)$$

$$Z_{m1nF1} = Z_{m2nF2} = 0.0493 + j0.3426\ \Omega/km$$

$$Z_{nF1m1} = Z_{nF2m2} = Z_{m1nF1} = Z_{m2nF2}$$

Mutual impedance between the messenger wire and the Rail

$$Z_{m1R11} = 9.869.10^{-4}.f + j4\pi.10^{-4}\ln(D_{ad}/D_{sa})$$

$$Z_{m1R11} = 0.0493 + j0.06283\ln(931.783/6.4897)$$

$$Z_{m1R11} = Z_{m2R12} = 0.0493 + j0.3120\,\Omega/km$$

$$Z_{m2R21} = Z_{m2R22} = Z_{m1R11} = Z_{m2R12}$$

Mutual impedance between the messenger wire and the static wires

$$Z_{m1S1} = 9.869.10^{-4}.f + j4\pi.10^{-4}\ln(D_{ad}/D_{sa})$$

$$Z_{m1S1} = 0.0493 + j0.06283\ln(931.783/3.2983)$$

$$Z_{m1S1} = Z_{m2S2} = 0.0493 + j0.3538\ \Omega/km$$

Mutual impedance between the negative feeder wire and the Rail line

$$Z_{NF1R21} = 9.869.10^{-4}.f + j4\pi.10^{-4}\ln(D_{ad}/D_{sa})$$

$$Z_{NF1R21} = 0.0493 + j0.06283\ln(931.783/7.8791)$$

$$Z_{NF1R21} = Z_{NF2R12} = 0.0493 + j0.2998\,\Omega/km$$

Mutual impedance between the negative feeder wire and the Rail line

$$Z_{NF1R22} = 9.869.10^{-4}.f + j4\pi.10^{-4}\ln(D_{ad}/D_{sa})$$

$$Z_{NF1R22} = 0.0493 + j0.06283\ln(931.783/8.5628)$$

$$Z_{NF1R22} = Z_{NF2R11} = 0.0493 + j0.2946\ \Omega/km$$

Mutual impedance between the negative feeder wire and the static wire

$$Z_{NF1S1} = 9.869.10^{-4}.f + j4\pi.10^{-4}\ln(D_{ad}/D_{sa})$$

$$Z_{NF1S1} = 0.0493 + j0.06283\ln(931.783/1.3647)$$

$$Z_{NF1S1} = Z_{NF2S2} = 0.0493 + j\ 0.4100\,\Omega/km$$

Mutual impedance between the negative feeder wire and the Rail line

$$Z_{NF1R21} = 9.869.10^{-4}.f + j4\pi.10^{-4}\ln(D_{ad}/D_{sa})$$

$$Z_{NF1R21} = 0.0493 + j0.06283\ln(931.783/10.864)$$

$$Z_{NF1R21} = 0.0493 + j0.2797\ \Omega/km$$

Mutual impedance between the negative feeder wire and the Rail line

$$Z_{NF1R22} = 9.869.10^{-4}.f + j4\pi.10^{-4}\ln(D_{ad}/D_{sa})$$

$$Z_{NF1R22} = 0.0493 + j0.06283\ln(931.783/11.976)$$

$$Z_{NF1R22} = Z_{NF2R11} = 0.0493 + \text{j}0.2736\ \Omega/km$$

Mutual impedance between the negative feeder wire and the static wire

$$Z_{NF1S2} = 9.869.10^{-4}.f + j4\pi.10^{-4}\ln(D_{ad}/D_{sa})$$

$$Z_{NF1S2} = 0.0493 + j0.06283\ln(931.783/12.179)$$

$$Z_{NF2S1} = Z_{NF1S2} = 0.0493 + j0.2726\,\Omega/km$$

B.4 How MATLAB /Simulink Mutual inductance element used to represent the catenary system

A.4.1 For the single track

C1=self-impedance of contact line 1

C1M1=Mutual impedance of the contact line 1and the messenger wire 1

C1F1= Mutual impedance of the contact line 1 and the negative feeder wire 1

The same is true for other conductors

C1= $(15 \times 0.2188/5, 15 \times 0.7652/314.159/5) = (0.6564, 0.00731)$

M1= $(15 \times 0.2396/5, 15 \times 0.7452/314.159/5) = (0.7188, 0.00712)$

C1M1= $(15 \times 0.0493, 15 \times 0.4208/314.159) = (0.7395, 0.0200)$

F1= $(15 \times 0.1520/5, 15 \times 0.7245/314.159/5) = (0.4560, 0.00692)$

C1F1= $(15 \times 0.0493, 15 \times 0.3371/314.159) = (0.7395, 0.0161)$

R11= $(15 \times 0.0733/5, 15 \times 0.6097/314.159/5) = (0.2199, 0.00582)$

C1R11= $(15 \times 0.0493, 15 \times 0.3242/314.159) = (0.7395, 0.01548)$

R11= R12

C1R11= C1R12

S1= $(15 \times 0.2636/5, 15 \times 0.7632/314.159/5) = (0.7908, 0.00729)$

C1S1= $(15 \times 0.0493, 15 \times 0.3538/314.159) = (0.7395, 0.01689)$

M1F1= $(15 \times 0.0493, 15 \times 0.3426/314.159) = (0.7395, 0.01636)$

M1R11= $(15 \times 0.0493, 15 \times 0.3120/314.159) = (0.7395, 0.0149)$

M1R12= $(15 \times 0.0493, 15 \times 0.3120/314.159) = (0.7395, 0.0149)$

M1S1= $(15 \times 0.0493, 15 \times 0.3546/314.159) = (0.7395, 0.0169)$

F1R11= $(15 \times 0.0493, 15 \times 0.2998/314.159) = (0.7395, 0.01432)$

F1R12= $(15 \times 0.0493, 15 \times 0.2946/314.159) = (0.7395, 0.01407)$

F1S1= $(15 \times 0.0493, 15 \times 0.4100/314.159) = (0.7395, 0.01958)$

R11R12= $(15 \times 0.0493, 15 \times 0.4069/314.159) = (0.7395, 0.0194)$

R11S1= $(15 \times 0.0493, 15 \times 0.3118/314.159) = (0.7395, 0.01489)$

R12S1= $(15 \times 0.0493, 15 \times 0.3055/314.159) = (0.7395, 0.01459)$

B.4.2 For the double track

For the double track the same procedure as the single track has to be followed, the only differences are instead of 15 kilometer 4 kilometer is used and the following parameters are equal.

C1=C2, M1=M2, F1=F2, R11=R21=R12=R22

C1M1=C2M2, C1F1=C2F2, C1R11=C2R21, C1R12=C2R22, C1S1=C2S2

MIF1=M2F2, M1S1=M2S2, M1R11=M2R21, M1R12=M2R22, FIS1=F2S2

F1R11=F2R21, F1R12=F2R22, S1R11=S2R21, S1R12=S2R22, R11R12=R21R2

C1C2=C2C1= $(4 \times 0.0493, 4 \times 0.3293/314.159) = (0.1972, 0.00419)$

C1M2=C2M1= $(4 \times 0.0493, 4 \times 0.3276/314.159) = (0.1972, 0.00417)$

C1F2=C2F1= $(4 \times 0.0493, 4 \times 0.2911/314.159) = (0.1972, 0.003705)$

C1R21=C2R11= $(4 \times 0.0493, 4 \times 0.3093/314.159) = (0.1972, 0.003937)$

B.5 Linear Transformer

The Linear Transformer block model shown consists of three coupled windings wound on the same core. The model takes into account the winding resistances (R1 R2 R3) and the leakage inductances (L1 L2 L3), as well as the magnetizing characteristics of the core, which is modeled by a linear (Rm Lm) branch

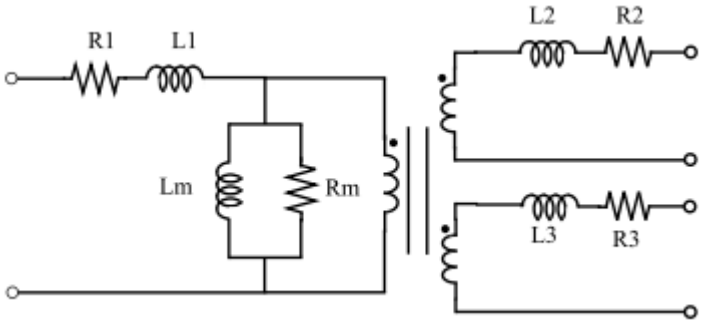

. G

Figure B.1: Linear transformer

In order to comply with industry, the resistance and inductance of the windings are specified in per unit (p.u.). The values are based on the transformer rated power Pn, in VA, nominal frequency fn, in Hz, and nominal voltage Vn, of the corresponding winding.

APPENDIX C

C.1 Current distribution in 2 × 25 power supply system

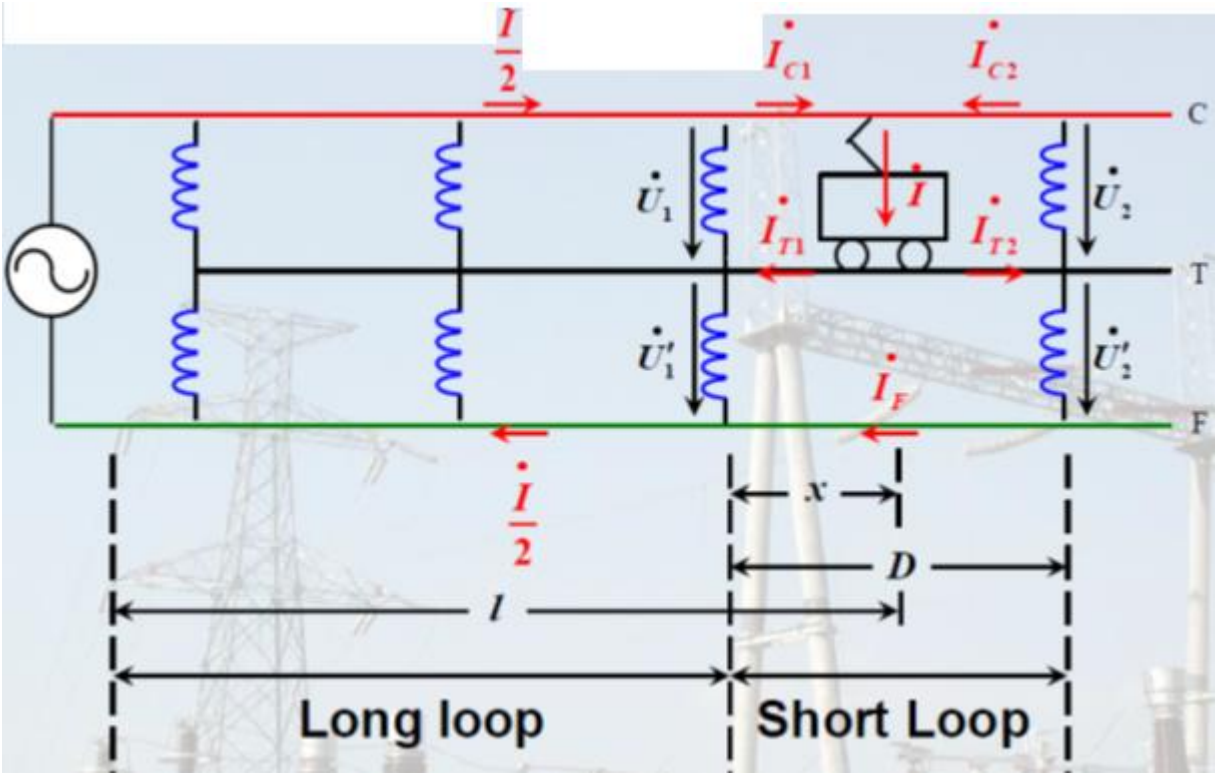

Figure C.1: Current distribution

C.1.1 Current distribution inside the long loop section

$$I_{CL} + \frac{1}{2}I_{T1} + \frac{1}{2}I_{T2} = I \quad \text{C.1}$$

$$I_{FL} - \frac{1}{2}I_{T1} - \frac{1}{2}I_{T2} = 0 \quad \text{C.2}$$

$$I_{T1} + I_{T2} = I \quad \text{C.3}$$

$$I_{CL} = \frac{1}{2}I \quad \text{C.4}$$

$$I_{FL} = \frac{1}{2}I \quad \text{C.5}$$

Conclusion: at long loop current at catenary and return feeder is half of the trains current

$$I_{FL} = \frac{1}{2}I = \frac{1}{2} * 550.88\ A$$

$$I_{FL} = 274.44\ A$$

And

$$I_{CL} = \frac{1}{2}I = 274.44\ A$$

$$274.44\ A + \frac{1}{2}I_{T1} + \frac{1}{2}I_{T2} = 550.88\ A$$

$$274.44\ A - \frac{1}{2}I_{T1} - \frac{1}{2}I_{T2} = 0$$

$$I_{T1} + I_{T2} = 550.88\ A$$

C.1.2 Current distribution inside the short loop section

$$I_{T1} = \frac{(D-x)}{D}I \quad \text{C.6}$$

$$I_{T2} = \frac{x}{D}I \quad \text{C.7}$$

$$I_{C1} = \frac{1}{2}\frac{(2D-x)}{D}I = (1 - \frac{x}{2D})I \quad \text{C.8}$$

$$I_{C2} = I_F = \frac{x}{2D}I \quad \text{C.9}$$

Conclusion: at short loop AT section, track current distribution is inversely proportional to the distance.

$$D = 15\ \text{km and}\ x = 14.9\ \text{km}$$

$$I_{T1} = \frac{(15 - 14.9)}{15} * 550.88\ A$$

$$I_{T1} = 3.67A$$

$$I_{T2} = \frac{14.9}{15} * 550.88\ A$$

$$I_{T2} = 547.2\ A$$

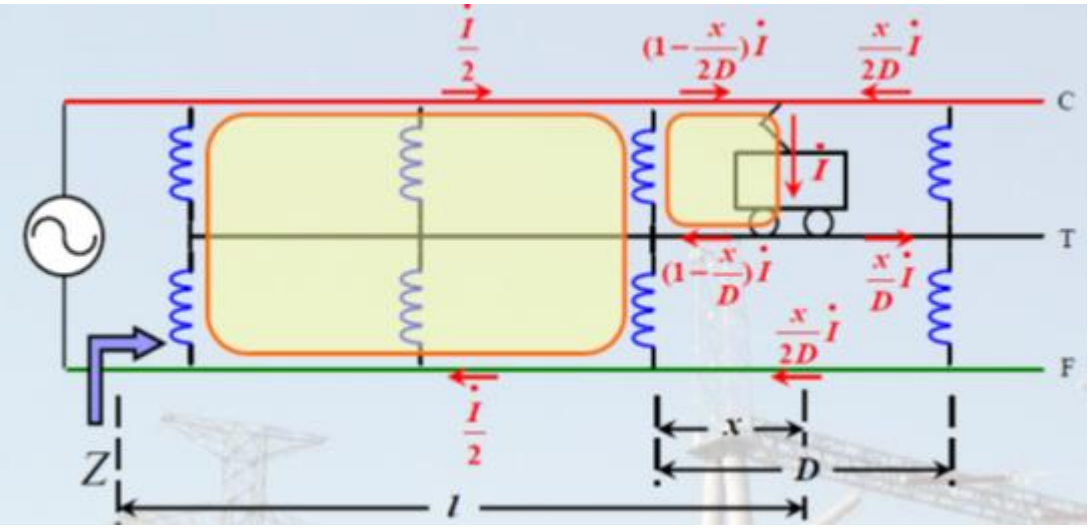

Figure C.2: shows current distribution in between two Autotransformers

C.2 voltage drop for a single train

$$\text{voltage drop} = \Delta\dot{U} = \frac{1}{2}\dot{E} - \dot{U} \qquad \text{C.10}$$

$$\Delta\dot{U} = \frac{1}{2}(Z_c + Z_F - 2Z_{CF})(l - x)\frac{I}{2} + \left(1 - \frac{x}{2D}\right)I(Z_c + Z_{CT})x + \frac{D-x}{D}I(Z_T - Z_{CT})x + \frac{x}{2D}I(Z_{TF} - Z_{CF})x \qquad \text{C.11}$$

$$\Delta\dot{U} = \frac{1}{4}(Z_c + Z_F - 2Z_{CF})lI + \left[-(Z_c + Z_R - 2Z_{CF}) - \frac{1}{4}(Z_c + Z_F - 2Z_{CF}) - \frac{x}{2D}(Z_c + 2Z_R + 2Z_{CF} - 3Z_{CR} - Z_{RF})\right]xI \qquad \text{C.12}$$

$$l = 64\text{km}$$

$$Z_{cc} = 0.2188 + j0.7652\ \Omega/\text{km} = 0.7958\ \Omega/\text{km}$$

$$Z_{FF} = 0.1520 + j0.7245\,\Omega/\text{km} = 0.74027\ \Omega/\text{km}$$

$$Z_{CF} = 0.0493 + j0.3371\ \Omega/\text{km} = 0.3406\ \Omega/\text{km}$$

$$Z_{CR} = 0.0493 + j0.3242\ \Omega/\text{km} = 0.3279\ \Omega/\text{km}$$

$$Z_{FR} = 0.0493 + j0.2946\ \Omega/km = 0.2986\ \Omega/km$$

$$Z_{RR} = 0.07334 + j0.6097\,\Omega/\text{km} = 0.6140\ \Omega/\text{km}$$

$$\Delta\dot{U} = \frac{1}{4}(0.7958\ \Omega/\text{km} + 0.74027\ \Omega/\text{km} - 2(0.3406\ \Omega/\text{km})64\ \text{km} * 550.88\ \text{A} + [(0.7958\ \Omega/\text{km} + 0.6140\ \Omega/\text{km} - 2(0.3406\ \Omega/\text{km}) - \frac{1}{4}(0.7958\ \Omega/\text{km} + 0.74027\ \Omega/\text{km} - 2(0.3406\ \Omega/\text{km}) - \frac{14.9}{30}(0.7958\ \Omega/\text{km} + 2(0.6140\ \Omega/\text{km}) + 2(0.3406\ \Omega/\text{km}) + 3(0.3279\ \Omega/\text{km}) - (0.2986\ \Omega/\text{km})]\ 14.9\ \text{km} * 550.88\ \text{A}$$

$$\Delta\dot{U} = 7534.89\ \text{V} + [0.7286 - \frac{1}{4}(0.8548) - 0.493(2.1227).\ 8208.112\ \text{V}$$

$$\Delta\dot{U} = 7534.89\ \text{V} + (-0.53159) \times 8208.112\ \text{V}$$

$$\Delta\dot{U} = 7534.89\ \text{V} - 4363.35\ \text{V}$$

$$\Delta\dot{U} = 3171.53\ \text{V}$$

$$\Delta\dot{U} = 3.173\ \text{KV}$$

The result of the voltage drop for the single train is approximatly equal to the voltage drop which we have seen in the simulation.

C.3 Short circuit calculation

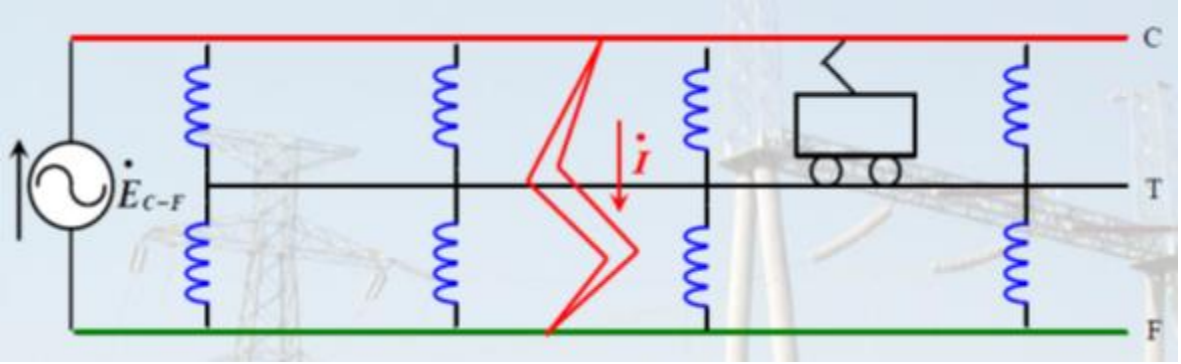

Figure C.3: Shows short circuit.

C.3.1 Short circuit between catenary and track

$$\text{Equivalent impedance} = Z = Z_{AA}l + Z_{BB}\left(1 - \frac{x}{D}\right)x$$

$$Z_{AA} = \frac{1}{4}(Z_C + Z_F - 2Z_{CF}) \qquad \text{C.13}$$

$$Z_{BB} = \frac{1}{2}(Z_C + 2Z_T + 2Z_{CF} - 3Z_{CT} - Z_{TF}) \quad \text{C.14}$$

$$I_{C-T} = \frac{E_{C-T}}{\frac{Z_S}{4} + Z_{AA}l + Z_{BB}\left(1-\frac{x}{D}\right)x} \quad \text{C.15}$$

$$Z_{AA} = \frac{1}{4}\big(0.2188 + j0.7652\ \Omega/km + 0.1520 + j0.7245\,\Omega/km - 2(0.0493 + j0.3371\ \Omega/km)\big).64km$$

$$Z_{AA} = \frac{1}{4}(0.2722 + j0.8155)$$

$$Z_{AA} = (0.0680 + j0.2038)$$

$$Z = (0.0680 + j0.2038)64 + (0.013 + j0.0687)\left(1 - \frac{14.9}{15}\right)14.9$$

$$Z = 4.3552 + j13.048$$

$$Z_S = Z_{eq} = 4.3552 + j13.048$$

$$\frac{Z_S}{4} = 1.0888 + j3.262$$

$$Z_{BB} = \frac{1}{2}(0.2188 + j0.7652\ \Omega/km + 2(0.07334 + j0.6097\,\Omega/km) + 2(0.0493 + j0.3371\ \Omega/km) - 3(0.0493 + j0.3242\ \Omega/km) - (0.0493 + j0.2946\ \Omega/km)$$

$$Z_{BB} = (0.13344 + j0.6958).0.09875$$

$$Z_{BB} = 0.013 + j0.0687$$

$$I_{C-T} = \frac{27.5\text{ kv}}{1.0888 + j3.262 + 4.3552 + j13.048 + 0.013 + j0.0687}$$

$$I = \frac{27.5\text{ kv}}{5.457 + j16.3787}$$

$$I = \frac{27.5\text{ kA}}{17.26} = 1.593\text{ kA}$$

C.3.2 Short circuit between the return feeder and the catenary

$$E_{C-F} = Z_S I_{C-F} + (Z_C I_{C-F} - 2Z_{CF} I_{C-F} + Z_F I_{C-F}) \quad \text{C.16}$$

$$I_{C-F} = \frac{E_{C-F}}{Z_s+(Z_C+Z_F-2Z_{CF})} \quad \text{C.17}$$

$$I_{C-F} = \frac{55\ \text{kv}}{4.3552+j13.048+0.2188+j0.7652+0.1520+j0.7245-2(0.0493+j0.3371)}$$

$$I_{C-F} = \frac{55\ \text{kv}}{4.3552 + j13.048 + 0.2722 + j0.8155)}$$

$$I_{C-F} = \frac{55\ \text{kv}}{4.5977 + j13.8635}$$

$$I_{C-F} = \frac{55\ \text{kv}}{14.6\ \Omega} = 3.767\ KA$$

I_{C-F} is the Short circuit current between the contact line and the negative feeder line

C.4 Percentage Voltage Regulation

One train at 15 km

$$\%\ \text{volatge regulation} = \frac{27413.13 - 26676.28}{27413.13} \times 100 = 2.68\ \%$$

One train at 45 km

$$\%\ \text{volatge regulation} = \frac{27380.40 - 25472.05}{27380.40} \times 100 = 6.97\ \%$$

When there is one train at 64 km

$$\%\ \text{volatge regulation} = \frac{27365.51 - 24778.16}{27365.51} \times 100 = 9.45\ \%$$

When two train at 15 and 45 km

$$\%\ \text{volatge regulation} = \frac{27260.71 - 24820.16}{27260.71} \times 100 = 8.95\ \%$$

When two train at 15 and 64 km

$$\%\ \text{volatge regulation} = \frac{27250.69 - 24181.15}{27250.69} \times 100 = 11.26\ \%$$

When two train at 45 and 64 km

$$\%\ \text{volatge regulation} = \frac{27181.30 - 23238.78}{27181.30} \times 100 = 14.50\%$$

When three cascaded train at 15 km

$$\%\ \text{volatge regulation} = \frac{27.08-24.65}{27.08} \times 100 = 8.97\ \%$$

When three cascaded train at 15 km

$$\%\ \text{volatge regulation} = \frac{26.96-20.73}{26.96} \times 100 = 23.1\%$$

When three cascaded train at 15 km

$$\%\ \text{volatge regulation} = \frac{26.95-19.82}{26.95} \times 100 = 26.45\%$$

APPENDIX D

Numerical data used in TPSS

In this following appendix some of the numerical values which used in TPSS are Stored.

Table D.1: Coordinates of the Different Conductors in the system

Point	(X,Y)
Contact wire	(0,5.3)
Messenger	(0,6.45)
Negative feeder	(-3.9175,7.2)
Earth wire	(-3.2675,6)
Reference point	(0,0)

Table D.2: Values of the train parameters

Name of the parameters	Symbols used	Values	unit
Maximum Train mass	m	5,000,000	kg
Adhesion coefficient	μ_a	0.3	//
Acceleration	a	0.2778	m/s^2
Slippage ratio	ξ	0	//
Coefficients for the train resistive force equation (found by calculation)	A B C	23450 N 510.556 94.25	N Ns/m Ns^2/m^2
Earth's gravity	g	9.81	m/s^2
Auxiliary power consumption	P_{aux}	42	kW
Power factor of the auxiliary power consumption	PF_{aux}	0.8	//
Efficiency	η_{loco}	0.8	//